

ROUGHNESS AT THE PAVEMENT-BRIDGE INTERFACE

by

Yi-Chin Hu
Tsu-Long Wu
Clyde E. Lee
Randy Machemehl

Research Report Number 213-1F

Roughness at the Pavement-Bridge Interface
Research Project 3-8-76-213

conducted for

Texas
State Department of Highways and Public Transportation

in cooperation with the
U. S. Department of Transportation
Federal Highway Administration

by the

CENTER FOR HIGHWAY RESEARCH
THE UNIVERSITY OF TEXAS AT AUSTIN

August 1979

PREFACE

This is the first and final published report on Research Project 3-8-76-213, "Roughness at the Pavement-Bridge Interface." It includes summaries of pertinent literature, methodologies for measurement and analyses of surface roughness, and recommendations for precluding and minimizing approach surface roughness.

Two unpublished theses based on various phases of the study have been submitted to The University of Texas at Austin in partial fulfillment of the requirements for the Master of Science degree in Civil Engineering. These are:

"A Study of Roughness at the Pavement-Bridge Interface," June 1977, by Y. C. Hu, and

"Roughness at the Bridge-Pavement Interface," August 1979, by T. S. Wu.

Copies of these are available for interlibrary loan from The University of Texas at Austin, Austin, Texas 78712.

ABSTRACT

Road surface roughness in the proximity of the pavement-bridge interface may lower riding quality and induce excessive dynamic wheel loads on highway structures. Twenty-one bridge sites in four Texas State Department of Highways and Public Transportation Districts, Lubbock, Houston, Austin, and San Antonio, are selected for study. The Surface Dynamics Profilometer is utilized to measure roadway profiles. Dynamic vehicular tire forces induced by three types of vehicles at two specified speeds are estimated using a computer simulation model. Possible causes and typical patterns of surface irregularities are identified and classified and various treatment methods are examined. A dynamic load index is developed to assess ride quality and predict subjective ratings.

SUMMARY

An extensive study of surface roughness along and adjacent to bridge approaches is presented. A survey of literature indicates that various aspects of the generalized problem have been investigated by a number of researchers. Most research efforts have recommended design and construction methodologies which have been incorporated into current practice.

Field data collection efforts have consisted of gathering design, construction, and maintenance histories and surface profile descriptions for bridge approaches in four SDHPT Districts. Computer simulation of vehicular tire forces for measured approach profiles indicates that dynamic tire forces induced by typical approach roughness may reach as much as 4.5 times their static values.

A large number of factors suspected of being related to approach roughness could not be identified as causative. These include traffic volume, bridge function, bridge type, bridge age or height of embankment fill. Rigid pavements could not be identified as being generally superior to flexible pavements; however, CRCP generally provided better performance than JRCP. Type of material utilized in approach embankments was found to be the factor best correlated with roughness problems. Timely performance of maintenance activities was, likewise, identified as having a strong relationship to the development and progression of approach problems.

IMPLEMENTATION STATEMENT

A concise summary of courses and manifestations of pavement surface roughness on bridge approaches is provided. Information presented may be utilized as a guide to design, and construction techniques which may be utilized to help preclude approach roughness problems. Data regarding surface maintenance may, likewise, be utilized as a guide to practices which may help alleviate roughness problems. Simulation based prediction of dynamic vehicular tire forces induced by specific roughness types, can be used to predict magnitudes and locations of dynamic loading on bridge approaches and bridge surfaces.

TABLE OF CONTENTS

PREFACE	iii
ABSTRACT	iv
SUMMARY	v
IMPLEMENTATION STATEMENT	vi
 CHAPTER 1. INTRODUCTION	
Roughness Indicators	1
Objectives	2
Scope of the Report	2
 CHAPTER 2. CAUSE EXAMINATION AND TREATMENT STUDY - A LITERATURE REVIEW	
Traffic	6
Climate and Environment	7
Material	8
Design	15
Construction	23
Maintenance	24
Summary	25
 CHAPTER 3. SITE INVESTIGATIONS	
District 14 (Austin) Sites	29
District 15 (San Antonio) Sites	36
District 5 (Lubbock) Sites	41
District 12 (Houston) Sites	47
Roughness Patterns	50
 CHAPTER 4. ANALYSIS OF DYNAMIC WHEEL LOADING	
Surface Dynamics Profilometer	57
DYMOL	58
Data Analysis and Result Presentation	62
Dynamic Loading Index	71
 CHAPTER 5. CONCLUSIONS AND RECOMMENDATIONS	
Conclusions	79
Recommendations	82

APPENDIX	84
REFERENCES	155

CHAPTER 1. INTRODUCTION

Road surface irregularities adjacent to highway bridges have long plagued highway users and highway maintenance agencies. These bumps, dips, and rolls not only create an unpleasant ride when a vehicle passes onto and off the bridge but also, in severe situations, may present a hazardous condition to fast moving traffic. The deterioration of both pavement and bridge structures is accelerated as a result of increased dynamic wheel loading caused by surface irregularities. Moreover, in order to correct these surface faults, costly repair work is often required. Under a heavy traffic flow situation, this maintenance operation may seriously disrupt the normal flow of traffic and thus significantly increase total user costs.

There is no general agreement on the specific longitudinal boundaries of bridge approaches. Many parts of the roadway may contribute to poor riding quality, such as the bridge deck and abutment, pavement structure, subgrade, embankment, and foundation. Though the physical condition of the pavement-bridge interface often provides an indication of the problem, the source of the problem usually lies somewhere else. For instance, the local climate could be a contributing source. In fact, the problem is so complicated that almost all aspects of design, construction, and maintenance are involved. These factors will be examined more closely later.

ROUGHNESS INDICATORS

Pavement distress is an obvious concern of this study. It includes at least three modes: fracture, distortion, and disintegration. A summary of

distress manifestations, with possible distress mechanisms, is shown in Fig 1.1.

One prevalent indicator of an unsatisfactory bridge approach is displacement of the pavement. As depicted in Fig 1.2, this may be either settlement or uplift of the pavement at the abutment or at the pavement end of an approach slab. Also shown in Fig 1.2, although not a frequent cause, is settlement or rotation of the abutment.

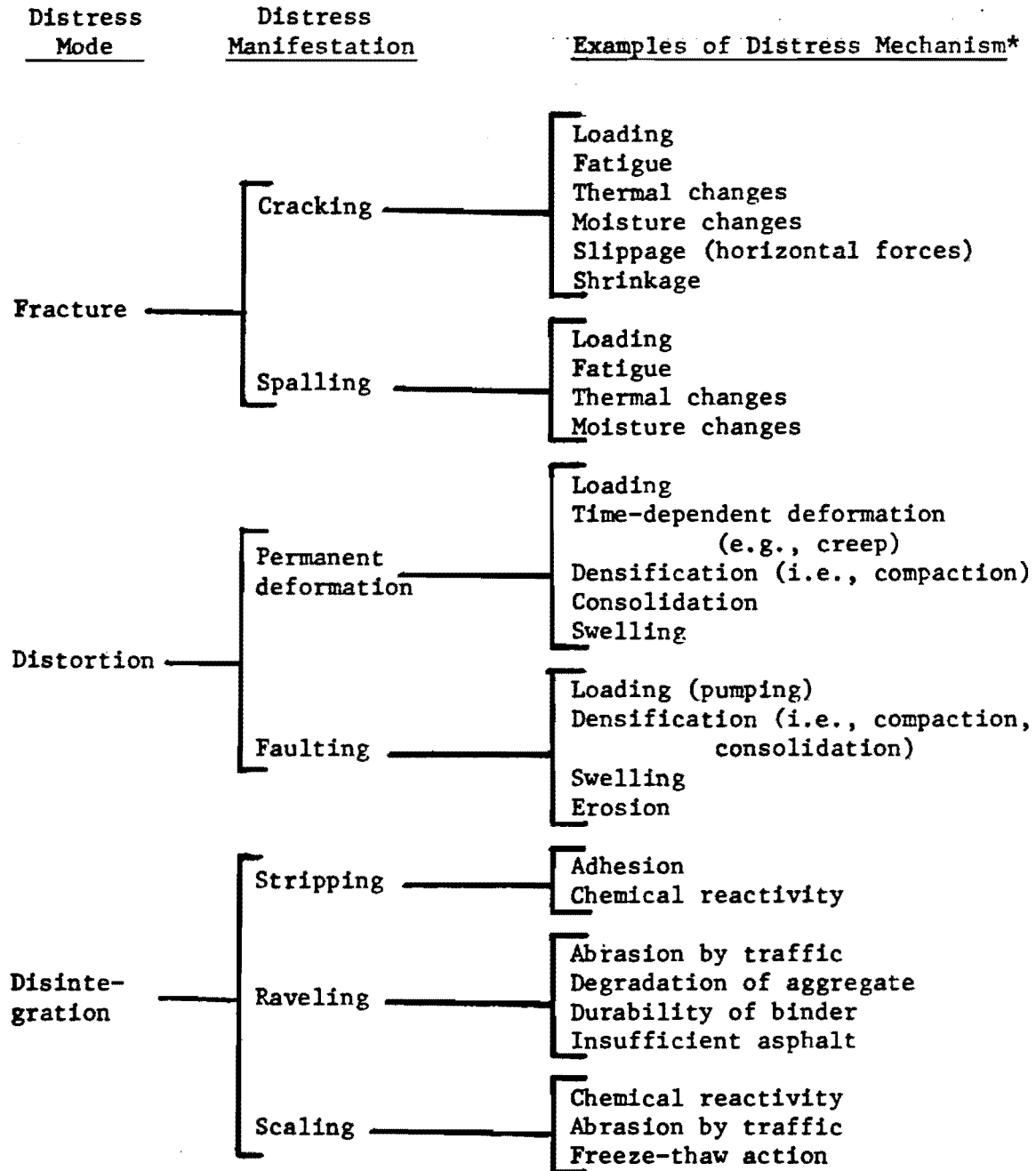
OBJECTIVES

This study is a continuing effort to examine roughness problems at pavement-bridge interfaces in the State of Texas. A number of representative cases in four districts, Austin, San Antonio, Lubbock, and Houston, are selected. The objectives are to locate and characterize the types of roughness, to identify their possible causes, and to suggest possible solutions or treatment techniques.

SCOPE OF THE REPORT

Chapter 2 includes a literature review in which causative factors and common treatments are classified and examined. Results of investigations at a number of selected field test sites are presented in Chapter 3. Data collected through questionnaires and on site studies form the basis of this analysis. Typical roughness patterns are identified and schematically illustrated.

Road surface profile measuring hardware and techniques are presented in the first section of Chapter 4. The second section describes a simulation model, which is used to predict dynamic vehicular tire forces which occur as the result of surface profile irregularities. The measured profiles are compared with rod-and-level elevations, and the applicability of profilometer



* Not intended to be a complete listing of all possible distress mechanisms.

Fig 1.1. Categories of pavement distress (from Ref 1).

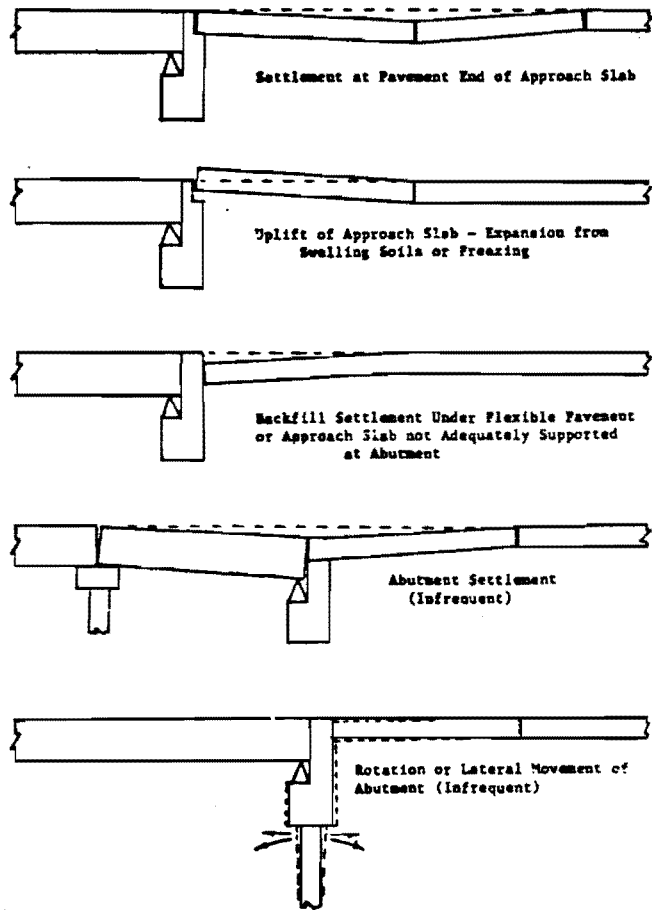


Fig 1.2. Typical bridge approach problems (from Ref 2).

records to dynamic load prediction is analyzed. The vehicle simulation analysis is presented in the subsequent section. Dynamic wheel load diagrams of simulation results are included in the appendix. A dynamic loading index is developed to permit quantitative expression of the potential for creation of dynamic vehicular loading by given surface profiles.

CHAPTER 2. CAUSE EXAMINATION AND TREATMENT STUDY

- A LITERATURE REVIEW

In order to develop necessary understanding of previously completed study efforts, a review of available literature was made. Factors affecting the riding quality of bridge approaches were examined and treatment methods that have been used were studied.

Factors which influence the performance of the pavement bridge interface are very complex and are interrelated with one another. There is no consensus about the causes and effective treatments of the problem. In this study, related factors are assembled into the following six groups:

- (1) traffic
- (2) climate and environment
- (3) materials
- (4) design
- (5) construction, and
- (6) maintenance.

TRAFFIC

Among the important factors to be evaluated for damages by traffic to highway pavements and bridge decks are the effects of vehicle characteristics, traffic volume, and speed of vehicle operation.

Major vehicle characteristics include weight and weight distribution, number of axles, axle arrangement, tire spacings, tire pressures, and elastic suspension system. One means of expressing the effects of vehicle axle weight upon pavement life is through the AASHTO equivalency factors (Ref 3).

These relationships can be utilized to numerically express the relative damage effects of any vehicle axle. The AASHTO equivalency factors indicate that the damage per pass by light passenger car axles is very small as compared with that by those of a heavy truck.

Most investigators agree that the magnitudes of dynamic loads increase with increasing speeds (Refs 4 and 5). Higher speeds increase the excitation of vehicle suspension systems when pavement roughness is present; however, the variation of dynamic wheel forces with speed depends heavily on the type of vehicle and the type of road roughness.

CLIMATE AND ENVIRONMENT

The most important factors under this category are temperature and moisture. Freezing temperatures in the presence of moisture directly induce frost action (Ref 6). In a broader sense, frost action means both frost heave and loss of subgrade support during frost-melt periods. This phenomenon is one severe cause of pavement roughness. Sometimes, structural damage during the spring thaw is so great that heavy loads are prohibited (Ref 7). Economic loss to the public resulting from selective shutdown of roads under such conditions may be very high.

For rigid pavements and bridge decks, temperature variations of the slab may affect the condition of the interface. With a rising temperature, the slab will expand and push against the abutment, causing displacement of the abutment if there are no well-maintained expansion joints and a properly installed anchorage system (Ref 8).

The effect of precipitation on pavement performance has not received the same attention as effect of frost action. However, since the load-bearing capacity of a pavement is determined considerably by the strength of the

subgrade, increases in water content due to rainfall or poor drainage conditions may lead to pavement breadup. Rainfall also provides part of the mechanism by which pumping of rigid pavements and shrinkage and swell of some subgrades may occur (Ref 9).

The presence of a water source near bridge abutments affects the potential for approach roughness. A study made in Kentucky (Ref 10) shows that a bridge over a river is more likely to have rough approaches than a bridge for a grade separation. Embankments near water sources have a tendency to absorb moisture, and the excess moisture often adversely affects material properties.

In general, the extent of damage at a bridge approach due to climate variables depends on the type of pavement, the amount of traffic, and particularly the type of embankment and foundation materials. For those areas with swelling clay or frost-susceptible soil, frequent moisture changes and freeze-thaw cycles will create roughness. Elaborate preventive measures are often warranted for such cases.

MATERIAL

Materials considered here include (1) original foundation soil, (2) embankment fill, (3) abutment backfill, and (4) swelling clay.

Foundation Material

It is believed that the post-construction settlement of foundation material is a common cause of roughness at bridge approaches (Ref 2). Subsurface exploration at the abutment site is utilized to predict the total amount of consolidation that can be anticipated in the embankment foundation and the time required for it to take place under imposed loads. Highly compressible foundation material at the bridge approach can be treated using several common methods as discussed below.

Removal by Excavation. This treatment can be adopted when soft material is reasonably shallow, required borrow is readily available, and embankment stability must be achieved in a relatively short period. Typical sections for various cases of excavation are shown in Fig 2.1. The cost of excavation is very high, and non-uniform post-construction settlement may occur if the undesirable material is not completely removed.

Removal by Displacement. As an alternative to excavation, displacement of soft materials by deliberate overstressing with the weight of the embankment, perhaps combined with a temporary surcharge, is sometimes employed (Ref 12). It is essential for this operation to have sufficient weight to force out the underlying soil, and the mudwave created before the leading fill front should be excavated to a sufficient depth, so that the displacement direction can be controlled and pockets of displaced soil will not be entrapped within the embankment. The method may result in the intrusion of fill into the area outside the boundary of the roadway, requiring more fill and more surcharge, thus adding to the cost of the project. In some cases, removal of the subsoil may be excellent; however, pockets of soft soil sometimes remain to produce differential settlements, which are intolerable for major highways. This method would therefore be more suited for secondary roads with low traffic volume.

Surcharge. This may be the most commonly used method for accelerating the rate of settlement. The embankment fill is placed to a height above the required for final elevation so that more settlement will occur during a given time period (Ref 13). The thicker surcharge will induce more and faster consolidation, but this benefit is partially offset by the high cost of placing the fill and subsequently removing the unneeded portion by the need for berms if the heavier surcharge is used.

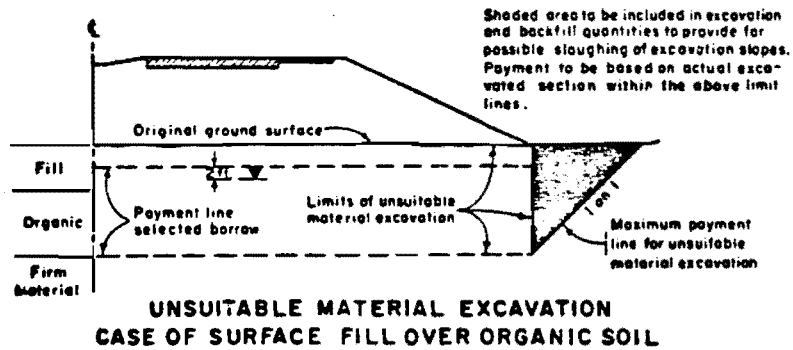
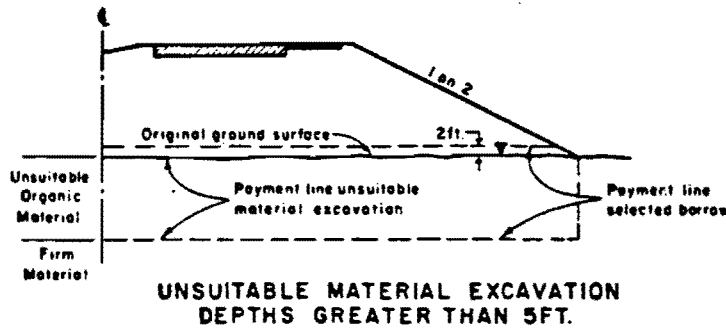
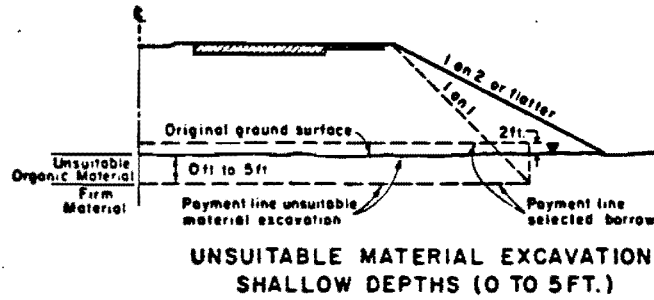


Fig 2.1. Typical sections for excavation of unsuitable material (from Ref 11).

Vertical Sand Drains. Layers of soft soils 10 to 15 feet (3 to 4.5 m) thick can often be stabilized by consolidation under surcharge only. For thick deposits of soft materials, however, stabilization can be attained more economically through installation of vertical sand drains, combined with pre-load fills (see Fig 2.2). Sand drains are pervious sand columns and are usually installed in a grid pattern. A blanket of pervious sand is placed on the tops of the drains to allow the water moving out of the drains to flow laterally from under the embankment. Sand drains can reduce the length of the water drainage path and, thus, the required surcharge thickness, the surcharge time, and the size of the berms, if any. There are many successful field experiences with this design (Ref 14), but the closed-end displacement-type installation may induce too much soil disturbance and reduce soil stability. Hence, nondisplacement types of drains, for which the hollow shaft flight auger is used, are often preferred to displacement types (Ref 15).

Embankment Material

The volume change of a roadway embankment is generally assumed to be less serious than that occurring in foundation material. It should be noted, however, that this assumption is valid only when good materials and good construction procedures are used (Ref 16). Since vertical stress beneath the centerline of the embankment decreases slowly with the depth (see Fig 2.3), high pressure, especially that associated with large fills, may induce severe settlement in the foundation and the embankment itself. Special select materials and increased density for the bridge approach embankment are specified by some agencies to ensure good performance (Ref 2).

Several experiments using lightweight material, instead of common borrow, for the embankment have been reported to be successful (Refs 18-20). Lightweight fill will reduce the embankment weight and the foundation stress

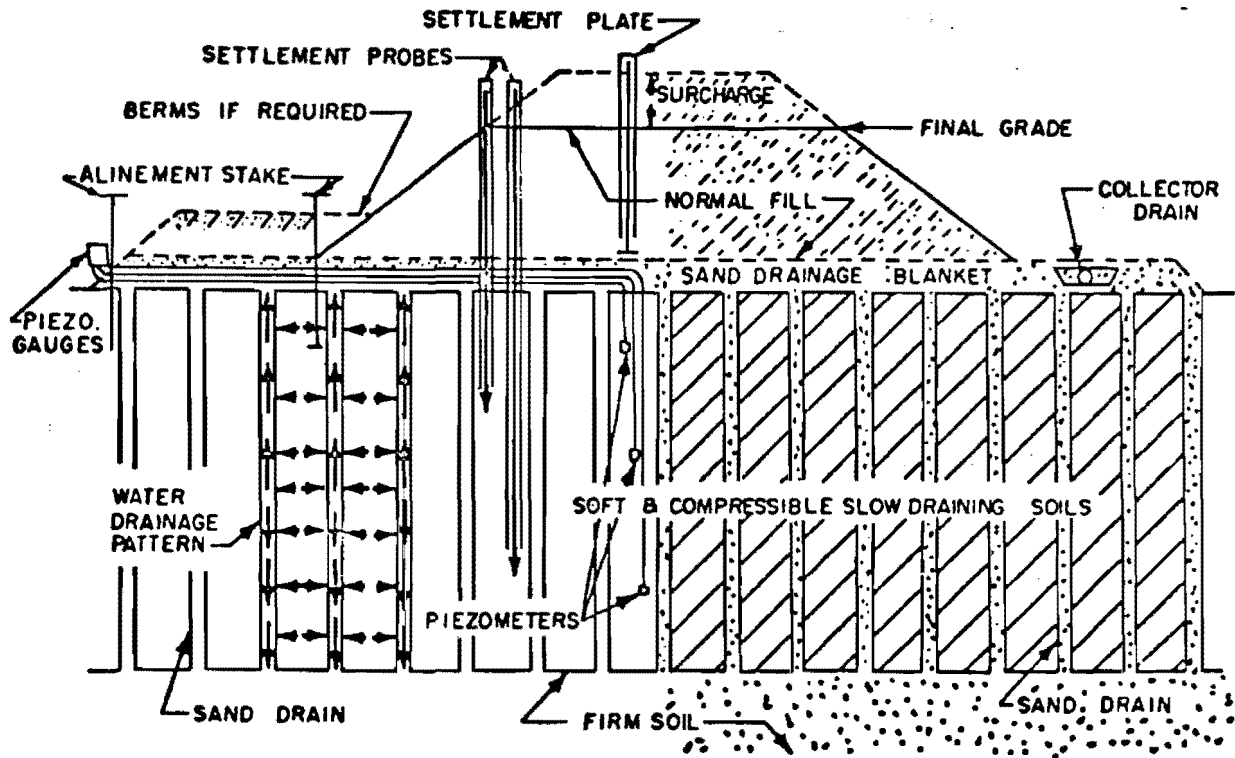
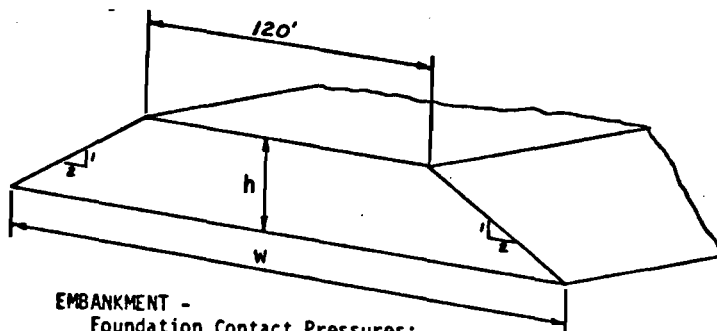
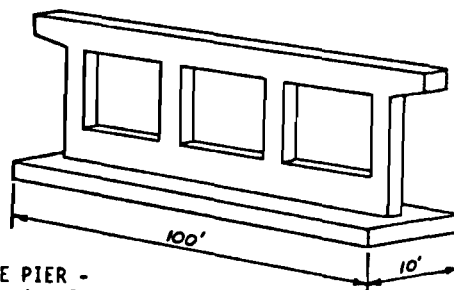


Fig 2.2. Design information for sand drain installation (from Ref 12).



EMBANKMENT -
 Foundation Contact Pressures:
 h = 20', w = 200'; q = 2.5 ksf
 h = 40', w = 280'; q = 5.0 ksf



BRIDGE PIER -
 Footing Contact Pressure
 q = 4 ksf (Total Load = 4000 kips)

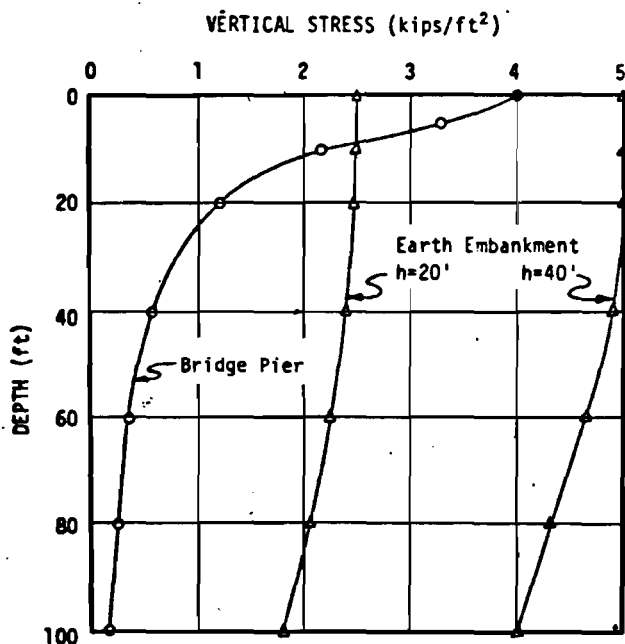


Fig 2.3. Comparison of vertical stresses beneath center lines of bridge pier and earth embankments.

considerably. As a result, the settlement is reduced and the berms are either reduced accordingly or eliminated completely.

So-called lightweight material includes sawdust, sewage ash, and fuel ash. Although costs for such materials are low, their properties differ greatly, and care must be exercised when they are used in the field. In some cases, frost susceptibility and deterioration in air of such materials may cause trouble. Precautionary actions should be taken, such as lime or cement stabilization to reduce frost heave and asphalt sealing to minimize air deterioration.

Abutment Backfill Material

Good condition of the abutment backfill is vital in bridge approach construction. Use of unsuitable backfill material, combined with poor compaction, has been a serious cause of roughness at bridge approaches.

In many instances specially graded granular material, such as sandy gravel, is specified for abutment backfill. It is not practical, however, to specify use of such high-quality material in all locations. The Road Research Laboratory (RRL) in England has experimentally compared the performance of sandy gravel and other materials (Refs 21-25). In the RRL experiments, well-graded sandy gravel was used as the abutment backfill at one side of a bridge, and another material was used at the other side. This arrangement eliminated the complicated variations of environment and traffic, and hence the performances of these two materials could be easily compared. It was found that (1) lightweight pulverized fuel ash, (2) a medium clay, (3) a uniformly-graded fine to medium sand, and (4) a stony-clay fill were very good or quite satisfactory as a substitute for sandy gravel. On the other hand, a silty clay turned out to be unacceptable and therefore should be avoided as abutment backfill.

Swelling Clay

Most highway agencies are concerned with settlement problems at bridge approaches, but those agencies located in areas of expansive clay are also concerned with swell. In these areas, special backfill is used on some occasions as a buffer to protect the bridge abutment and the approach slabs (Ref 2). Other treatments include removal of swelling clay, lime stabilization, and preswelling of the soil before construction through ponding. Plastic sheets and bituminous membranes have also been used to form moisture barriers above expansive clay (Ref 26).

DESIGN

Design factors discussed include (1) type of pavement, (2) type of abutment, (3) type of abutment support, (4) embankment slope stability, and (5) approach slabs.

Type of Pavement

Pavement is usually classified as either rigid or flexible. The major difference between them is the manner in which tire forces are distributed upon the subgrade. The load-carrying capacity of flexible pavements develops from the load distributing characteristics of the layered system. Such pavements consist of a series of layers, generally with an asphalt concrete surface at the top. The thickness design of the pavement is influenced appreciably by the behavior of the subgrade. Rigid pavements, including both JRCP and CRCP, because of their rigidity and high modulus of elasticity, tend to act as rigid plates; thus certain weak spots in the subgrade can be bridged over by the pavement. For this reason, a rigid pavement, at least for a short period of time, may allow better performance at bridge approaches (Ref 10).

Type of Abutment

As pointed out in Chapter 1, the condition of the bridge abutment is sometimes a factor in causing irregular approach surfaces. Such conditions include rotation of abutments on pile groups and settlement of abutments on spread footings.

There are three general types of abutments which are frequently used.

- (a) Closed, or retaining wall, type abutments (Fig 2.4) usually consist of a central pier to support the bridge deck and two wing walls to retain the backfill. This type of abutment is treated as a retaining wall in structural design. One objectionable feature is the inherent difficulty in placing and compacting material against the wall and between wing walls. Vertical alignment of the abutment may be disturbed if heavy equipment is permitted to work near the wall. In addition, placement of the embankment after construction of the abutment may cause excessive foundation settlement. To overcome these problems, backfilling is not started until the first bridge span is in place and as much of the adjacent embankment as is practical is placed before abutment construction.
- (b) Stub, or shelf, type abutments (Fig 2.5) are constructed after the embankment has settled to the final elevation. It can be supported on spread footings, drilled shafts, or piles. Since the difficulty of compaction is eliminated, many engineers believe that this type of abutment provides the best bridge approach performance.
- (c) Spill-through, or open, type abutments (Fig 2.6) consist of two or more vertical columns extending from the natural ground to carry a beam that supports the bridge seat. Proper compaction of the fill around the columns and under the abutment cap is nearly impossible

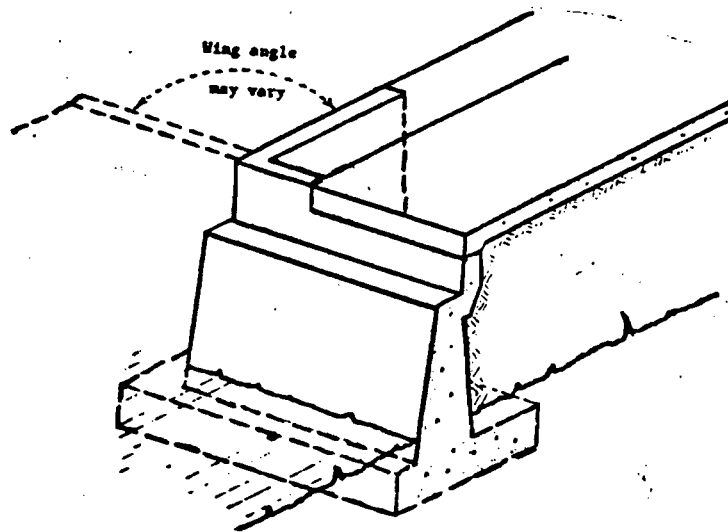


Fig 2.4. Typical closed or retaining wall abutment (from Ref 2).

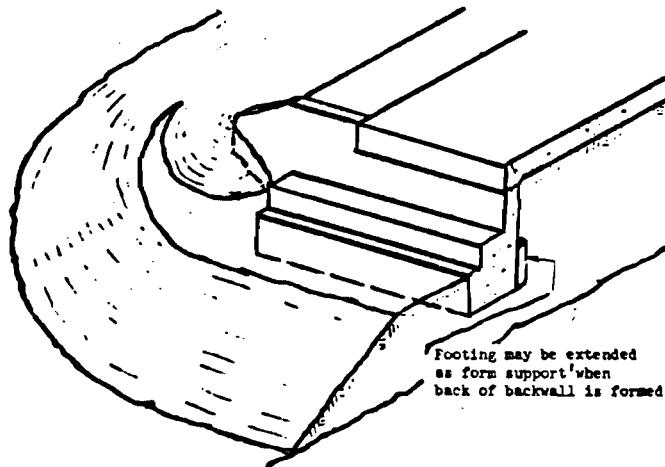


Fig 2.5. Typical stub or shelf abutment (from Ref 2).

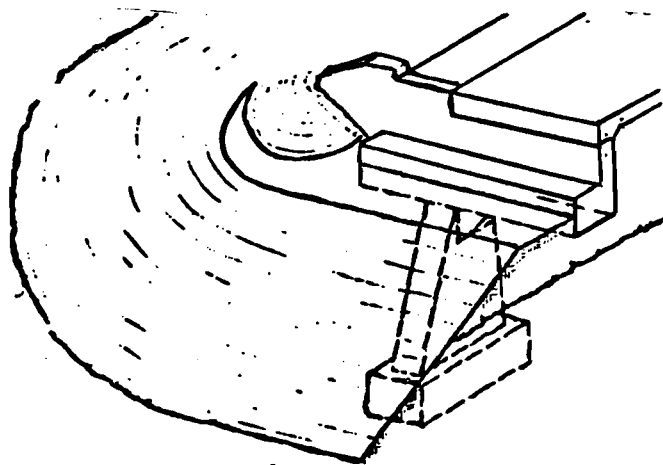


Fig 2.6. Typical spill-through or open abutment (from Ref 2).

to attain. It is believed, therefore, that this type of abutment may be highly susceptible to bridge approach problems.

Type of Abutment Support

Regardless of the abutment type adopted, there are only two principal types of abutment support. These include spread footings (shallow foundation) and piles or drilled shafts (deep foundation).

Abutments on spread footings may have less differential settlement between abutment and approach slab than abutments on deep foundations (Ref 2). The total settlements of abutments on shallow foundations may, however, be intolerably large. Many agencies, therefore, strongly recommend use of deep foundations at all abutments in embankment fills (e.g., Ref 27). Moreover, drainage for abutments on shallow foundations can be very critical. Some special granular material has to be used to offset possible settlement or erosion (Ref 2).

Embankment Slope Stability

Approach embankment slope failure is a serious cause of surface roughness near the interface area. Several methods used to maintain slope stability are summarized here.

Drainage System. Along with paved surface drains, provision for the removal of subsurface water is an essential part of the abutment design. Information concerning area ground water conditions in association with abutment type and backfill materials is utilized to choose among the several alternative drainage schemes shown in Fig 2.7 (Ref 2).

Membrane. Various types of asphaltic membranes are often used to reduce changes in moisture content for sites with highly plastic or expansive soils. Three types commonly referred to as surface, buried, and envelope membranes are shown in Fig 2.8. Envelope type membranes used on the Gulf Freeway in

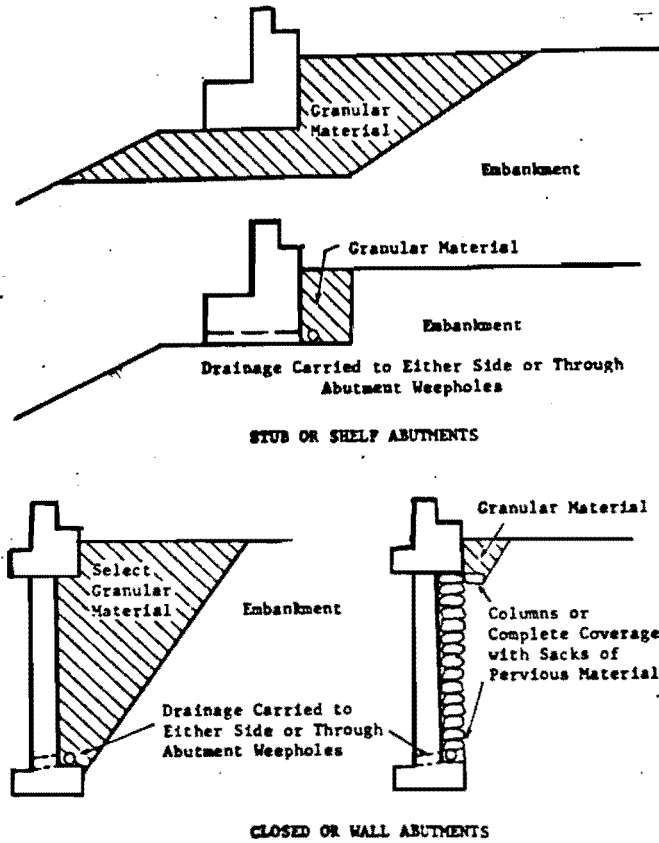


Fig 2.7. Typical methods used to provide abutment drainage (from Ref 2).

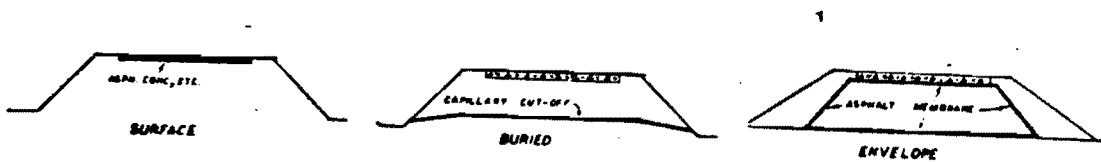


Fig 2.8. Functional types of membranes (from Ref 28).

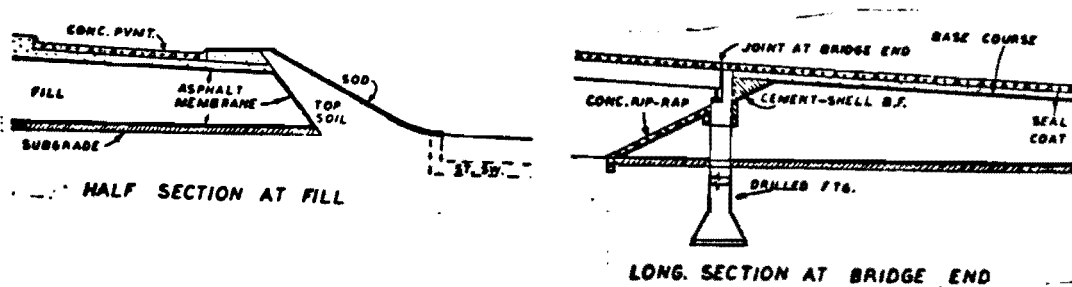


Fig 2.9. Typical embankment sections with envelope-type membranes, Gulf Freeway (from Ref 28).

Houston (see Fig 2.9) provided excellent stabilization of the plastic abutment fills and the strength of the fill did not decrease significantly during a 14-year monitoring period.

Stabilizing Berm. When the weight of the embankment causes shear stresses greater than the shearing strength of the foundation soil, the underlying soil may be displaced laterally. The purpose of a berm placed against the outer embankment slope is to offer some counterweight to resist the overturning moment on the failure arc (see Fig 2.10). It can also be used to correct failures which occur during or after construction.

Benching. Because even small movements of the embankment may create problems at bridge approaches, benching of the natural ground is sometimes employed to provide a stable horizontal foundation with a larger contact plane. A typical section is depicted in Fig 2.11.

Approach Slab

Many agencies consider the use of reinforced portland cement concrete approach slabs to be the most satisfactory means for controlling surface irregularities at bridge approaches. However, in regions of serious swelling clay problems, approach slabs sometimes become so troublesome that they have to be removed.

Approach slabs are designed in a wide range of shapes, lengths, widths, and depths. Some frequently used types are shown in Fig 2.12.

In many cases, the use of approach slabs may shift the bump to the pavement end of the slab (see Fig 1.1). This shifting, in fact, does not solve the roughness problem. Therefore, special joints for use between roadway pavement and approach slabs have been developed to correct the condition.

Figure 2.13 illustrates five examples.

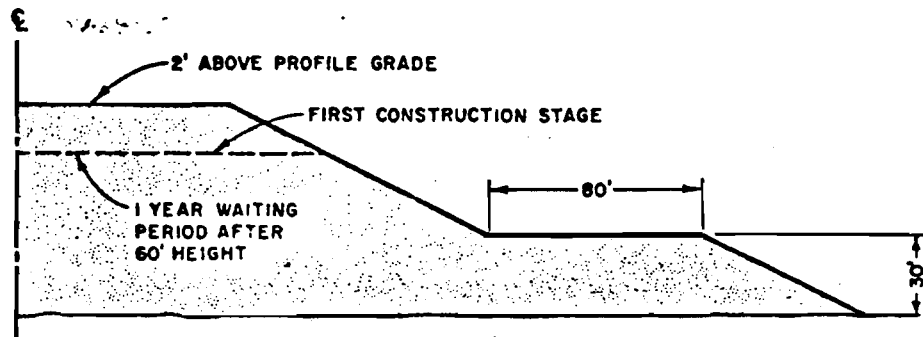


Fig 2.10. Typical half-section of stabilizing berm (from Ref 12).

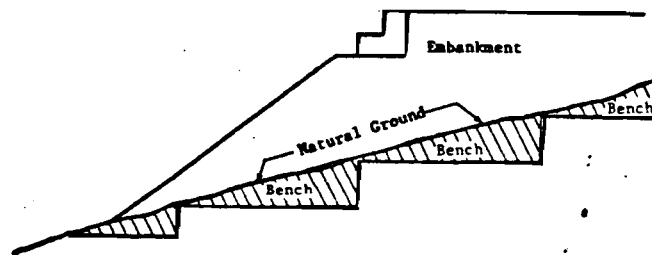


Fig 2.11. Abutment end section with natural ground benched (from Ref 2).

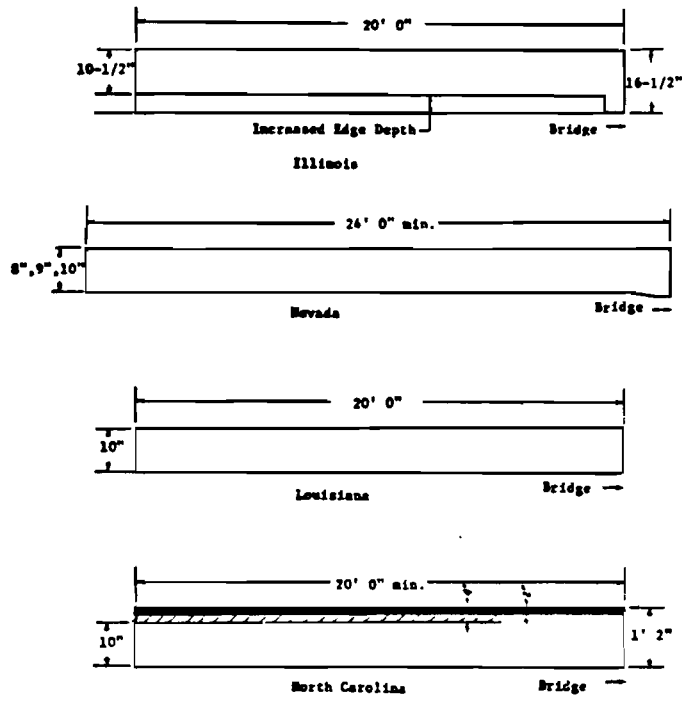


Fig 2.12. Commonly used bridge approach slabs (from Ref 2).

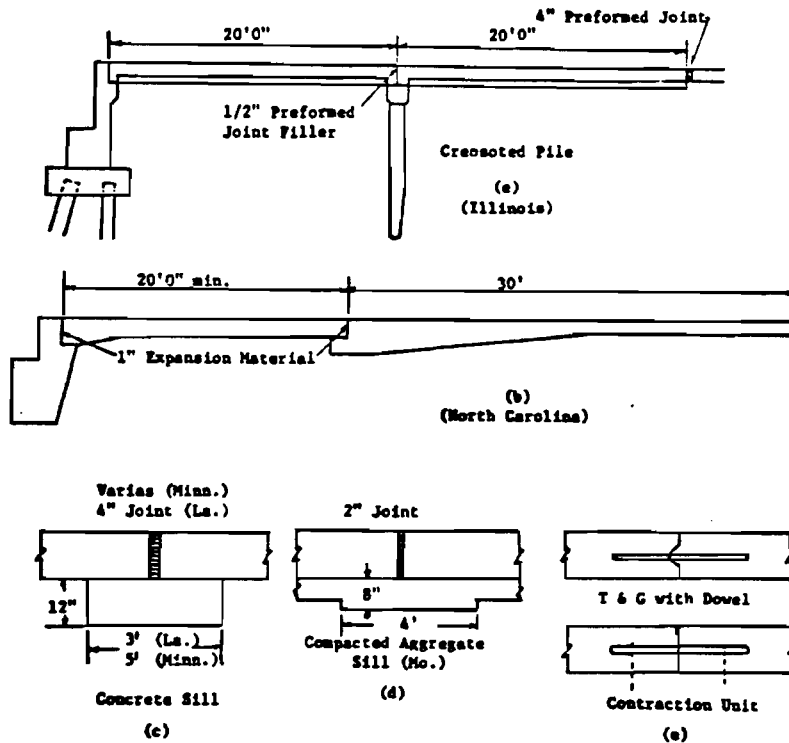


Fig 2.13. Joints used between roadway pavement and approach slabs (from Ref 2).

CONSTRUCTION

Two construction techniques which are sometimes helpful in precluding roughness are discussed here: (1) slow rate construction and (2) compaction.

Slow Rate Construction

This is probably the most economical construction technique because it involves no additional construction material. The only requirement is sufficient time.

Slow rate construction is employed where the foundation soil would undergo shear failure if the embankment were constructed under normal procedures. However, due to its relatively rapid consolidation characteristics, such a soil might become strong enough during a controlled or partially delayed construction period to prevent such a possibility.

In case of slow rate construction, an elapsed time of three to six months between embankment construction and paving operations is common. A waiting time so long that it extends into the next construction season is common for major structures (Ref 2).

Compaction

Improper placement and compaction of material in approach embankments is one primary source of surface roughness. Therefore, stringent specifications and inspection of soil compaction are extremely important. Some state highway agencies require the compactive density be as high as 102 percent of the maximum density specified in the ASSHTO T-99 test (Ref 27). On the whole, most agencies believe that their current specifications for embankment construction are satisfactory (Ref 17). However, as noted earlier, special difficulties may be associated with the abutment backfill. Thus, a special quality control program may be required for this critical area.

MAINTENANCE

Timely and proper maintenance of bridge approaches can smooth the roadway surface, decrease dynamic wheel loads, and reduce the deterioration rate. Depending on the problem and its cause, maintenance may be simple and inexpensive, such as slab jacking or heater planing, or it may entail complete rehabilitation through an overlay (Ref 1). Illustrated in Fig 2.14 are the routine bituminous leveling techniques. Settlement is corrected by adding additional asphalt to the approach pavement; however, when swelling has lifted the approach, additional asphalt is added to the first span of the bridge.

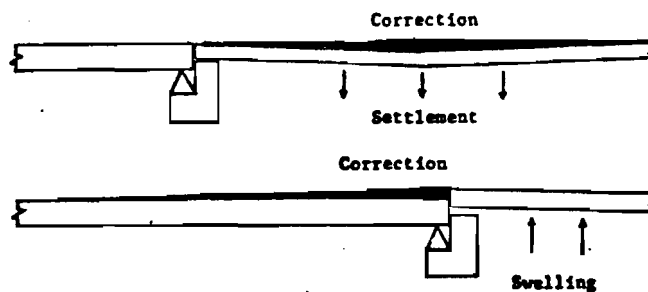


Fig 2.14. Use of bituminous leveling to correct settlement or swelling (From Ref 2).

SUMMARY

The above review indicates that there are many causative factors which can create roughness in the proximity of the bridge-pavement interface. A study sponsored by the Ohio Department of Transportation concluded that the correlation between bridge approach performance and design/construction parameters was very poor and that differential approach settlement had no general correlation with the embankment height (Ref 27). However, it seems appropriate to emphasize four major causes:

- (1) excessive settlement of the embankment and its foundation,
- (2) embankment slope failure over a soft foundation,
- (3) volume change of the expansive clay due to moisture variations,
and
- (4) horizontal movement of a concrete slab due to temperature or moisture variations in the slab.

These four major factors, together with various treatment methods, are summarized in Table 2.1. Remedial treatments should be considered in design and appropriately implemented in construction processes. Heavy trucks may worsen the problem, while maintenance can help alleviate the problem. The environment may have either positive or negative effects on the overall situation.

TABLE 2.1. SUMMARY OF BRIDGE APPROACH PROBLEMS AND TREATMENTS

<u>Treatments</u>	<u>Excessive Settlement</u>	<u>Slope Failure</u>	<u>Swelling Clay</u>	<u>Slab Movement</u>
Drainage	X	X	X	
Membrane	X	X	X	
Berm		X		
Benching		X		
Approach slab	X			
Anchorage system				X
Lightweight fill	X	X		
Lime stabilization	X	X	X	
Good subbase material	X			X
Granular fill	X	X	X	
Removal of bad foundation material	X	X	X	
Surcharge	X	X	X	
Sand drain	X	X	X	
Compaction	X	X	X	
Water ponding			X	

CHAPTER 3. SITE INVESTIGATIONS

In order to characterize surface roughness in the proximity of the pavement-bridge interface site, investigations were conducted in four SDHPT Districts. The conditions of District 14 (Austin), District 15 (San Antonio), District 5 (Lubbock), and District 12 (Houston) were sampled. Engineers in those areas were asked to select about a dozen representative bridge sites in their districts and provide general information by filling out specially developed questionnaires. Personal opinions and experiences with the pavement-bridge interface problems were exchanged through informal discussions between engineers and researchers.

The overall riding quality of each site was evaluated subjectively by SDHPT engineers and was categorized into either "good" or "bad" subgroups. Based on such information, several locations of interest, i.e., those with either typical or special design features or those in quite good or quite bad condition, were chosen in each district for road surface profile measurements. Roughness patterns were identified for further analysis of their potential for inducing dynamic vehicular tire forces.

QUESTIONNAIRE

Based on the literature review of roughness problems at bridge approaches, two questionnaires were designed to obtain data which might enable objective analysis of approach problems. Questionnaire A (Fig 3.1), which was a form listing general information about site conditions and history of bridge and pavement performance, was developed and used in District 14. Initial

BRIDGE "BUMP" CHECK LIST A

Dist. No. _____ Highway _____

Location _____

Inservice Date: _____

Traffic Description: ADT _____
 % Trucks _____

No. of Bents _____ Span Lengths _____

Type of Footing: _____

Bridge Deck Description: _____

Approach Slab: _____

Joint Connection Type: _____

Fill: _____

Height of Fill: _____

Fill or Cut Soil, Description: _____

Soil Borings Available _____

Roadway Pavement Type _____ JRCP/CRCP/FP/Other _____

Maintenance Performed:

Date _____	Description _____
Date _____	Description _____
Date _____	Description _____

Resident Engr. During Construction _____

Comments _____

Maint. Engr./Foreman _____

Comments _____

Fig 3.1. Questionnaire A

experience with this format indicated the need for more detailed information, and Questionnaire B (Fig 3.2) was thus developed for use in Districts 15, 5, and 12. Information on representative bridge sites was hence collected so that both successful and unsuccessful practices could be evaluated.

DISTRICT 14 (AUSTIN) SITES

Table 3.1 summarizes basic information about selected bridges in District 14. All the bridges have asphaltic concrete pavements on the adjacent roadways. Settlement in the fill material on the bridge approaches appeared to be the most prevalent cause of roughness problems. Drilled shafts were commonly adopted to support bridges; spread footings were used only with low fills (e.g., 5 feet). Approach slabs are seldom used in this area because of the difficulties in maintenance, especially where swelling clay is involved. Heavy and light traffic are observed in both subgroups.

The following observations seem to indicate that many problems are related to bridge age, depth of fill, and quality of backfill materials:

- (1) All the problem sites have been in service less than 10 years while all the sites in good condition have been in service for more than 10 years. Two of the four sites in good condition have been under traffic for more than 20 years.
- (2) Four out of five problem sites have fill heights of more than 15 feet (4.5 m) while only one out of four in the good subgroup has a fill above that height.
- (3) Clayey fill material was used for all the problem sites while three out of four sites in good condition were built on rock or certain other stable material. The only site with high PI fill in the good subgroup had very good backfill material. The relatively low fill

BRIDGE "BUMP" CHECKLIST B

Dist. No. _____ Highway _____

Location _____

1. Bridge Approach Condition: ___good ___bad

2. Roadway Pavement Type: ___JRCP ___CRCP ___ACP ___Other _____

3. Bridge:

Function: ___for grade separation ___for crossing major river

___other _____

Type of Footing: _____

Bridge Deck Description: _____

Joint Connection Type: _____

4. Climatic Condition: _____

5. Traffic Description: ADT _____

% Truck _____

Speed Limit _____

6. Abutment Type: ___retaining wall abutment (closed type)

___stub or shelf type

___open column or spill-through type

___other _____

7. Embankment Slope Stability Experience and Treatment

Slide: ___yes ___no Description: _____

Sufficient Drainage: ___yes ___no

Asphaltic Membrane for Stabilization: ___yes ___no

if yes, ___envelope type ___buried type ___surface type

(Continued)

Stabilization Berm: yes no

Benching of Sloping Ground: yes no

Other Treatment: _____

8. Embankment Material:

Fill or Cut Soil, Description: _____

Soil Boring Available: _____

Height of Fill: _____

Swelling Clay: yes no, treatment: _____

9. Backfill Material:

Description: _____

Lime or Cement Stabilization: _____

Other Treatment: _____

10. Foundation Material:

Description: _____

Boring Available: _____

Vertical Sand Drain: yes no

if yes, spacing _____

method of installation _____

Removal of Bad Material: none dredging displacement

Other Treatment: _____

11. Construction History:

Date of Start of Emabnkment Construction: _____

Date of End of Embankment Construction: _____

Waiting Period: _____ Inservice Date: _____

(Continued)

Fig 3.2. Continued

12. Compaction:

Specification Used: _____

Moisture Content Control: _____

Lift Thickness Control: _____

Type of Equipment Used: _____

Dry Density Requirement: _____

Comment: _____

13. Special Design:

Approach Slab: yes no

Other: _____

Comment: _____

14. Maintenance Performed:

Date _____ Description _____

Date _____ Description _____

Date _____ Description _____

Date _____ Description _____

Difficulties Encountered: _____

Comment: _____

Resident Engineer During Construction _____

Comments _____

Maintenance Engineer/Foreman _____

Comments _____

District Contact Man _____

Fig 3.2. Continued

TABLE 3.1. BRIDGE INFORMATION, DISTRICT 14
AUSTIN, TEXAS

Condition	Bad	Bad	Bad
Location	US 290 over MKT RR	Loop 427 over Mustang Creek	US 183S over Loop 343
Pavement Type	ACP	ACP	ACP
Bridge Type	PC	Simple RC	PC
Bridge Function	Grade separation	River crossing	Grade separation
Type of Support	Drilled shafts	Drilled shafts	Drilled shafts
Joint Type	Fix	Fix	Open
ADT (1973)	8,330	--	15,680
Z Truck	6.7	--	17.5
Height of Fill (ft.)	20	10	15
Fill Material	Yellow clay	High PI yellow clay	Yellow clay
Backfill Material	--	Highly plastic material	--
Years in Service (to 1975)	8	3	9
Maintenance Performed	Patching and leveling	Leveling up	Leveling up bridge ends
Approach Slab	Yes	No	No
Note	Premix patch over approach slabs	Lime 6" subgrade	Settlement observed

TABLE 3.1. (Continued)

Condition	Bad	Bad	Bad
Location	US 183S over Boggy Creek	US 290 over Loop 360S	IH 35 over Chandler Creek
Pavement Type	ACP	ACP	ACP
Bridge Type	PC	PC	Simple RC
Bridge Function	River crossing	Grade separation	River crossing
Type of Support	Drilled shafts	Drilled shafts	Spread footings
Joint Type	Fix	Fix	Fix
ADT (1973)	16,010	24,450	19,350
% Truck	16.1	5.3	11.6
Height of Fill (ft.)	24	15	5
Fill Material	Yellow clay	Clay	Rock
Backfill Material	—	—	Granular material
Years in Service (to 1975)	9	6	40
Maintenance Performed	—	Patching bridge ends	Hot mix overlay
Approach Slab	No	No	No
Note	Settlement observed	Settlement observed	

TABLE 3.1. (Continued)

Condition	Good	Good	Good
Location	SH 29 over San Gabriel River	US 290 over MP RR	SH 71 over Bee Creek
Pavement Type	ACP	ACP	ACP
Bridge Type	Continuous I-beam	PC	Simple RC
Bridge Function	River crossing	Grade separation	River crossing
Type of Support	Drilled shafts	Drilled shafts	Drilled shafts & spread footing
Joint Type	Open	Fix	Fix
ADT (1973)	1,390	35,600	2,690
Z Truck	9.0	3.4	6.8
Height of Fill	10	20	8+
Fill Material	High PI material	Stable material	Rock
Backfill Material	Base material	--	--
Years in Service (to 1975)	16	14	28
Maintenance Performed	No patching in last 3 years	--	No patching since 1970
Approach Slab	No	No	No
Note			

and light traffic of that section might also have helped decrease the potential for creating surface irregularities.

DISTRICT 15 (SAN ANTONIO) SITES

Generally speaking, the sites in District 15 exhibit problems which are different from those in District 14. Since the soil containing montmorillonite and illite of high swelling potential is dominant in this district, the roughness problems generally result from large volume changes in the expansive soils, rather than settlements as encountered in District 14.

From informal discussions with engineering personnel and from an on-site inspection of the sites in San Antonio, it was revealed that the joint between adjacent rigid pavements and one bridge approach slab had opened as much as 4 inches (Fig 3.3). The gap enabled water on the pavement surface to penetrate into the fill material and increase the potential for swelling. At another site, pressure of the expansive soil had moved the abutment and caused the rocker supporting the bridge to tilt (Fig 3.4). The curb near this bridge end was also lifted about 3 inches (Fig 3.5). The vertical curvature in the pavement surface can be easily seen by referencing the lane markers and the curb to the guardrail shown in the background.

Engineers in District 15 feel that approach slabs are necessary, but that special designs which keep moisture on the roadway surface from penetrating into the fill material are needed. Finger joints with a lateral drain have been effective at several sites (Fig 3.6) and the expansion joint has been eliminated between the pavement and the approach slab with good results at other locations (Fig 3.7). Granular backfill materials have been used for drainage at some sites.



Fig 3.3. Gap between the approach slab and the pavement,
IH 37 over Fair Ave., San Antonio, Texas.



Fig 3.4. Tilted rocker, Southcross St. over
IH 37, San Antonio, Texas.

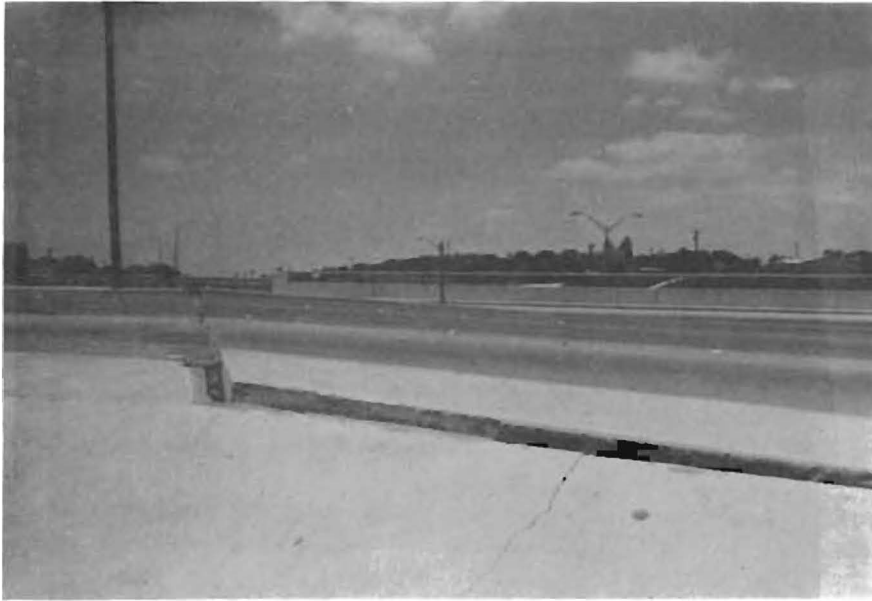


Fig 3.5. Lifted curb, Southcross St. over
IH 37, San Antonio, Texas.

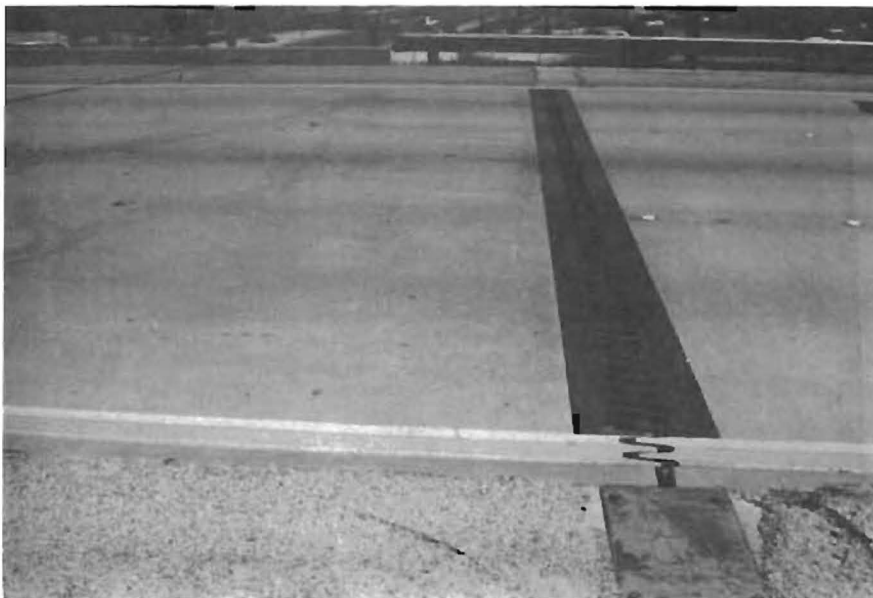


Fig 3.6. Finger joint and drain, IH 10 over W. W. White
Blvd., San Antonio, Texas.

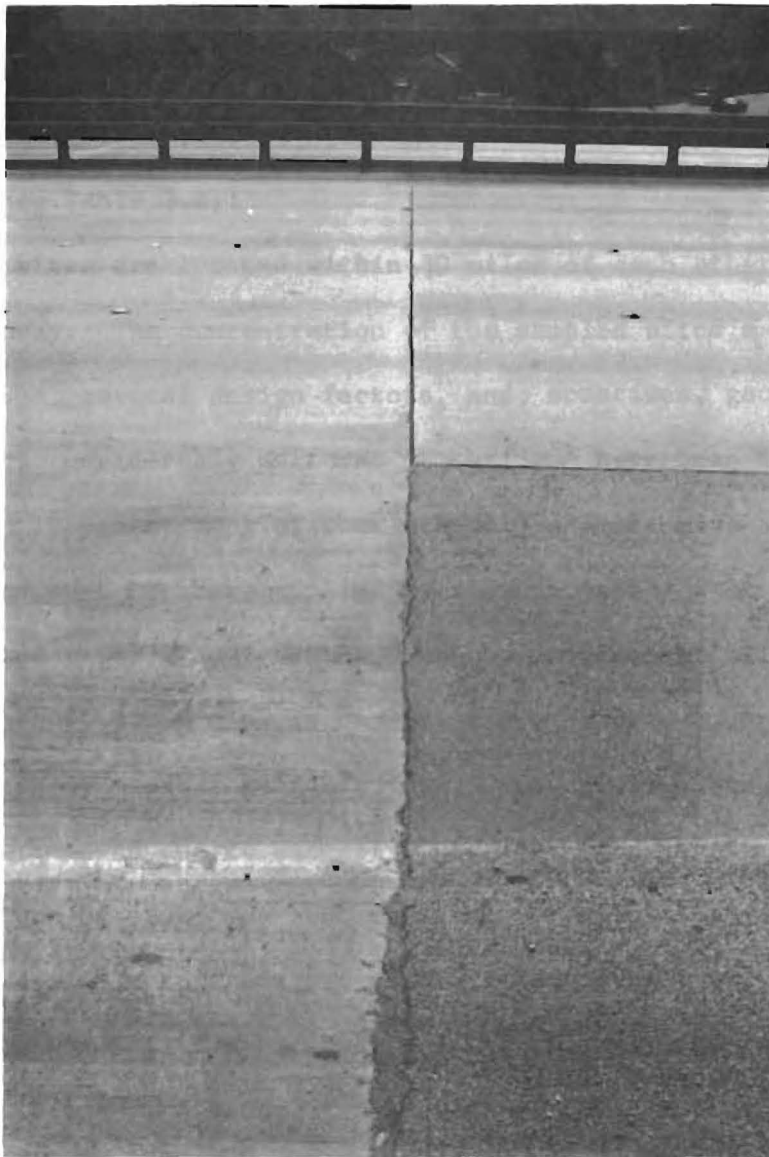


Fig 3.7. Joint deletion between the pavement and the approach slab, IH 37 over Durango St., San Antonio, Texas.

Information about bridge sites in the rural areas of District 15 is summarized in Table 3.2. The sites are all on IH 10 east of San Antonio and have asphaltic concrete pavements on the approach roadways.

The following observations are made based upon on-site visits and collected data (see Table 3.2):

- (1) All sites are located within 30 miles of each other on the same highway. The concentration of the sampled sites makes the traffic volume, several design factors, and, sometimes, geological conditions considerably uniform. No bridges have been in service more than 10 years; most of them are only 4 years old. Little maintenance work has been applied up to this point.
- (2) Washed river gravel was used as the backfill at all locations. Though swelling clay is common, the riprapped embankment slopes generally exhibit good stability. At one site, the approach slabs were removed due to excessive heaving.
- (3) The use of stub-type abutments, deep foundations, approach slabs, and Hyster compactors are common practice in this district. All three sites in the bad subgroup incorporate lime stabilized fill to a depth of 6 inches. The original foundation materials in the bad subgroup are all clays while those in the good classification are sand or sandy clay.

DISTRICT 5 (LUBBOCK) SITES

Information about selected bridge sites in District 5 is summarized in Table 3.3. In this area, four sections were designated as having good ride quality and two as having bad. Some observations can be made as follows:

TABLE 3.2. BRIDGE INFORMATION, DISTRICT 15
SAN ANTONIO, TEXAS

Condition	Bad	Bad	Bad
Location	IH 10E over FM 725	IH 10E over Guadalupe River	IH 10 over Plum Creek
Milepost	604.4	605.1	631.8
Pavement Type	ACP	ACP	ACP
Bridge Type	RC	--	--
Bridge Function	Grade Separation	River Crossing	River Crossing
Type of Support	Drilled shafts with bells	Drilled shafts with bells	--
Joint Type	Open	Open & finger	Open
ADT (1974)	9,000	8,610	6,770
Z Truck	15	15	15
Abutment Type	Stub	Stub	Stub
Embankment Slope Stability	Good Stability	Good Stability	Good Stability
Height of Fill (ft.)	10	13-17	22-28
Fill Material	Clay cliche gravel	Black sandy clay	Gray sandy clay
Backfill Material	Washed river gravel	Washed river gravel	Washed river gravel
Foundation Material	Yellow & gray clay	Blue shaley clay	Blue clay
Swelling Clay	Yes	--	--
Years in Service (to 1976)	9	9	4
Compaction Equipment	Hyster	Hyster	Hyster
Maintenance Performed	None	None	None
Approach Slab	Yes (WBL removed)	Yes	Yes
Note	Lime 6" subgrade	Lime 6" subgrade	Lime 6" subgrade

TABLE 3.2. (Continued)

Condition	Good	Good	Good
Location	IH 10E over Allen Creek	IH 10E over Nash Creek	IH 10W over San Marcos River
Milepost	623.2	619.2	626.9
Pavement Type	ACP	ACP	ACP
Bridge Type	RC	RC	--
Bridge Function	River crossing	River crossing	River crossing
Type of Support	Drilled shafts with bells	Concrete piles	Steel H piles
Joint Type	Open	Open	Open
ADT (1974)	7,750	7,670	6,770
Truck	15	15	15
Abutment Type	Stub	Stub	Stub
Embankment Slope Stability	Good Stability	Good Stability	Good Stability
Height of Fill (ft)	10	15-20	20
Fill Material	Gray sandy clay	Red sandy clay & gravel	Gray sandy clay
Backfill Material	Washed river gravel	Washed river gravel	Washed river gravel
Foundation Material	Blue sandy clay	Gray & brown sand	Brown & gray sandy clay
Swelling Clay	No	No	--
Years in Service (to 1976)	4	4	4
Compaction Equipment	Hyster	Hyster	Hyster
Maintenance Performed	None	None	None
Approach Slab	Yes	Yes	Yes
Note	Line 6" subgrade		

TABLE 3.3. BRIDGE INFORMATION, DISTRICT 5
LUBBOCK, TEXAS

	Spur 326 over AT & SF RR	US 87 at 98th St.	US 84 at Brazos River (Southbound)
Condition	Good	Good	Good
Pavement type	ACP	ACP	ACP
Bridge type	Continuous steel I beam	Simple PC girder	Concrete box girder
Bridge function	Grade separation	Grade separation	River crossing
Type of Support	Drilled shafts	Drilled shafts	Drilled shafts
Bridge deck condition	Linseed oil treatment	Linseed oil treatment	Asphalt overlay
ADT (1977)	8080	9960	1860
% truck	10	10	13
Speed limit (mph)	30	55	55
Abutment type	Stub	Stub	Stub
Embankment slope stability	Good stability	Riprap moved	Good stability
Height of fill (ft)	25	18	—
Swelling clay	No	Yes	No
Backfill material	Sandy loam	Sandy loam	Sandy loam
Years in service (to 1978)	23	8	50
Compaction Equipment	Pneumatic and sheepsfoot	Hyster and pneumatic	No special equipment
Maintenance performed	Hole patching	None	Overlay
Approach slab	Yes	Yes	Yes
Note	New overlay on approach slabs	Approach slabs removed	Old bridge over Brazos

TABLE 3.3. (Continued)

	US 84 at Brazos River (northbound)	FM 1065 at Los Linguish Creek	Loop 289 at US 87 South
Condition	Good	Bad	Bad
Pavement type	ACP	Two-course sur- face treatment	ACP
Bridge type	Concrete slab (pan form)	Concrete slab (simple span)	Concrete slab (arch shape)
Bridge function	River crossing	River crossing	Grade separation
Type of support	Drilled shafts	Concrete piles	Drilled shafts
Bridge deck condition	Asphalt overlay	Rough	Epoxy overlay
ADT (1977)	1860	150	21020
Z truck	13	9.7	10.9
Speed limit (mph)	55	55	55
Abutment type	Stub	Stub	Stub
Embankment slope stability	Good stability	Good stability	Good stability
Height of fill (ft)	—	9	19
Swelling clay	No	Yes	No
Backfill material	Sandy loam	Sandy gravel	Sandy loam
Years in service (to 1978)	20	27	13
Compaction equipment	---	Sheepsfoot and pneumatic	Hyster and pneumatic
Maintenance performed	Overlay	---	Epoxy overlay and asphalt patching
Approach slab	Yes	Yes	Yes
Note	New bridge over Brazos	Approach slabs removed	Epoxy is wearing off

- (1) It is interesting to note that the bridge surface condition has a definite correlation with the subjective ride quality assessment. Pavement surface distress has been corrected to some extent through various types of surface treatment. The decks of good bridges were virtually all treated either by linseed oil or asphalt. One bad bridge had no surface treatment at all, while the other had one epoxy overlay, which was wearing rapidly.
- (2) Average daily traffic counts on the two bad sections were both the highest (21,020) and the lowest (150), indicating that traffic cannot be identified as a critical factor. A similar conclusion can be drawn for bridge function, bridge type, and bridge age. That is, the number of bridges examined in this analysis is too small to imply, for example, that approach surface conditions for bridges at grade separation are less troublesome than for those at river crossings.
- (3) Use of the stub-type abutment, which is believed to be the least likely to cause roughness problems, is common practice in Lubbock. Sandy loam or sandy gravel, with no special stabilization, was generally used as the backfill material for both good and bad subgroups.
- (4) The predominant soil in this area is windblown cover sand. Swelling clay is encountered in some locations but has not been identified as a predominant problem. Approach slabs are commonly used and serve well in general, although in some sections of swelling clay they have been removed because of excessive movement.
- (5) Deep foundations, either piles or drilled shafts, are utilized for all bridges considered. Embankment slopes, protected by

concrete riprap, are quite stable for most cases. Asphalt concrete pavement is used on all sampled roadways with the exception of one farm-to-market road which has a two-course surface treatment.

- (6) The approach performance has no general relationship with height of fill. A 25-foot high embankment falls into the good subgroup, while a bad case has a fill of only 9 feet.
- (7) Lubbock is located in northwestern Texas and has an elevation of above 3000 feet. The average temperature during the winter months is about 40°F. Extended periods of subfreezing temperatures are rare over the whole State of Texas, and therefore, the problem of frost action is not critical.

DISTRICT 12 (HOUSTON) SITES

Basic information about the bridge sites in this district is tabulated in Table 3.4. Due to insufficiency of data, this table is not so detailed as Tables 3.2 and 3.3. Nevertheless, based on the summary table and on-site inspection, overall observations can be made as follows:

TABLE 3.4. BRIDGE INFORMATION, DISTRICT 12
HOUSTON, TEXAS

	IH 610 (S. Loop) at Calais St.	IH 610 (S. Loop) at SH 288	IH 610 (N. Loop) at McCarty Rd.
Condition	Good	Good	Good
Pavement type	CRCP	CRCP	JRCP
Bridge type	Continuous concrete slab	Continuous con- crete slab	Simple PC
Bridge function	Grade separation	Grade separation	Grade separation
Type of support	Drilled shafts	Drilled shafts	Drilled shafts
ADT (1977)	129,180	129,180	73,550
Abutment type	Stub	Stub	Stub
Approach slab	Yes	Yes	Yes
	IH 45 at S. Belt	SH 225 at Shell overpass	SH 225 at Scar- borough Lane
Condition	Bad	Bad	Bad
Pavement type	JPCP	JRCP	JRCP
Bridge type	Simple PC	Simple PC	Simple PC
Bridge function	Grade separation	Grade separation	Grade separation
Type of support	Piles	Piles	Piles
ADT (1977)	81,390	35,810	74,790
Abutment type	Stub	Stub	Stub
Approach slab	Yes	Yes	Yes
	IH 10 at W. Belt	IH 610 (N. Loop) at HB & T RR	
Condition	Bad	Bad	
Pavement type	JRCP	JRCP	
Bridge type	Simple PC	Simple PC	
Bridge function	Grade separation	Grade separation	
Type of support	Piles	Drilled shafts	
ADT (1977)	132,210	73,550	
Abutment type	Stub	Stub	
Approach slab	Yes	Yes	

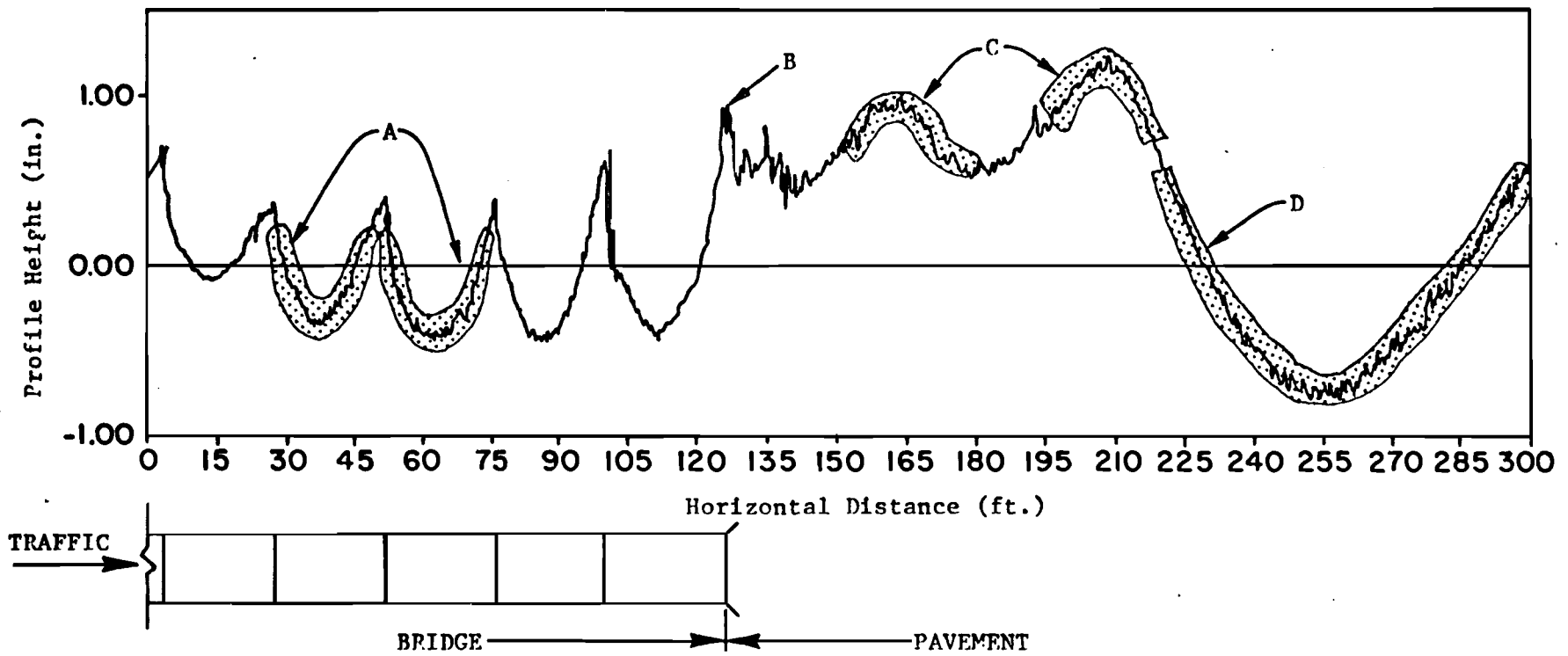
- (1) Eight bridge sites were selected and five of those were categorized as bad. The pavement type is rigid on all sections (either CRCP or JRCP). Data suggest that CRCP provides better riding quality, because the two sections with CRCP are in the "good" classification.
- (2) The use of approach slabs, stub-type abutments, and deep foundations (piles or drilled shafts) is common to all. All bridges under study were constructed for grade separations. The common height of fill ranges from 15 to 20 feet. Traffic is heavy for both subgroups. Since Houston is a port, a higher percentage of trucks (17 percent) is present. The speed limit is 55 mph, and in some sites there is a posted minimum speed of 40 mph.
- (3) The predominant soil in this area is Beaumont clay. Hence foundation and embankment materials are generally not good. High PI fills are sometimes used because only small quantities of sandy material are available and the quality is not remarkably better than the clay.
- (4) The normal annual rainfall here is about 46 inches. A large portion of the rainfall occurs within short periods of time, providing an important source of moisture variations in subsoils. The rather frequent wetting-drying cycle, together with the Beaumont clay, easily induces soil volume changes. This is likely one critical reason why movement of the approach slab was observed in almost every case. Virtually all approach slabs, though designed in different ways, have translated up or down relative to the bridge abutments. Envelope-type asphaltic membranes used with success for stabilization on the Gulf Freeway (Ref 28) were not applied to bridge sites under examination in this study.

- (5) All the bridges were constructed during the 1960s. Modern compaction equipment, such as the sheepsfoot and pneumatic-tired rollers, were extensively employed during construction. Sandy material, stabilized by lime/cement, was used in abutment backfilling. Presumably such procedures would improve bridge approach performance.

ROUGHNESS PATTERNS

The road profile of each section in the four districts was measured using the Surface Dynamics Profilometer. Profile data thus obtained include the whole bridge and extend on both ends about 200 feet from the structure. After examining all the in-hand road profiles, some typical roughness patterns were identified and are schematically illustrated in Figs 3.8 through 3.12. These patterns include the following components:

- (1) roughness on the bridge -
 - (a) camber or sag formed by bridge span (Fig 3.8),
 - (b) opening at the bridge joints (Figs 3.9, 3.12), and
 - (c) discontinuity between the bridge and the pavement/
approach slab (Figs 3.8, 3.10, 3.11, 3.12);
- (2) roughness in the bridge approach area -
 - (a) long wave profile (Fig 3.8),
 - (b) tilted or distorted approach slab (Figs 3.10,
3.11, 3.12),
 - (c) gap between the approach slab and the pavement
(Figs 3.10, 3.11),
 - (d) hump or sag near bridge end (Figs 3.8, 3.9), and
 - (e) gap at pavement joint (Figs 3.10, 3.12).



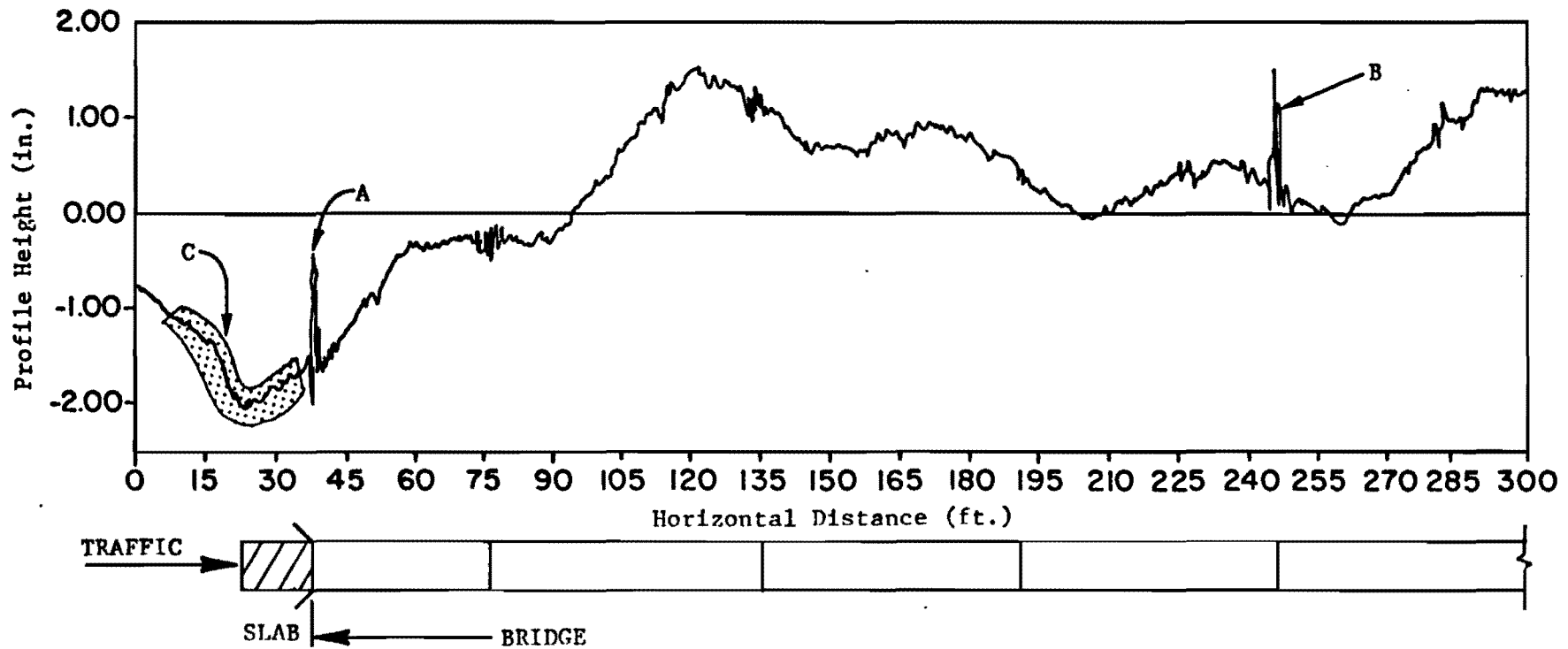
A. Sag formed by each span

B. Discontinuity at bridge-pavement interface

C. Hump near bridge end

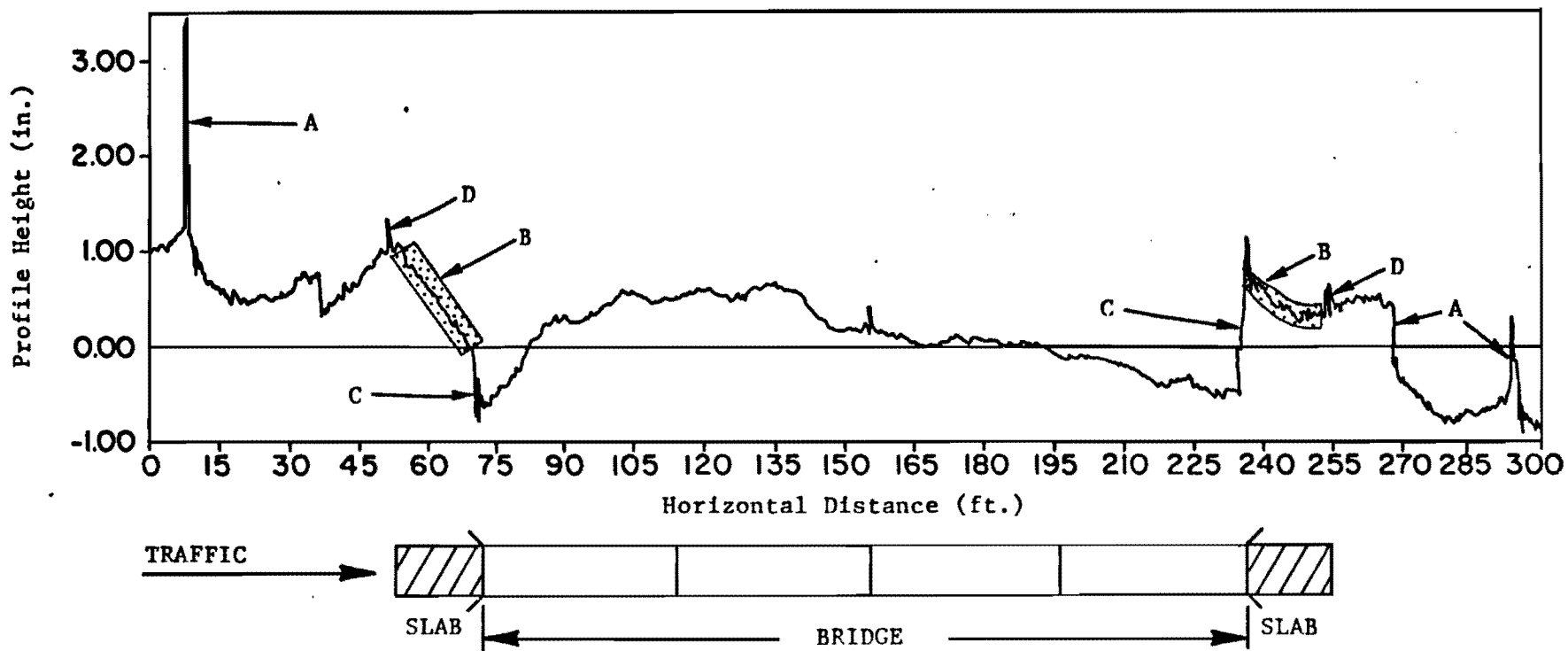
D. Long waves on bridge approach

Fig 3.8. Bridge profile, FM 1065 over Los Linguish Creek (Lubbock), end of bridge.



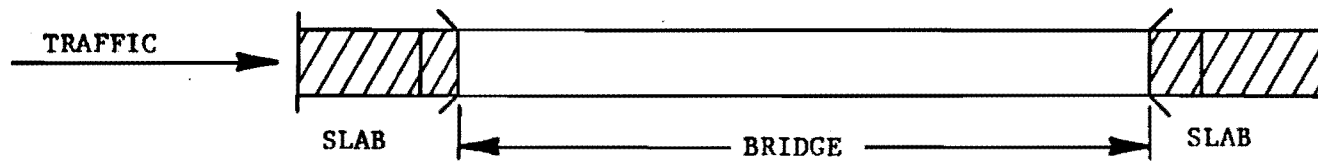
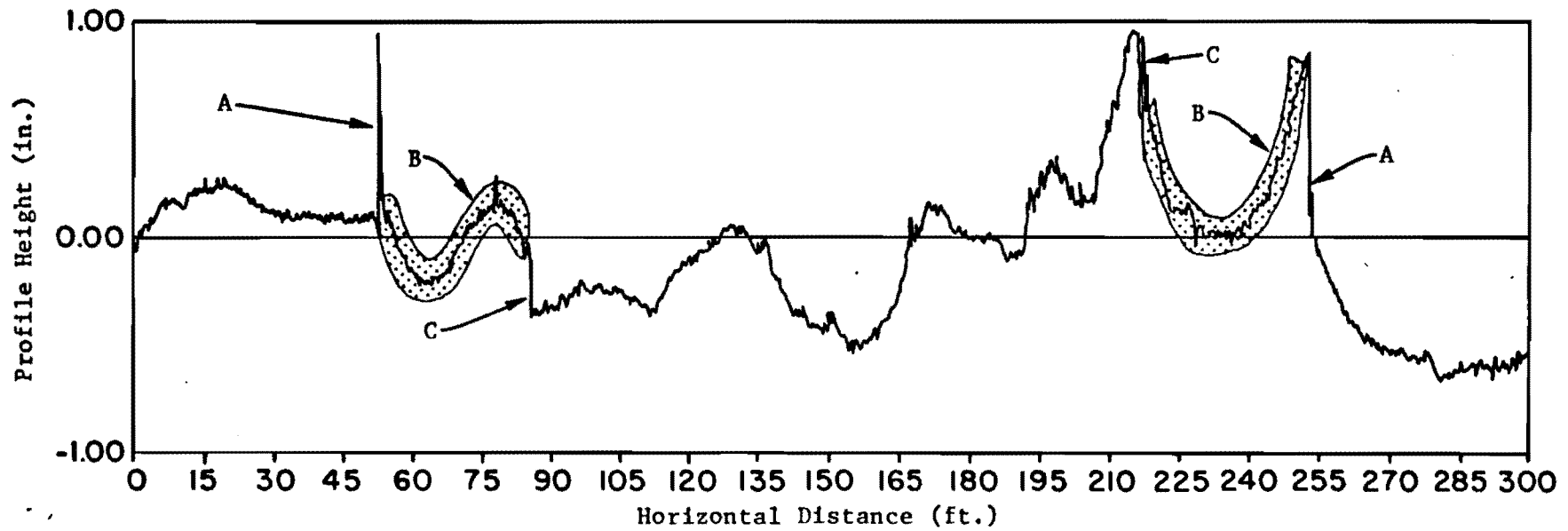
- A. Discontinuity between approach slab and bridge
- B. Open joint between bridge decks
- C. Sag near bridge end

Fig 3.9. Bridge profile, Loop 289 over US 87 South (Lubbock), start of bridge.



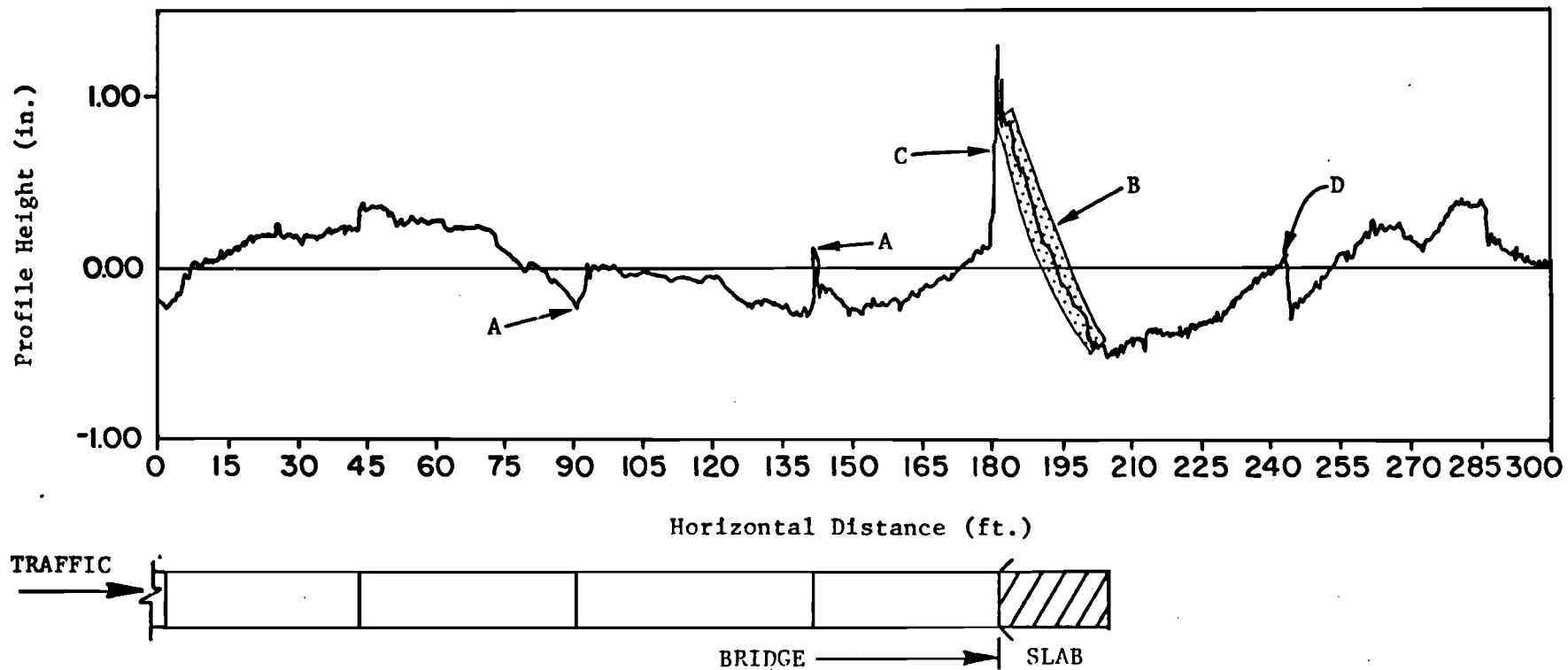
- A. Gap at pavement joint
- B. Tilted or distorted approach slab
- C. Joint between approach slab and bridge
- D. Joint between approach slab and pavement

Fig 3.10. Bridge Profile, SH 225 over Scarborough Lane (Houston).



- A. Discontinuity between approach slab and pavement
- B. Distorted approach slab
- C. Discontinuity between approach slab and bridge

Fig 3.11. Bridge profile, South Loop over Calais Street (Houston).



- A. Opening between bridge decks
- B. Tilted approach slab
- C. Discontinuity between approach slab and bridge
- D. Gap at pavement joint

Fig 3.12. Bridge profile, IH 10 over West Belt (Houston), end of bridge.

The potential for those patterns to produce dynamic vehicular tire forces is assessed in later sections.

CHAPTER 4. ANALYSIS OF DYNAMIC WHEEL LOADING

As noted earlier, roughness in the vicinity of the pavement-bridge interface may lower the riding quality of the roadway and induce excessively large dynamic loads. In this study, the Surface Dynamics Profilometer was the fundamental tool used to measure and record longitudinal road profiles in each wheel path and thus provide the basic data for assessing riding quality. A computer simulation model called DYMOL was used to predict the magnitude of dynamic vehicular tire forces created by specific types of vehicles moving at specified velocities over the defined profile. Critical types of roughness encountered in Austin, Houston, San Antonio, and Lubbock were identified in each section and the interaction of vehicles with these roughness patterns was analysed. However, certain inherent characteristics of the profilometer may distort road profile measurements. Therefore the effect of this distortion was analyzed before using the profilometer measured profile records for DYMOL simulations.

SURFACE DYNAMICS PROFILOMETER

The profilometer (Fig 4.1) is a specially instrumented two-axle van-type vehicle which measures variations in the elevation of each wheel path along the roadway. The profile is detected by two small sensor (feeler) wheels at the center of the test vehicle. The relative vertical movement between the sensor wheel and the vehicle body is measured by a linear potentiometer. An accelerometer, mounted above each potentiometer, senses the vertical acceleration of the vehicle body at these locations. An analog computer in the vehicle immediately double integrates the acceleration to produce vertical displacements. These displacements, combined with the movement

measured by the potentiometers, yield an estimation of the roadway profile in each wheelpath. The results are written onto a 4-track analog tape, and a strip chart depicting the profile is produced. Interested readers are

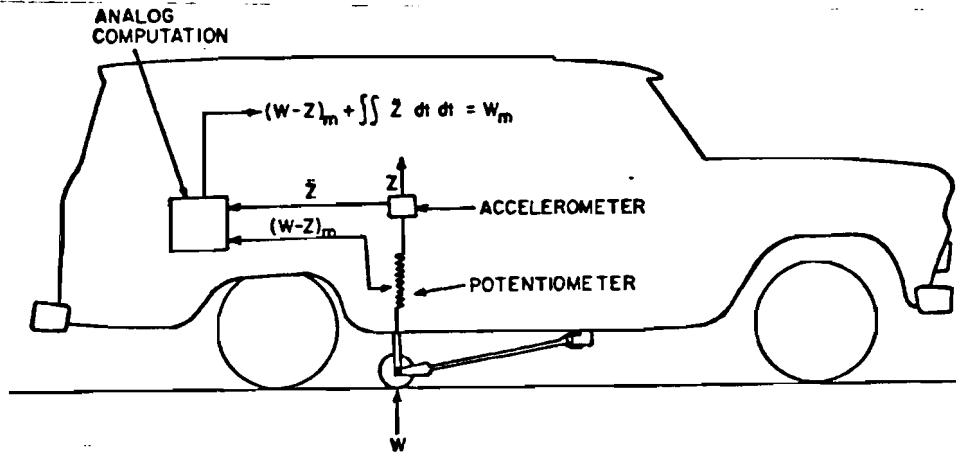


Fig 4.1. Principle of the high speed Surface Dynamics Profilometer (from Ref 9).

referred to the related reports for details and some inherent problems (Ref 29-3]).

DYMOL

DYMOL is a FORTRAN program developed at the Center for Highway Research at The University of Texas at Austin (Ref 32). It simulates the behavior of vehicles interacting with a road profile in each wheel path and can be used to predict the magnitude, duration, and location of the induced dynamic wheel loads.

The DYMOL program can be used to simulate five typical types of vehicles, as shown in Fig 4.2. Specific vehicle configurations, including weights and axle spacings, can be selected by the user. Each vehicle model consists of a series of masses, springs, and dashpots which are connected with one another. In a statistically designed validation program, the simulation model predicted maximum dynamic wheel forces within about ± 10 percent of measured values (Ref 32).



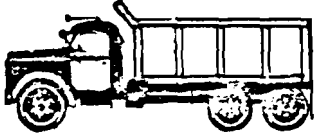


	Class	Designation
	I	2-D
	II	2S-1
	III	3-A
	IV	2S-2
	V	3S-2

Fig 4.2. Five representative types of vehicles (from Ref 32).

In this study, the vehicle was assumed to be initially at rest on a level surface with elevation equal to that of the start of the pavement section under analysis. Vehicles were "driven" at specified velocities over the section profile. Output included listings and plots of dynamic loads applied to the surface by the moving wheels of the modeled vehicle.

Analyses of Profilometer Measurement Capability

The Profilometer-measured road profile data are sometimes distorted due to slight phase shifting characteristics. In order to examine the effect of this distortion, rod-and-level measurements of the roadway surface profile at three bridge sites were made to compare with those measured by the profilometer. These sites were (1) Loop 427 over Mustang Creek, Taylor, (2) IH 10 over Plum Creek, San Antonio, and (3) Test Section No. 8, Austin. Emphasis was placed on the bridge and areas where more intensive readings were made.

The measurements were plotted to scale, and after examining the general trend of the whole section, the grade was corrected to a straight, sloping line. This slope was subtracted from the measured elevations and the results were compared with the profilometer-measured profiles.

Observations and Explanations

Though the rod-and-level measurements and the profilometer measured profile did not agree exactly, it was found that the high-frequency (short wavelength) bumps and dips were represented quite consistently in both profiles. The phenomenon can be explained by the following facts:

- (1) Vertical curves in an actual profile cannot be adequately approximated by a straight line.

- (2) The dynamic response of the profilometer filtering cannot be corrected exactly by a simple slope adjustment technique.
- (3) Most importantly, distortion of the profilometer measurements is more apparent in long wavelength than in short wavelength roughness, due to the inherent characteristics of the instrumentation.

As a result, the profilometer can measure high frequency roughness on the roadway with acceptable accuracy and with great consistency.

Vehicular Response to Long-Wave Profile Roughness

It is understandable that a vehicle will respond differently to road profile waves of the same amplitude but of different wavelength. The dynamic loads produced by a wave 10 feet long and of 1-inch amplitude will be much greater than those loads resulting from a 100-foot wave of the same amplitude. Since the profilometer is able to record short wavelength roughness fairly accurately but distorts the long waves, it is important to investigate the relative effects of different wavelengths on dynamic wheel loads which result from a wheel interacting with a rough road profile. If the effects of the profilometer distortion are not significant, the profilometer records can be used as input to DYMOL, and an adequate analysis of dynamic loading by traffic at the pavement-bridge interface can be made.

Filtering and Phase-Shift Correction

Several techniques for obtaining a corrected profile record that represents the actual roadway section have been used. None of these has yet been wholly successful. However a profile analysis program was utilized to correct the phase shift by moving long waves various distances computed on the basis of the frequency response curve of the profilometer.

Comparison of the Dynamic Loads

The original profilometer profile of a test section and a phase-shift corrected profile are plotted in Fig 4.3. It can be observed that the short wavelength bumps and dips agree while the long waves disagree greatly. For predicting dynamic wheel loads, a simulated two-axle dump truck was "driven" at 55 mph on both the measured and the adjusted profile. In Fig 4.4, the light solid line represents the dynamic loads produced by the measured profile, and the dark dotted line, those produced by the adjusted profile. Most of the time, discrepancies between the predicted dynamic loads from the two profiles are less than 10 percent of the static weight. The maximum discrepancies do not exceed 15 percent of the static weight. Considering that the simulation model was found to predict dynamic wheel forces within about 10 percent in the validation experiments of the DYMOL program, errors of this range are quite acceptable.

It is concluded, therefore, that the errors created by the distorted long waves are within a tolerable range. And the DYMOL program can be a satisfactory tool for predicting dynamic wheel loads that result from profiles containing long-wave roughness even though the profilometer distorts these waves somewhat.

DATA ANALYSIS AND RESULT PRESENTATION

In this study, three representative types of vehicles, a two-axle dump truck (2-D), a three-axle concrete mixer (3-A), and a five-axle tractor trailer (3S-2), were modeled at speeds of 40 and 55 mph. Two general types of dynamic loading oscillations were observed. These include high frequency oscillations, with frequencies from 8 to 12 Hz due to movements of the unsprung mass of the vehicle undercarriage, and low frequency oscillations,

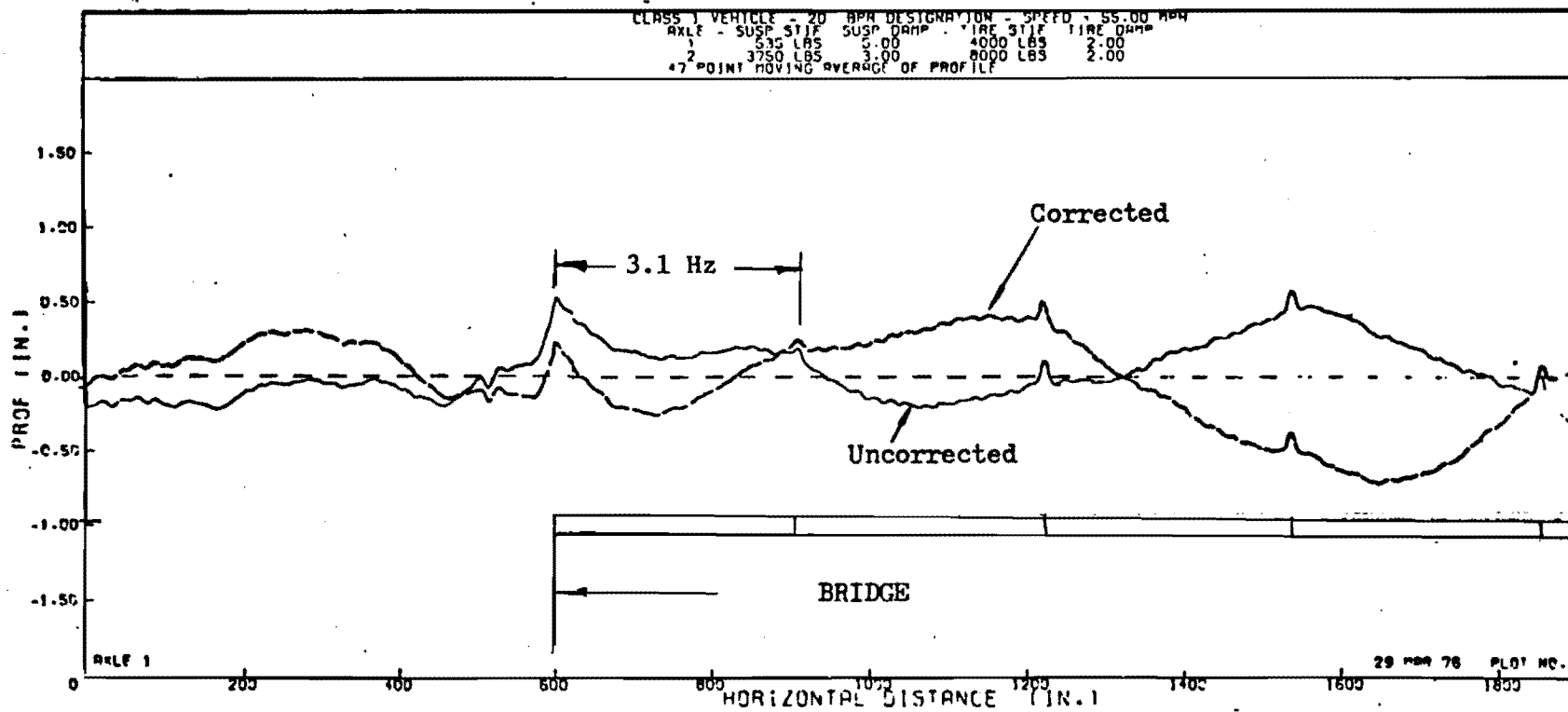


Fig 4.3. Phase-shift corrected and uncorrected profile,
 SH 71 over Bee Creek, SW. of Austin.

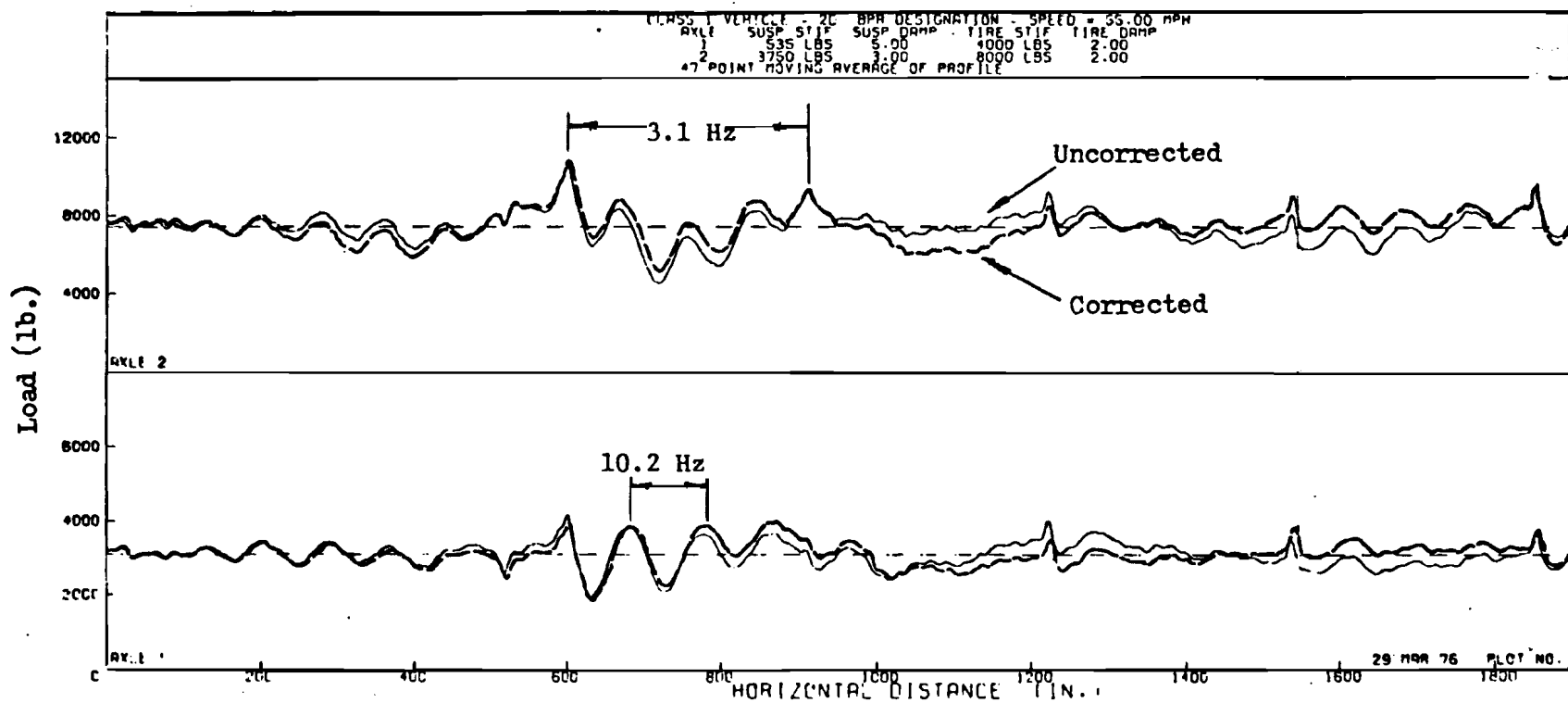


Fig 4.4. Dynamic wheel loads resulting from phase-shift corrected and uncorrected profile, SH 71 over Bee Creek, SW. of Austin.

with frequencies from about 1.5 to 3 Hz associated with movements of the sprung mass of the vehicle. Dynamic wheel loads exercised on the road surface are the combination of these two types of oscillations.

To examine the dynamic wheel loads which result from vehicles traversing the bridge-pavement interface areas, high and low frequency oscillations are treated separately. The amplitudes of the wheel force curves for both frequencies are measured and expressed as percentages of the static weight of the axle considered. A graphical presentation is designed to show the load variations by the thickness of a line. Class limits for categories of wheel force amplitude are set at 0-20, 20-40, 40-60, 60-80, and more than 80 percent of the static weight. If amplitudes of wheel force curves vary less than 20 percent from the static weight, no line is plotted. A line of one-unit thickness is used for 20-40 percent, two-unit for 40-60 percent, three-unit for 60-80 percent, and four-unit for 80 percent or more. The profile of the roadway over which the vehicle travels is attached at the top of the graph. The seriousness of the dynamic loading over each section can be judged by the overall "blackness" of the graph.

Graphical analysis of simulation results is presented in Figs A4.1 through A4.35, in the appendix. Twenty-one bridge sites including three in Austin, four in San Antonio, six in Lubbock, and eight in Houston, are presented. The length of profile for each case is approximately 300 feet. If the bridge is long enough, the start of the bridge and the end of the bridge are shown separately. Otherwise the entire bridge is presented in one figure. As mentioned earlier, the high and low frequency load variations of each section are shown in two graphs, noted as A and B. The types of vehicles are shown on the left. "V" is used to designate velocity in mph,

and "A" indicates the axle number of the simulated vehicle. The location of the peak loading, as directly read from the DYMOL output, is identified with a small triangle, and its magnitude is recorded as a percentage of the static weight on the far right end. The shaded area on each graph represents the range appreciably affected by dynamic vehicular loading. Significance of the shaded area is discussed later.

Table 4.1 provides an overview of roughness patterns and induced dynamic loads for the selected sites. High and low-frequency dynamic loads are again separated. An X indicates the load classification when the dynamic variations of the specified amplitude are induced anywhere in the section. The maximum peak load and the mean peak load for each site are also tabulated as a percentage of the static weight. The standard deviation is calculated by

$$\sigma = \sqrt{\frac{\sum_{i=1}^N (X_i - \bar{X})^2}{N - 1}}$$

where

X_i = the peak load induced by each axle in the section (%),

\bar{X} = the mean peak load of the sampled axles (%), and

N = total number of axles, equal to 20 in this study.

The next two rows give the values of $\mu-1\sigma$ and $\mu-2\sigma$. Assuming the peak loads induced by different axles are normally distributed, these two numbers are the approximate values that 84 percent and 98 percent of the induced peak loads will exceed. For instance, the mean peak load created by the roughness of the section of FM 1065 over Los Linguish Creek (Lubbock), start of bridge (see Fig A4.13), is 203 percent. The standard deviation is 35 percent. With

TABLE 4.1. ROUGHNESS PATTERNS AND DYNAMIC LOADS

Subjective Rating		Bad		Bad		Good		Good		Bad		Bad	
Site (Lubbock)		FM 1065 over Los Linguish Creek, start of bridge		FM 1065 over Los Linguish Creek, end of bridge		Spur 326 over AT & SF RR, start of bridge		Spur 326 over AT & SF RR, end of bridge		Loop 289 over US 87 South, start of bridge		Loop 289 over US 87 South, end of bridge	
Referenced Figure		A4.13		A4.14		A4.15		A4.16		A4.17		A4.18	
Main Roughness Pattern		Sag formed by each span		Sag formed by each span		Open joints with approach slab		Tilted approach slab		Gap: approach slab and bridge		Open joint: bridge decks	
Amplitudes, % of Static Weight	Class	Frequency											
		High	Low	High	Low	High	Low	High	Low	High	Low	High	Low
	0 - 20	X	X	X	X	X	X	X	X	X	X	X	X
	20 - 40	X	X	X	X	X	X	X	X	X	X	X	X
	40 - 60	X	X	X	X	X	X	X	X	X	X	X	X
	60 - 80	X	X	X	X	X	X	X	X	X	X	X	X
80+	X	X	X	X	X	X	X	X	X	X	X	X	
Maximum Peak Load, %		294		312		280		211		214		277	
Mean Peak Load, %		203		210		204		177		187		215	
Standard Deviation, %		35		44		40		19		18		34	
$\mu - 1\sigma$, %		168		166		164		158		169		181	
$\mu - 2\sigma$, %		133		122		124		139		151		147	

TABLE 4.1. CONTINUED

Subjective Rating		Good		Good		Good		Good		Good					
Site (Lubbock)		US 87 South over 98th St.		US 84 over Brazos, old structure, start of bridge		US 84 over Brazos, old structure, end of bridge		US 84 over Brazos, new structure, start of bridge		US 84 over Brazos, new structure, end of bridge					
Referenced Figure		A4.19		A4.20		A4.21		A4.22		A4.23					
Main Roughness Pattern		Long wave profile near bridge end		Opening at bridge joint		Tilted approach slab		Tilted first span		Discontinuity: bridge and approach slab					
		Frequency													
		Class		High		Low		High		Low		High		Low	
Amplitudes, % of Static Weight	0 - 20	X	X	X	X	X	X	X	X	X	X	X	X	X	X
	20 - 40	X	X	X		X	X	X	X	X	X	X	X	X	X
	40 - 60	X	X			X	X								
	60 - 80	X	X			X									
	80+	X	X			X									
Maximum Peak Load, %		264		146		256		172		165					
Mean Peak Load, %		180		132		161		145		145					
Standard Deviation, %		38		8		34		14		11					
$\mu - 1\sigma$, %		142		124		127		131		134					
$\mu - 2\sigma$, %		104		116		93		117		123					

TABLE 4.1. CONTINUED

Subjective Rating		Bad	Bad	Bad	Bad	Bad	Bad	Good					
Site (Houston)		IH 45 over S. Belt, start of bridge	IH 45 over S. Belt, end of bridge	SH 225 Shell overpass, start of bridge	SH 225 Shell overpass, end of bridge	SH 225 over Scarborough Lane	South Loop over Calais St.						
Referenced Figure		A4. 24	A4. 25	A4. 26	A4. 27	A4. 28	A4. 29						
Main Roughness Pattern		Discontinuity: bridge and approach slab	Opening at pavement joint	Tilted approach slab	Long wave on bridge approach	Opening at pavement joint	Discontinuity: approach slab & pavement						
Amplitudes, % of Static Weight	Class	Frequency											
		High	Low	High	Low	High	Low	High	Low	High	Low	High	Low
	0 - 20	X	X	X	X	X	X	X	X	X	X	X	X
	20 - 40	X	X	X	X	X	X	X	X	X	X	X	X
	40 - 60	X	X	X	X	X	X	X	X	X	X	X	X
	60 - 80	X	X	X	X	X	X	X	X	X	X	X	X
80+	X	X	X	X	X	X	X	X	X	X	X	X	
Maximum Peak Load, %		434	358	314	351	449	256						
Mean Peak Load, %		254	233	201	222	310	196						
Standard Deviation, %		91	54	32	42	55	30						
$\mu - 1\sigma$, %		163	179	169	180	255	166						
$\mu - 2\sigma$, %		72	125	137	138	200	136						

TABLE 4.1. CONTINUED

Subjective Rating		Good		Good		Bad		Bad		Bad		Bad					
Site (Houston)		S. Loop over SH 288		N. Loop over McCarty Rd.		IH 10 over W. Belt, start of bridge		IH 10 over W. Belt, end of bridge		N. Loop over RR, start of bridge		N. Loop over RR, end of bridge					
Referenced Figure		A4.30		A4.31		A4.32		A4.33		A4.34		A4.35					
Main Roughness Pattern		Discontinuity: approach slab and pavement		Opening between approach slab and bridge		Opening between approach slab and bridge		Tilted approach slab		Tilted approach slab		Tilted approach slab					
Amplitudes, % of Static Weight	Frequency																
	Class	High		Low		High		Low		High		Low		High		Low	
	0 - 20	X	X	X	X	X	X	X	X	X	X	X	X	X	X	X	
	20 - 40	X	X	X	X	X	X	X	X	X	X	X	X	X	X	X	
	40 - 60	X	X	X	X	X	X	X	X	X	X	X	X	X	X	X	
	60 - 80	X	X	X	X	X	X	X	X	X	X	X	X	X	X	X	
80+	X							X	X	X	X	X	X	X	X		
Maximum Peak Load, %		303		213		203		239		297		301					
Mean Peak Load, %		232		181		165		192		217		180					
Standard Deviation, %		34		18		21		25		39		46					
$\mu - 1\sigma$, %		198		163		144		167		178		134					
$\mu - 2\sigma$, %		164		145		123		142		139		88					

the assumption of a normal distribution, 84 percent of the induced peak loads will be higher than 168 percent of the static axle weight, and 98 percent of those loads will be higher than 133 percent of the static axle weight.

The section of SH 225 over Scarborough Lane (Houston) is another example. The major roughness is due to a large opening at a pavement joint. The induced maximum dynamic peak load for one axle is almost 4.5 times its static weight. The mean peak load is 310 percent and the standard deviation is 55 percent. As a result, 84 percent of the dynamic loads are higher than 2.55 times the static weight and about 98 percent of those loads are twice their static weights.

At this point, it seems worthwhile to emphasize the significance of approach slabs. There are thirty-five sections, presented in Figs A4.1 through A4.35 respectively, and twenty-eight sections have approach slabs. Among those twenty-eight about 80 percent (twenty-two sections) have primary roughness problems related to approach slabs, which are tilted or distorted or have a gap between the approach slab and the bridge/pavement. As noted already, the use of approach slabs is common in San Antonio, Lubbock, and Houston. Great care in choice of design and construction processes may improve performance in the vicinity of the bridge-pavement interface.

DYNAMIC LOADING INDEX

Though Table 4.1 provides useful information, it is not adequate for identifying the most critical types of roughness inducing dynamic loads. For example, the X shows the induced load class, but it does not show where and by how many axles the loads were created. Therefore, in order to better quantify the dynamic loading problem, a dynamic load index was developed. It is the sum of the products of the mean of each load classification and

the number of axles which induce the dynamic load in that classification. The index includes all dynamic loads within the influence range of the roughness under consideration. If, for a total of 20 axles, the roughness creates oscillations with amplitudes less than 20 percent of the static weight, this index is $10\% \times 20 = 2.0$ (10 percent is the mean of that classification). On the other extreme, if all axles are excited and large loading oscillations with amplitudes greater than 80 percent are induced, the index will be $100\% \times 20 = 20.0$, where 100 percent is the assumed mean value of that classification since the upper bound is not set. The index is bounded by these two limits.

The proper choice of the length of influence range is vital for development of the index. The area of most severe roughness itself must be included. It was found, however, that the range must extend beyond the end of the most severe roughness a distance of at least one dynamic load cycle. The cycle length varies with vehicle speeds and loading frequencies. The lowest frequency in each load category was selected for use so that the longest cycle length could be included. When the speed is 40 mph, the rounded cycle length is 8 feet for high-frequency oscillations, and 40 feet for low-frequency oscillations. When the speed is 55 mph, the rounded cycle lengths are 10 and 50 feet for high and low-frequency oscillations respectively. The ranges thus developed are marked on the graphs (Figs A4.1 through A4.35 with light shading.

A combination of several types of roughness, not an isolated discontinuity, normally creates maximum dynamic loading. The section of Scarborough Lane (Houston) exemplifies this statement. A detailed analysis of that site is shown in Fig 3.10. Besides the previously mentioned gap at the pavement joint, there are at least three other types of roughness present.

These include (1) a tilted or distorted approach slab, (2) a discontinuity between the approach slab and the bridge, and (3) a discontinuity between the approach slab and the pavement. The dynamic loads induced by one roughness pattern will often influence the loads by another. Therefore, dynamic wheel loads are, quite often, the composite result of several types of roughness.

Numbers of axles in each load classification for major roughness patterns, with references to analysis figures, and derived dynamic load indices are summarized in Table 4.2. These indices are useful for identifying the potential for creating large magnitude dynamic loads. Small index values indicate little tendency to produce excessive dynamic tire forces. The smaller the indices, the smoother the roadway. It is interesting that these indices may be correlated with subjective ratings and can be therefore useful for indicating a measure of ride quality. For the cases examined in San Antonio, Lubbock, and Houston, an index value of 9.0 is an appropriate division between good and bad riding quality. If one of the indices for a site is greater than 9.0, the overall rating for that site is almost certainly bad. This is true for 16 out of 18 sites in those three districts, with only two exceptions. The site of Spur 326 over the AT & SF Railroad (Lubbock) has an index equal to 13.8 for high-frequency oscillations but is rated as good. Another exception is the site of South Loop (IH 610) over SH 288 (Houston) which is rated as good although the largest index value for that section is 9.5. However, in general, the index seems to be well correlated with subjective ride quality ratings for those three districts. In Austin only three sites (two bad and one good) are considered and all the index values are lower than 9.0. The Austin data is simply too limited in quantity to make significant statements about the correlation between

TABLE 4.2. DYNAMIC WHEEL LOAD INDICES

Subjective Rating	Bad		Bad		Good		Bad		Good		Good		Bad	
Site Location	Mustang Creek (Austin)		Boggy Creek (Austin)		Bee Creek (Austin)		Hackberry St. (S.A.)		Durango St. (S.A.)		W. W. White Blvd. (S.A.)		Plum Creek (S.A.)	
Description of Roughness Patterns	Hump near bridge ends.		Dropoff at bridge end.		Sharp rise at bridge end.		Gap between slab & pvmt.		Distorted approach slab.		Finger joint with drain between pvmt. & slab.		Tilted slab and hump near bridge ends.	
Predicted Dynamic Vehicular Loading														
End of Bridge	Start	End	End	Start	Start	End	Start	End	Start	End	Start	End	Start	End
Referenced Figures	A4.1	A4.2	A4.3	A4.4	A4.5	A4.6	A4.7	A4.8	A4.9	A4.10	A4.11	A4.12	A4.11	A4.12
Dynamic Tire Forces (%) <u>High Frequency Oscillation</u>	Number of Observations													
	0 - 20	8	1	1	2	0	0	15	16	5	6	2	0	
	20 - 40	11	15	12	14	8	10	3	2	14	14	15	14	
	40 - 60	1	3	6	2	8	6	2	0	1	0	2	2	
	60 - 80	0	1	1	1	2	3	0	2	0	0	1	1	
	80+	0	0	0	1	2	1	0	0	0	0	0	3	
Loading Index	4.6	6.8	7.4	7.1	9.8	9.1	3.4	3.6	5.2	4.8	6.4	8.9		
<u>Low Frequency Oscillation</u>	0 - 20	11	7	12	9	1	4	4	4	9	3	0	0	
	20 - 40	9	11	6	9	15	15	13	11	7	12	11	8	
	40 - 60	0	2	2	2	3	1	3	3	4	4	2	6	
	60 - 80	0	0	0	0	1	0	0	2	0	1	4	4	
	80+	0	0	0	0	0	0	0	0	0	0	3	2	
Loading Index	5.0		4.0	4.6	6.8	5.4	5.8	6.6	5.0	6.6	10.1	10.2		

TABLE 4.2. CONTINUED

Subjective Rating	Bad		Good		Bad		Good	Good		Good		
Site Location (Lubbock)	Los Linguish Creek		AT & SF RR		US 87 S		98 th St.	Brazos (old)		Brazos (new)		
Description of Roughness Pattern	Sag formed by each span		Poor joints with approach slab		Gap between approach slab and bridge		Open joint between bridge decks	Long wave profile near bridge end	Opening at bridge joint	Tilted approach slab	Tilted first span	Discontinuity between approach slab and bridge
Predicted Dynamic Vehicular Loading												
End of Bridge	Start (S)	End (N)	Start (S)	End (N)	Start (E)	End (W)	End (N)	Start (NW)	End (SE)	Start (SE)	End (NW)	
Referenced Figure	A4.13	A4.14	A4.15	A4.16	A4.17	A4.18	A4.19	A4.20	A4.21	A4.22	A4.23	
Number of Observations												
Dynamic Tire Forces (Z): High Frequency Oscillation	0 - 20	1	4	0	10	4	0	10	16	8	13	15
	20 - 40	5	10	1	7	5	2	6	4	8	7	5
	40 - 60	8	1	9	1	8	6	0	0	2	0	0
	60 - 80	5	1	5	2	2	5	3	0	0	0	0
	80+	1	4	6	0	1	7	1	0	2	0	0
Loading Index	10.1	8.6	13.8	5.0	8.3	14.1	5.9	2.8	6.2	3.4	3.0	
Dynamic Tire Forces (Z): Low Frequency Oscillation	0 - 20	5	1	10	4	15	20	7	20	11	8	11
	20 - 40	0	8	7	4	5	0	4	0	7	12	9
	40 - 60	5	2	1	5	0	0	3	0	2	0	0
	60 - 80	4	2	2	7	0	0	4	0	0	0	0
	80+	6	7	0	0	0	0	2	0	0	0	0
Loading Index	11.8	11.9	5.0	9.0	3.0	2.0	8.2	2.0	4.2	4.4	3.8	

TABLE 4.2. CONTINUED

Subjective Rating		Bad		Bad		Bad
Site Location (Houston)		S. Belt		Shell Overpass		Scarborough Lane
Description of Roughness Pattern		Discontinuity between bridge and approach slab	Opening at pavement joint	Tilted approach slab	Long wave on bridge approach	Opening at pavement joint
Predicted Dynamic Vehicular Loading						
End of Bridge		Start (NW)	End (SE)	Start (W)	End (E)	Start (W)
Referenced Figure		A4.24	A4.25	A4.26	A4.27	A4.28
		Number of Observations				
Dynamic Tire Forces (Z): <u>High Frequency Oscillation</u>	0 - 20	3	0	2	10	3
	20 - 40	7	6	10	2	0
	40 - 60	3	11	5	5	1
	60 - 80	4	0	1	2	3
	80+	3	3	2	1	13
Loading Index		9.7	10.3	8.4	6.5	15.9
Dynamic Tire Forces (Z): <u>Low Frequency Oscillation</u>	0 - 20	8	5	3	5	6
	20 - 40	2	8	4	1	4
	40 - 60	2	3	10	2	5
	60 - 80	5	3	3	5	2
	80+	3	1	0	7	3
Loading Index		8.9	7.5	8.6	12.3	8.7

TABLE 4.2. CONTINUED

Subjective Rating		Good	Good	Good	Bad		Bad
Site Location (Houston)		Calais St.	SH 288	McCarty Rd.	W. Belt		R.R.
Description of Roughness Pattern		Discontinuity between approach and pvt.	Discontinuity between approach slab and pvt.	Opening between approach slab and bridge	Opening between approach slab and bridge	Tilted approach slab	Tilted approach slab
Predicted Dynamic Vehicular Loading							
End of Bridge		End (W)	Start (W)	End (SE)	Start (E)	End (W)	Start (NW) End (SE)
Referenced Figure		A 4. 29	A 4. 30	A 4. 31	A4. 32	A4. 33	A4.34 A4.35
		Number of Observations					
Dynamic Tire Forces (%): <u>High</u> Frequency <u>Oscilla- tion</u>	0 - 20	3	0	2	0	0	3 15
	20 - 40	8	11	9	12	6	10 3
	40 - 60	5	5	7	7	9	6 0
	60 - 80	1	1	2	1	3	1 0
	80+	3	3	0	0	2	0 2
Loading Index		8.9	9.5	7.8	7.8	10.4	7.0 4.4
Dynamic Tire Forces (%): <u>Low</u> Frequency <u>Oscilla- tion</u>	0 - 20	4	4	9	6	4	4 4
	20 - 40	8	10	9	9	6	4 10
	40 - 60	4	3	2	5	8	6 3
	60 - 80	4	3	0	0	2	4 2
	80+	0	0	0	0	0	2 1
Loading Index		7.6	7.0	4.6	5.8	7.6	9.4 7.3

ride quality and loading index.

CHAPTER 5. CONCLUSIONS AND RECOMMENDATIONS

In this study, roughness problems in the vicinity of the bridge-pavement interface are examined. Information on representative bridge sites in the Austin, San Antonio, Lubbock, and Houston districts of the State Department of Highways and Public Transportation was obtained through a special survey questionnaire. With the aid of on-site inspections, twenty-one locations were selected for road surface profile measurements. A vehicle computer simulation program was used to analyze the interaction of vehicles with roadway profiles. The following conclusions and recommendations are based upon study and analysis of these data.

CONCLUSIONS

- (1) Based upon observations of this study, the magnitude of traffic volume cannot be identified as a causative factor of surface roughness at bridge approaches. Since the temperature in Texas is neither extremely cold nor extremely hot, frost action and slab movement due to temperature variations are not serious. No significant correlation was consistently found between the performance of bridge approaches with bridge function, bridge type, bridge age, or the height of embankment fill.
- (2) While flexible pavement is dominant in Austin, San Antonio, and Lubbock, rigid pavement is primarily used in the Houston area. No obvious superiority of one type over another was found. However, compared with JRCP, CRCP provides better performance.

- (3) Stub-type abutments, generally recognized as most desirable, were utilized at all sites investigated. Deep foundations are used almost exclusively as supports for bridges and appear to be very effective in minimizing total settlement. No special treatments for slope stability have been applied; that is, membranes, berms, or benching has not been utilized. There are no special treatments for soft foundations. Though light-weight material offers promise for use in fills, no such material is used in these four districts.
- (4) The type of material utilized in the approach roadway structure is related to the pavement-bridge interface roughness problem. Highway compressible clayey material was used as embankment fill for all problem sites in District 14. Expansive soil appeared to be the major cause of roughness in District 15. Heavy rainfall in conjunction with expansive Beaumont clay induced severe surface irregularities in Houston. No similar cause can be identified for the Lubbock area. However, based on those sites studied, Lubbock seems to have a less serious situation than the others.
- (5) Penetration of water through pavement joints or cracks, especially when expansive soils are involved, may become a major creator of roughness. Elimination of expansion joints and use of finger joints with transverse drains has been effective measures for reduction of the water intrusion problem.
- (6) Timely maintenance and slow rate construction techniques certainly offer promise for reduction of surface irregularities. Modern compaction equipment, which has been extensively used since the 1960s, also offers promise for problem minimization. Stringent

specifications and inspections of soil compaction are essential to obtaining satisfactory bridge approaches.

- (7) Roughness at bridge approaches can occur either on the bridge or on the roadway. A number of typical roughness patterns have been identified. Except in Austin, the use of approach slabs as the transition between the bridge and the pavement is a common practice. However, for those sections having approach slabs, about 80 percent of the identified roughness problems are related to the existence of approach slabs. In San Antonio and Lubbock, approach slabs have been removed in some locations, and the road profile has remained relatively smooth following this modification.
- (8) The Surface Dynamics Profilometer provides a safe, convenient means of obtaining the road profile information that is needed for locating and identifying critical patterns of roughness at the pavement-bridge interface. Rod-and-level measurements at three sites in Texas have revealed that short wavelength roughness is represented adequately by the Surface Dynamics Profilometer but that long waves in the profile are somewhat distorted. Dynamic wheel loads can, however, be predicted satisfactorily by simulation from the profilometer records since vehicular response to long-wave roughness is relatively insignificant.
- (9) The DYMOL vehicle simulation program is a power tool for prediction of the relative effect of roughness in creating dynamic wheel loads. The analysis process developed for DYMOL output seems to be acceptable. The derivation of a dynamic load index is useful for quantitative evaluation of roughness conditions. The index is also useful for prediction of riding quality.

- (10) The most serious case encountered in this study is SH 225 over Scarborough Lane (Houston). The primary roughness pattern, consisting of a wide gap at the pavement joint, induced peak dynamic axle loads of 4.5 times static weight. If a normal distribution is assumed for dynamic loading, about 98 percent of the dynamic axle loads will be twice their static weights. The importance of joint sealing or repair cannot be overlooked.

RECOMMENDATIONS

- (1) To avoid or alleviate interface roughness problems, generally recognized good design and construction practices offer the most promise. Stub-type abutments, deep foundations for bridges, adequate investigations of the foundation site, appropriate specifications and inspections of soil compaction, and sometimes a slow-rate construction schedule should be considered. Benching the natural ground to support the approach embankment is also recommended.
- (2) High-volume-change materials should be used with caution in embankment construction, and special attention should be given to the drainage system. On the one hand, the surface water should be prevented as much as possible from penetrating into the underlying layers. On the other hand, water having intruded into the soil should be removed quickly and completely. Select granular-type material, probably with additives for stabilization, is always desirable as the abutment backfill.

- (3) Though in many cases bridge approach roughness is associated with approach slabs, the banning of approach slab use is not considered to be proper. The decision to use the specially designed reinforced approach slabs should be based on traffic volume, soil condition, construction cost, and an estimate of the possible problems if they are not used. It is impractical, however, to specify any particular design for approach slabs as being better than any other; local past experience will provide valuable guidance.
- (4) When undesirable surface roughness adjacent to the bridge-pavement interface does occur, maintenance should be performed immediately. Scheduled preventive maintenance may prove to be a more effective and economical solution. Points of major concern include pavement joints, bridge joints, and the joints between the approach slab and the bridge-pavement.
- (5) Even though the effect of a distorted profile from the Surface Dynamics Profilometer is not critical in the simulation analysis made by DYMOL, a good representation of the real profile is highly desirable. More study should be devoted to defining the capability of the Surface Dynamics Profilometer to measure long-wave roughness.
- (6) Extensive soil exploration, along with detailed and accurate information on the design, construction, and maintenance history of the bridge site, is essential for determining the extent and the specific causes of one particular interface roughness. Analyses of this depth are beyond the scope of this study. Further in-depth research efforts are surely warranted in the investigation of roughness problems in the proximity of the bridge-pavement interface.

APPENDIX

Dynamic Wheel Load Diagrams

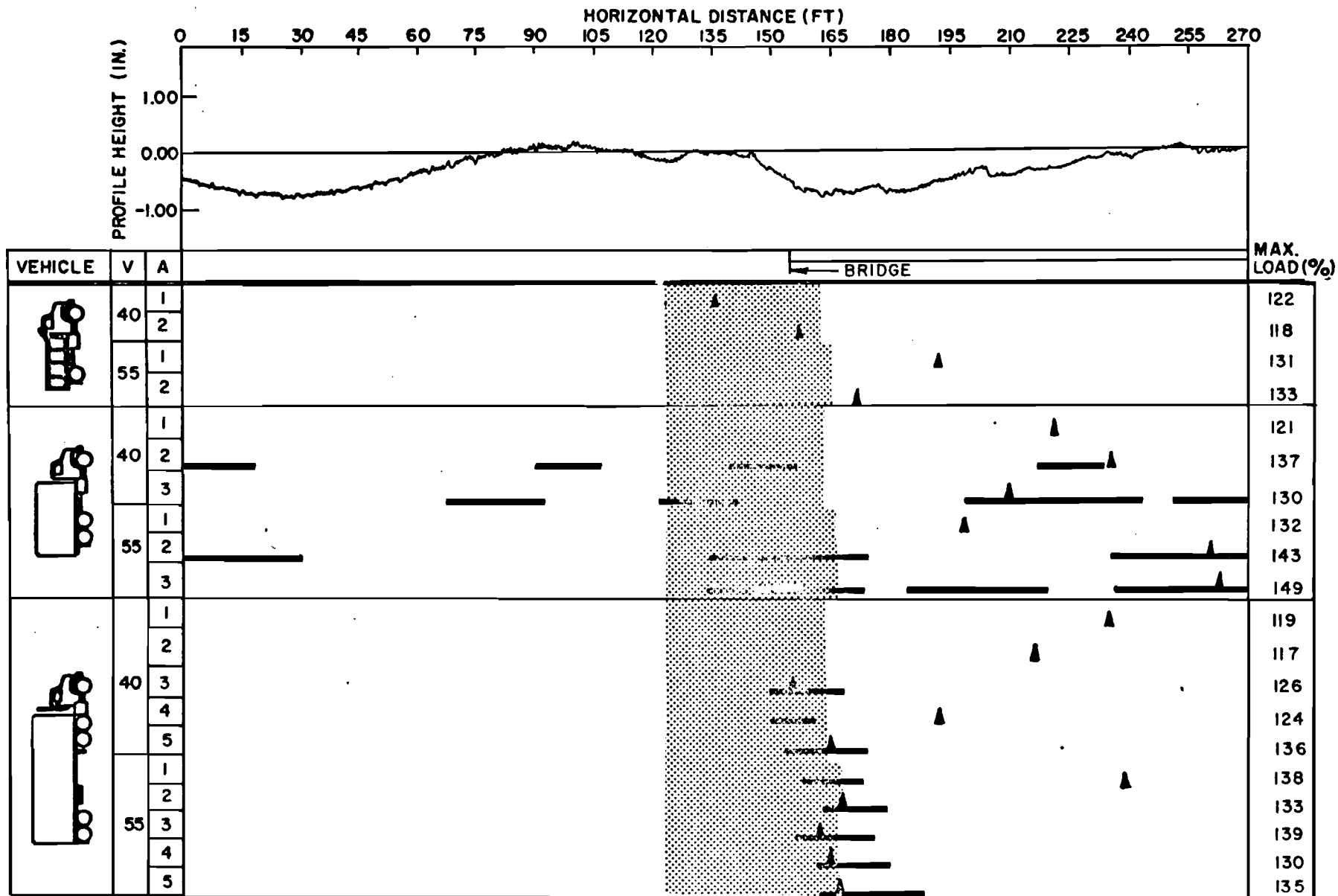


Fig A4.1A. Dynamic wheel load diagram, high frequency oscillation, Loop 427 over Mustang Creek (Austin), start of bridge.

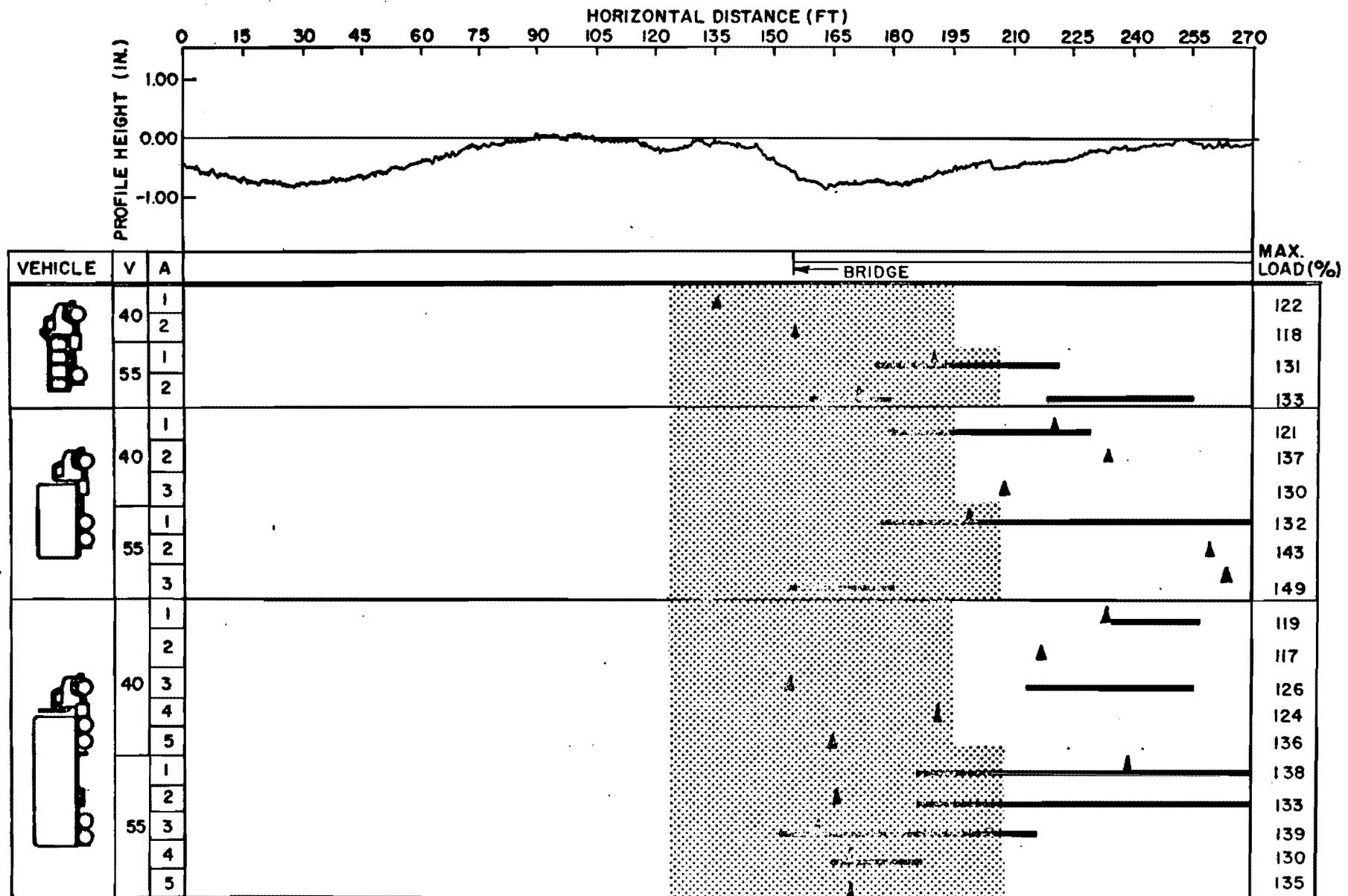


Fig A4.1B. Dynamic wheel load diagram, low frequency oscillation, Loop 427 over Mustang Creek (Austin), start of bridge.

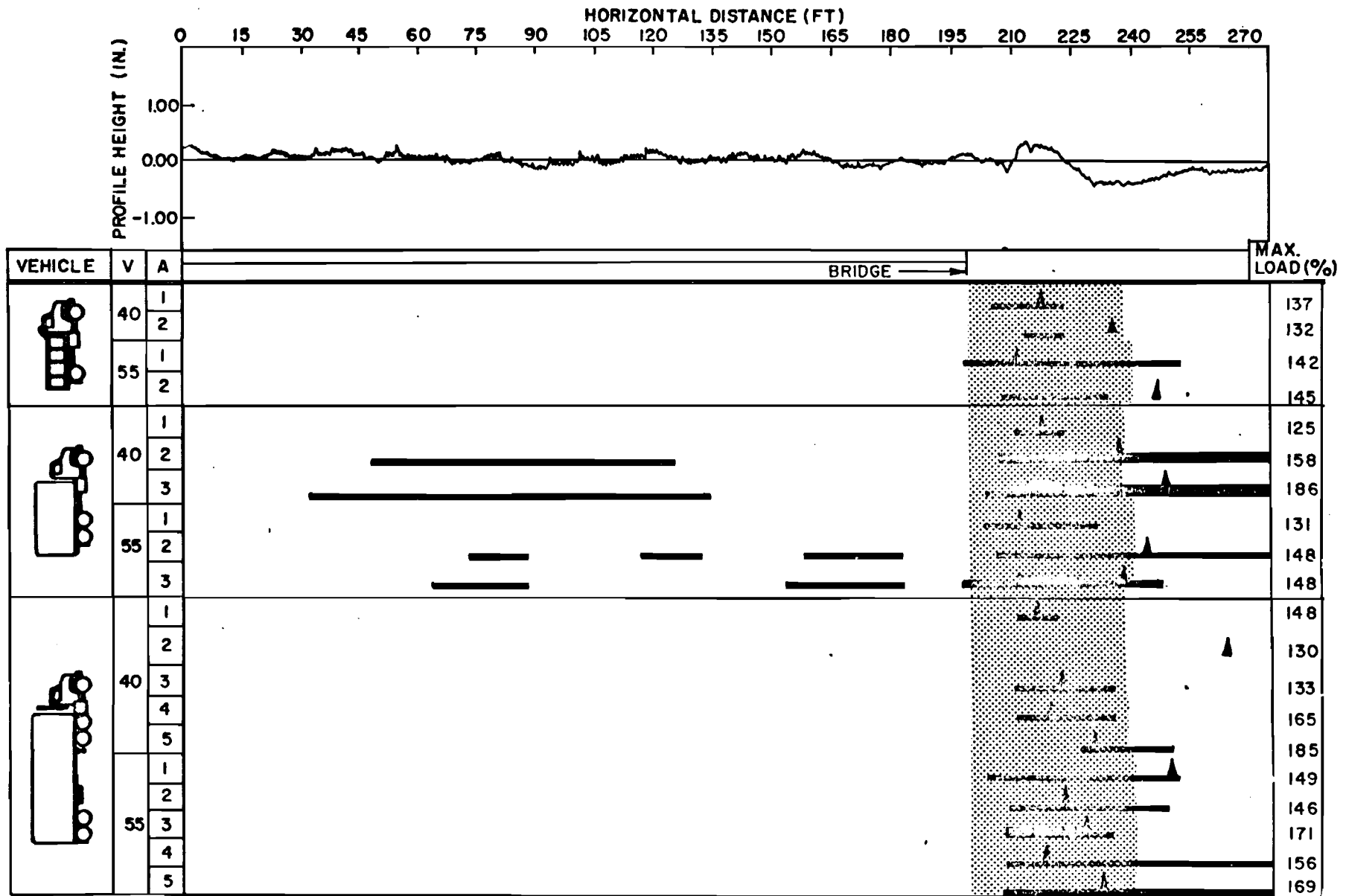


Fig A4.2A. Dynamic wheel load diagram, high frequency oscillation, Loop 427 over Mustang Creek (Austin), end of bridge.

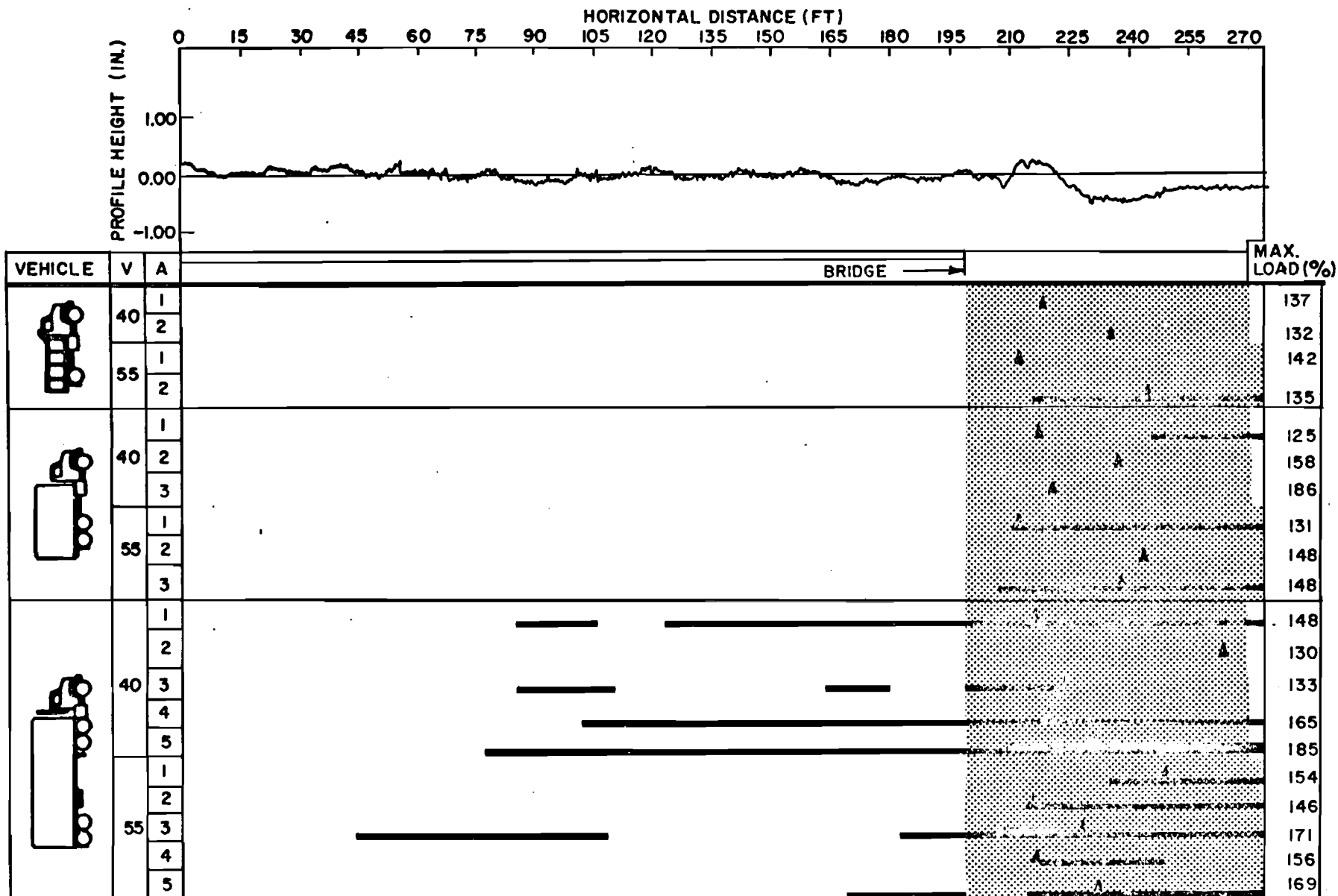


Fig A4.2B. Dynamic wheel load diagram, low frequency oscillation, Loop 427 over Mustang Creek (Austin), end of bridge.

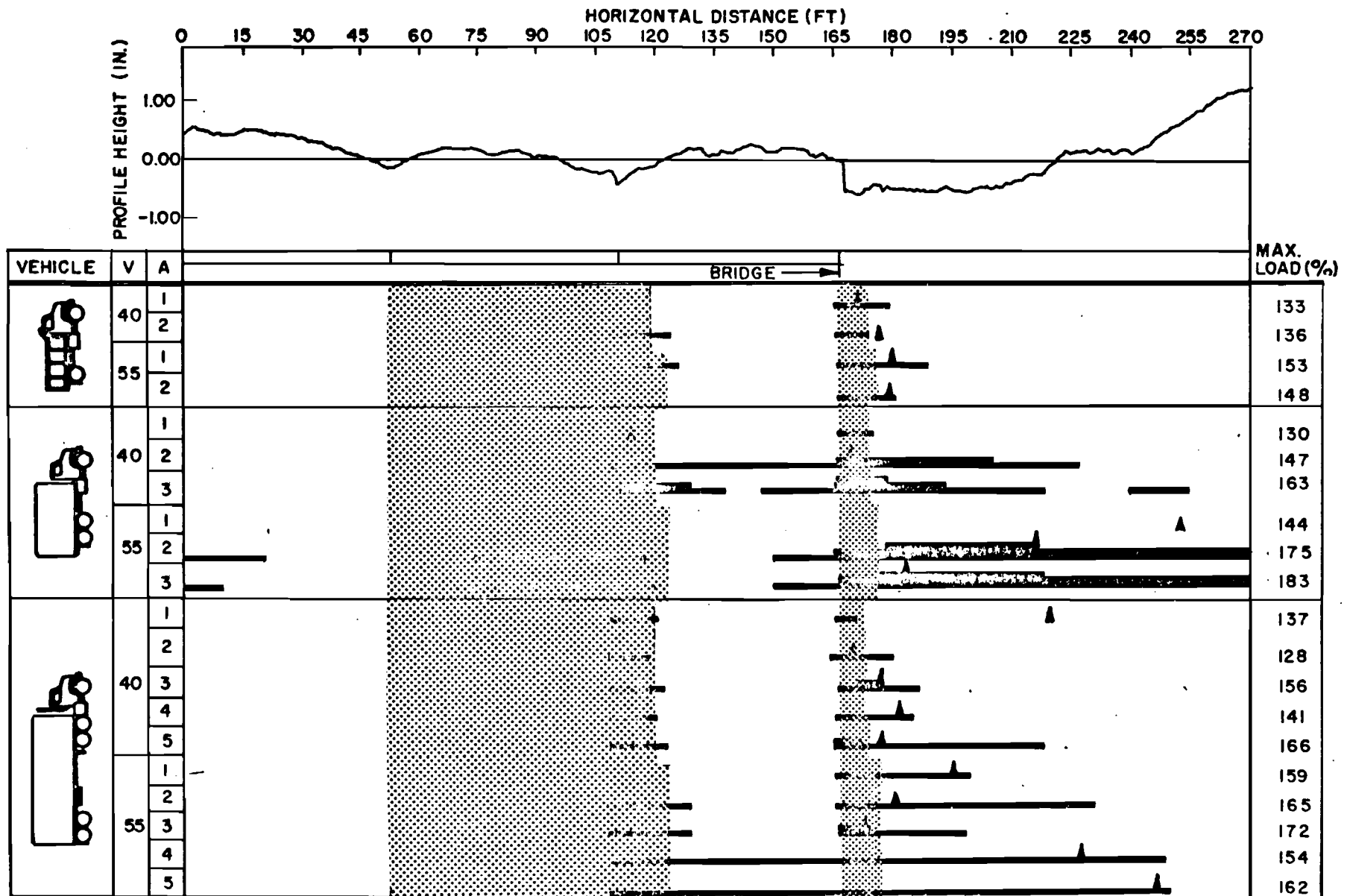
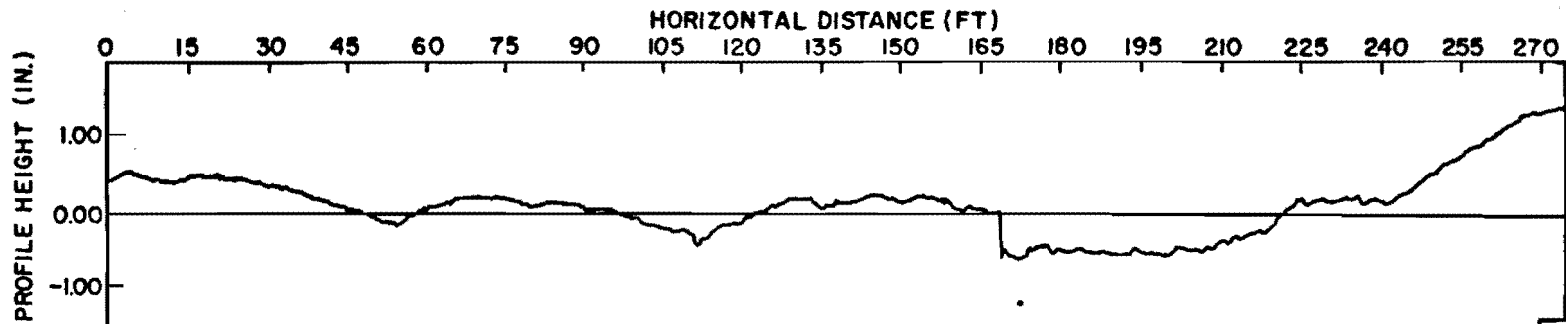


Fig A4.3A. Dynamic wheel load diagram, high frequency oscillation, US 183 over Boggy Creek (Austin), end of bridge.




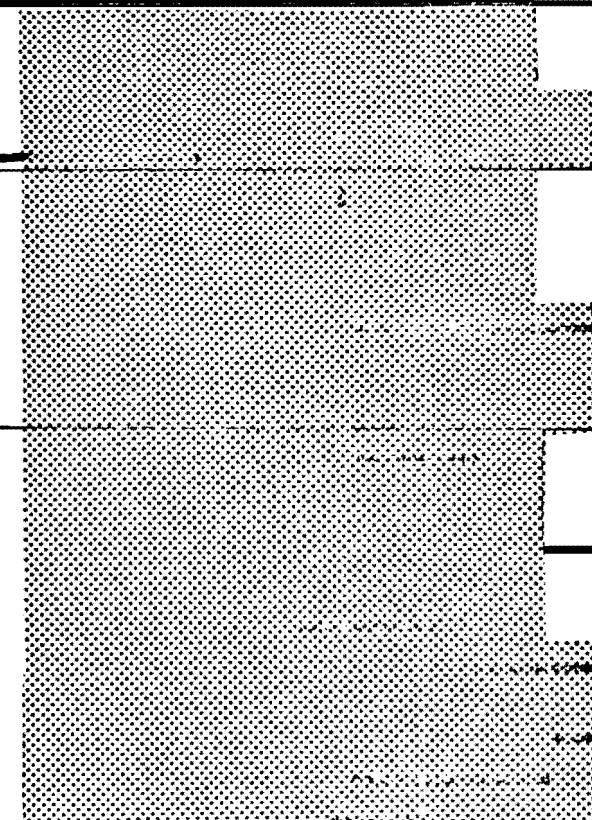
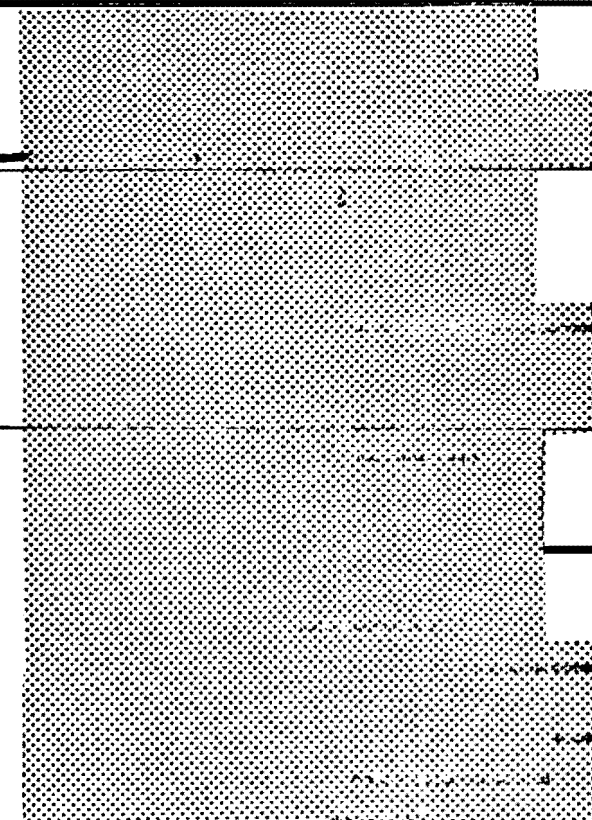

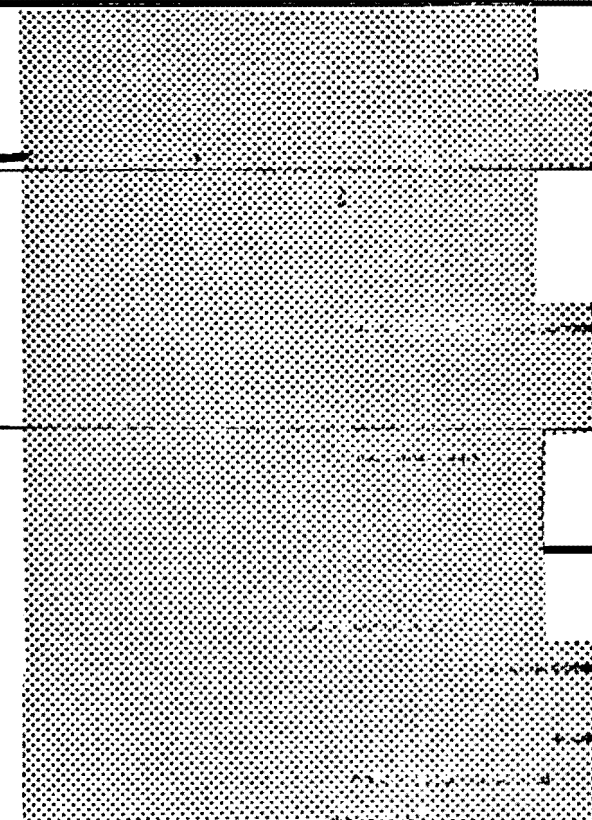
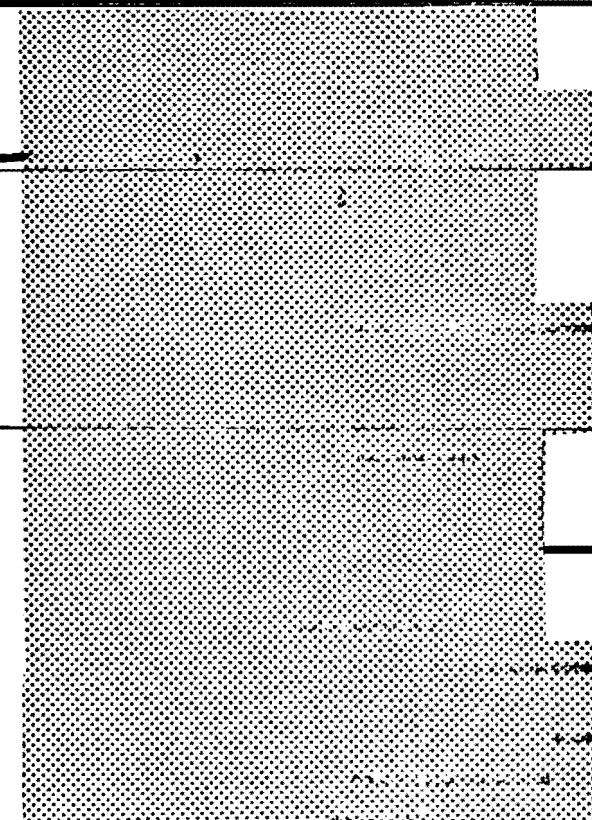

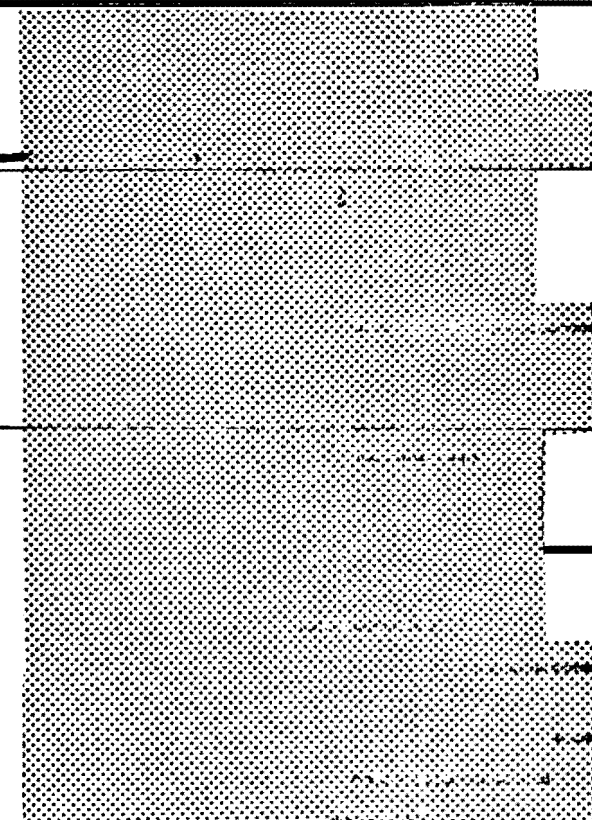
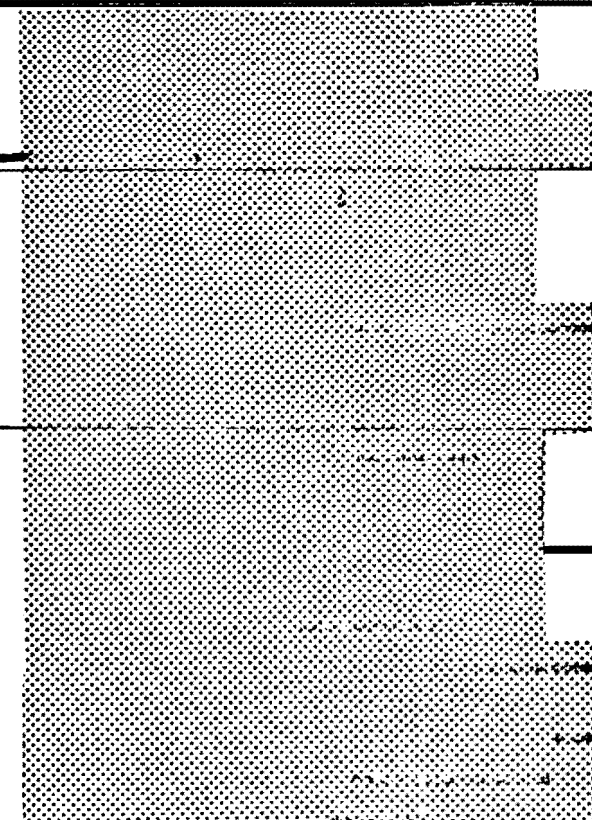
VEHICLE	V	A	BRIDGE	MAX. LOAD (%)				
	40	1		133				
		2		136				
	55	1			153			
		2			148			
	40	1				129		
		2				147		
		3				163		
	55	1					144	
		2					175	
		3					183	
	40	1						137
		2						128
		3	156					
		4	141					
		5	166					
	55	1		159				
		2		165				
		3		172				
		4		154				
		5		162				

Fig A4.3B. Dynamic wheel load diagram, low frequency oscillation, US 183 over Boggy Creek (Austin), end of bridge.

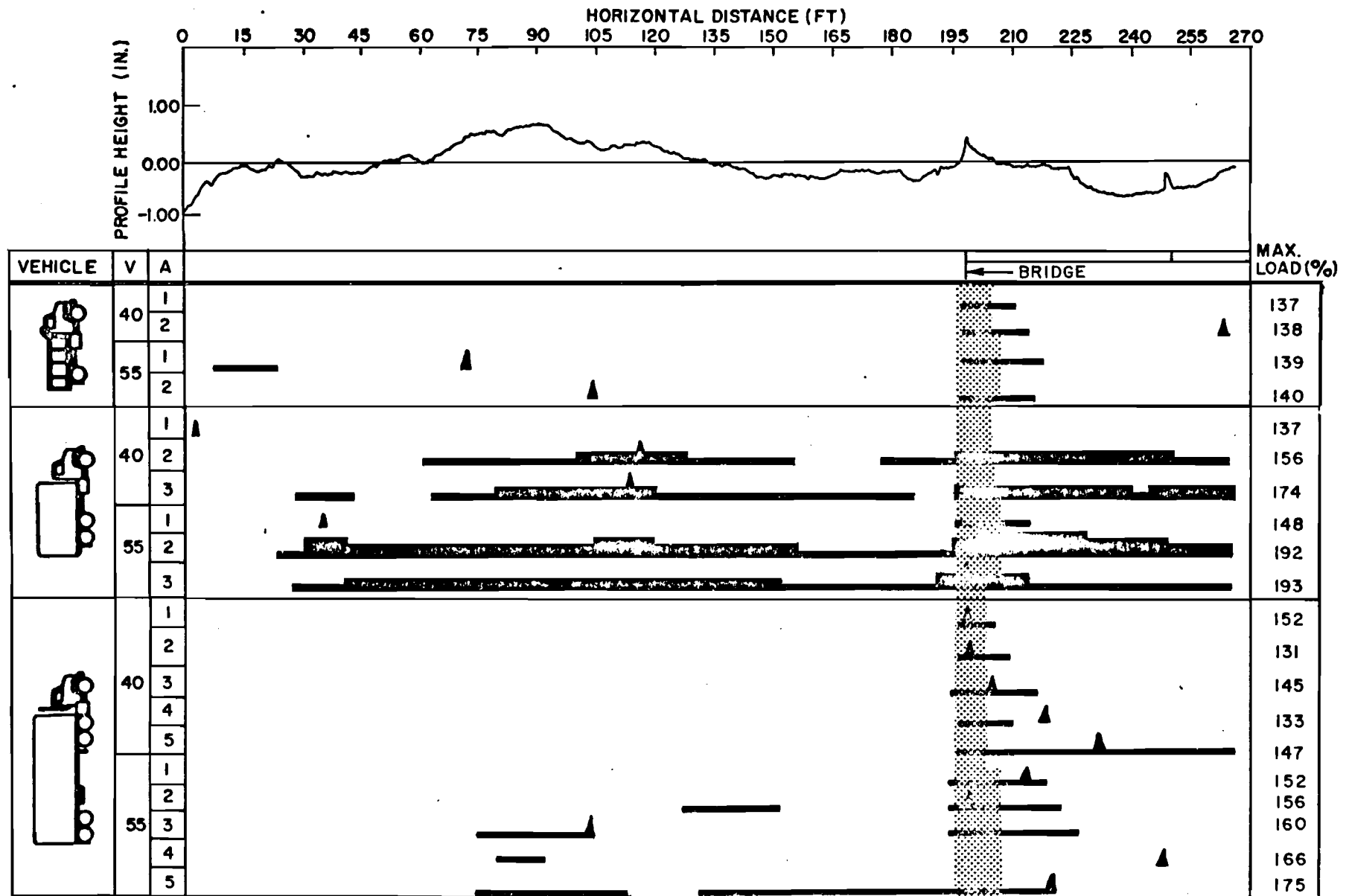


Fig A4.4A. Dynamic wheel load diagram, high frequency oscillation, SH 71 over Bee Creek (Austin), start of bridge.

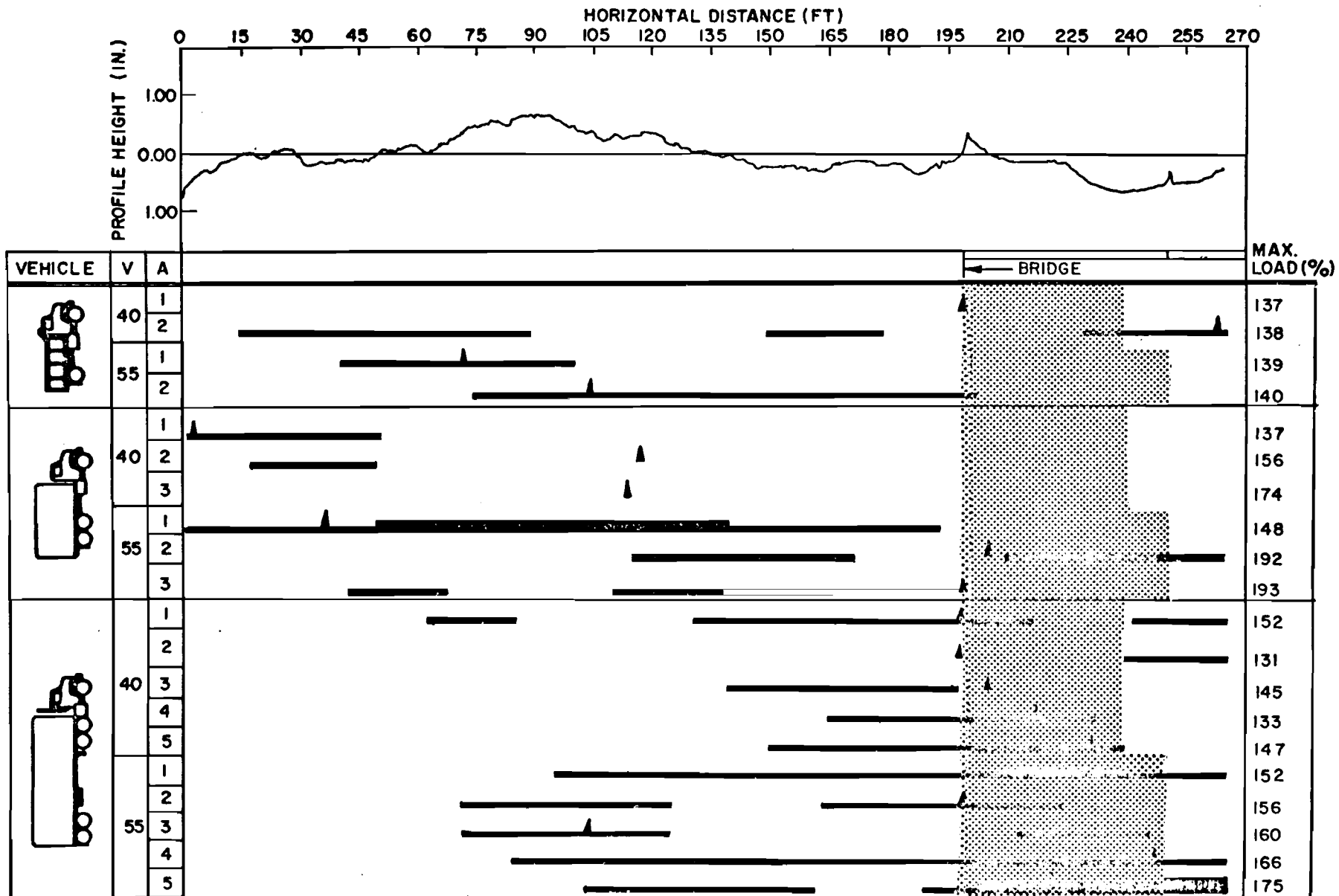


Fig A4.4B. Dynamic wheel load diagram, low frequency oscillation, SH 71 over Bee Creek (Austin), start of bridge.

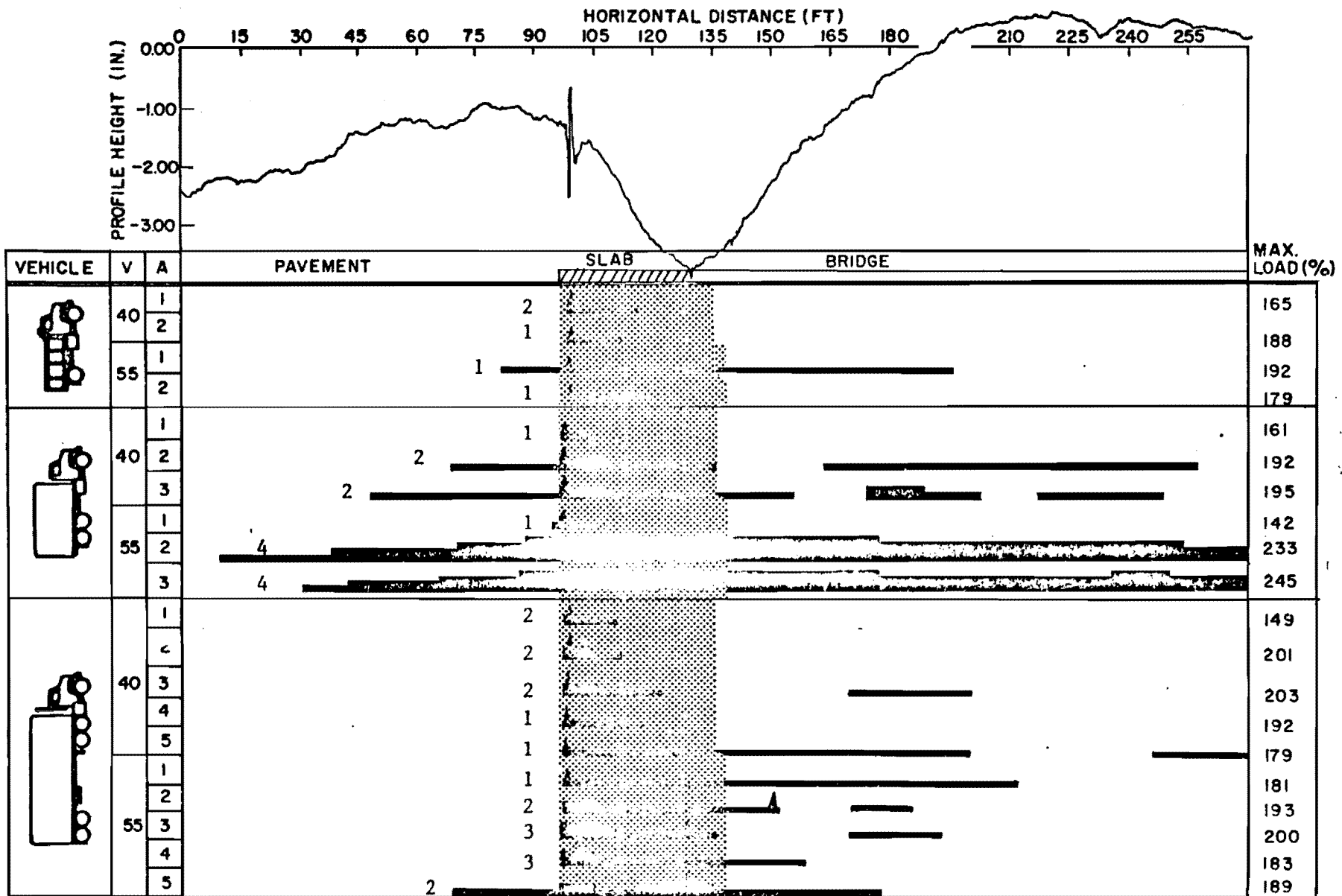


Fig A4.5A. Dynamic wheel load diagram, high frequency oscillation, IH 37 over Hackberry St., (S.A.), start of bridge.

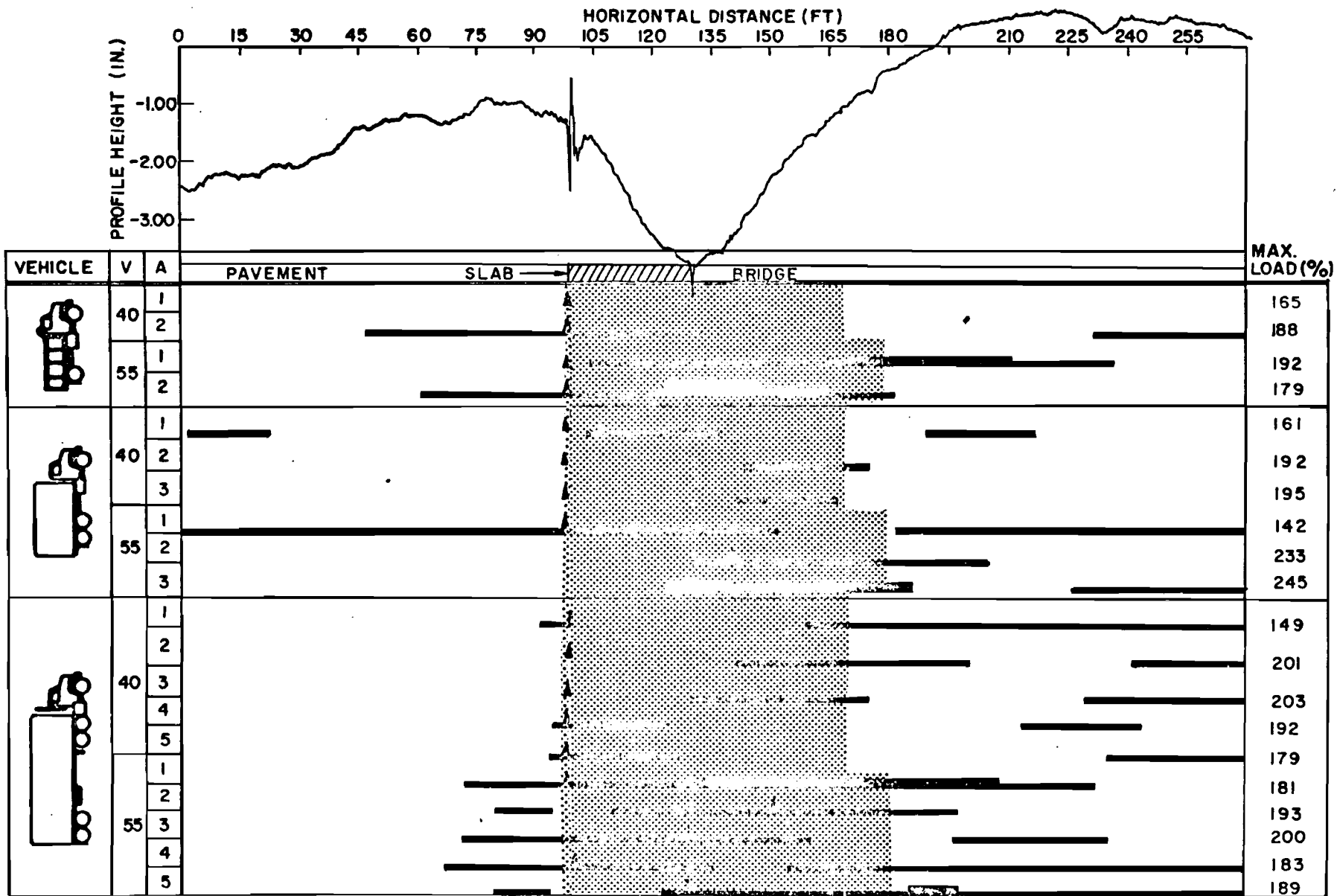


Fig A4.5B. Dynamic wheel load diagram, low frequency oscillation, IH 37 over Hackberry St., (S.A.), start of bridge.

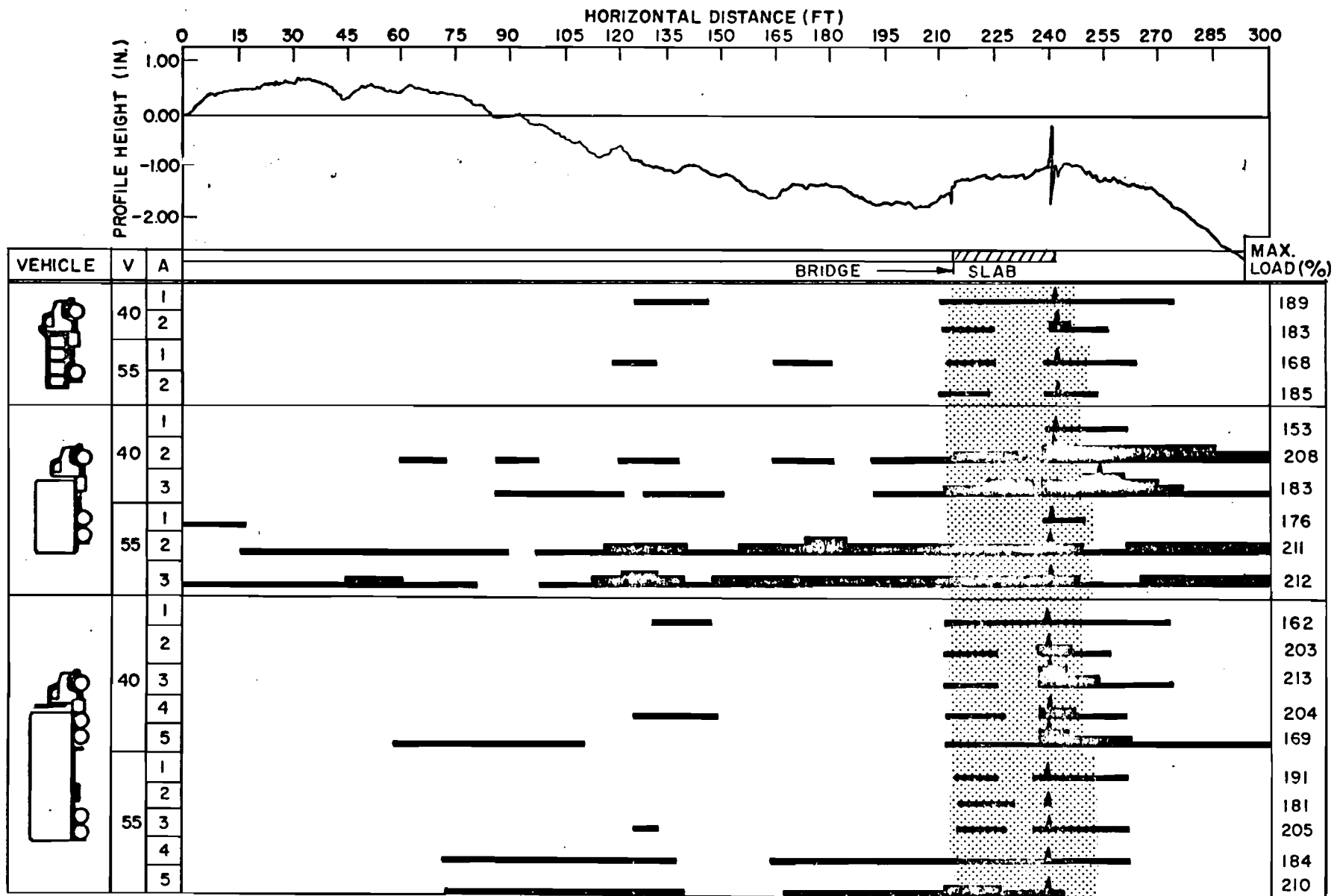


Fig A4.6A. Dynamic wheel load diagram, high frequency oscillation, IH 37 over Hackberry St., (S.A.), end of bridge.

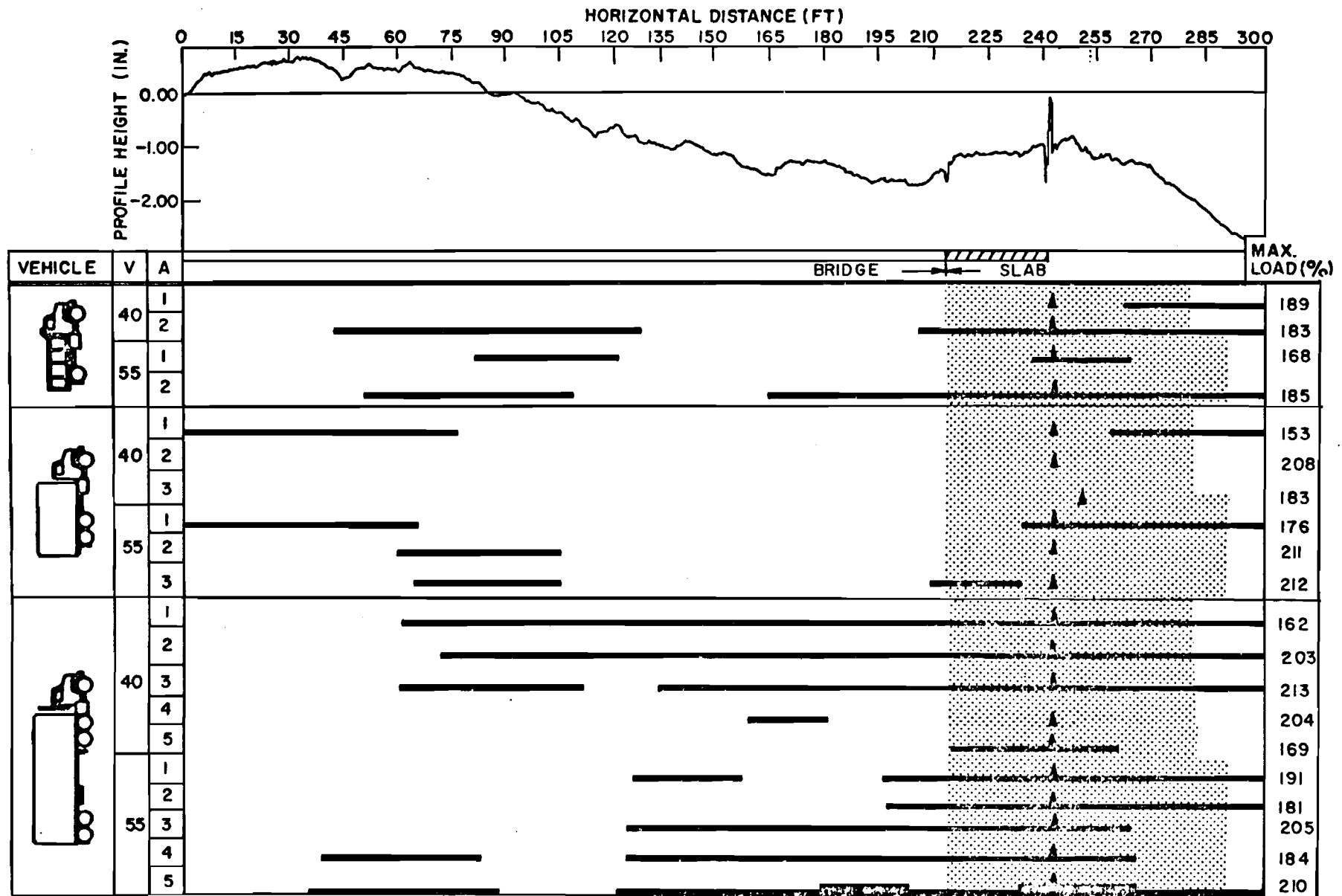


Fig A4.6B. Dynamic wheel load diagram, low frequency oscillation, IH 37 over Hackberry St., (S.A.), end of bridge.

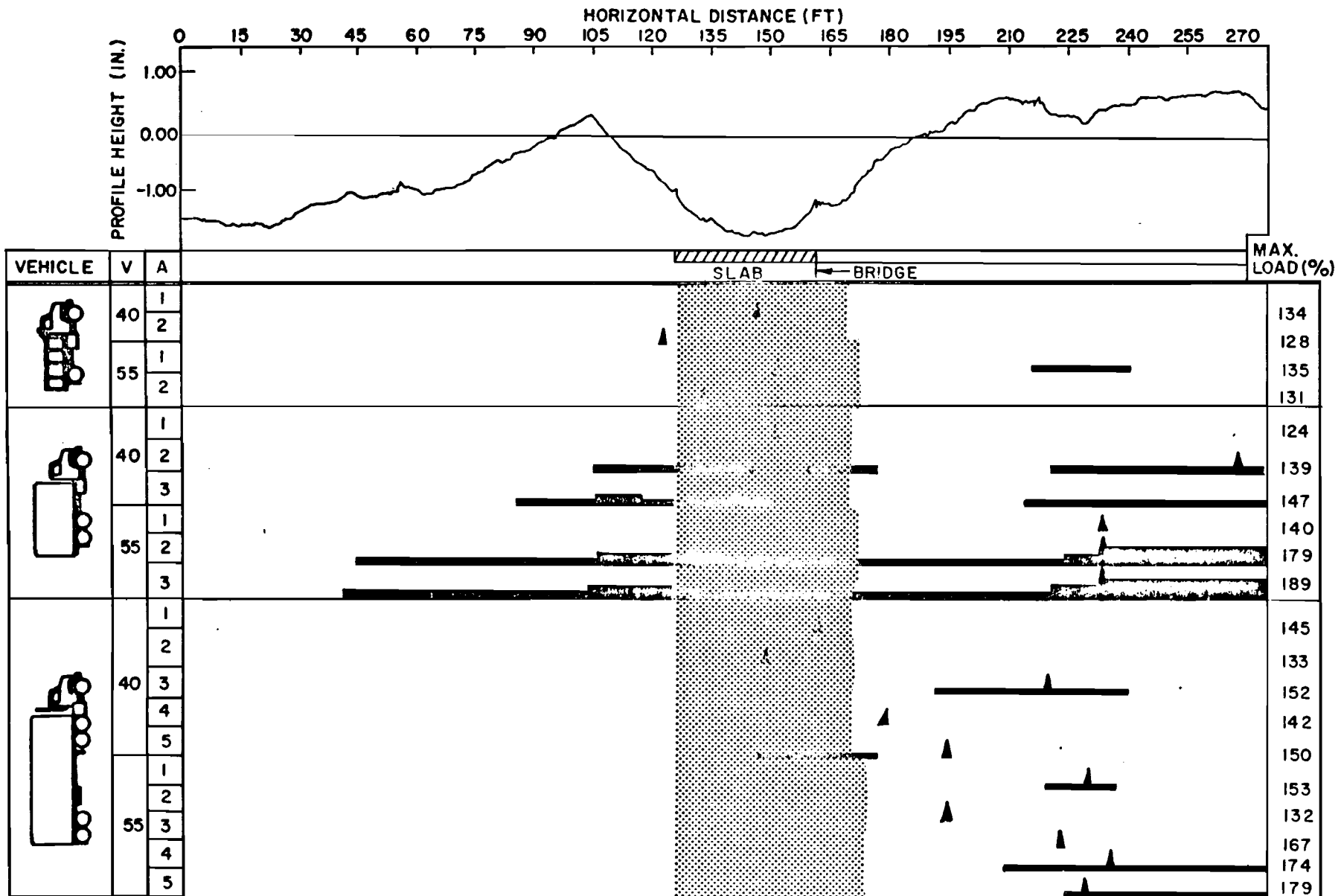


Fig A4.7A. Dynamic wheel load diagram, high frequency oscillation, IH 37 over Durango St., (S.A.), start of bridge.

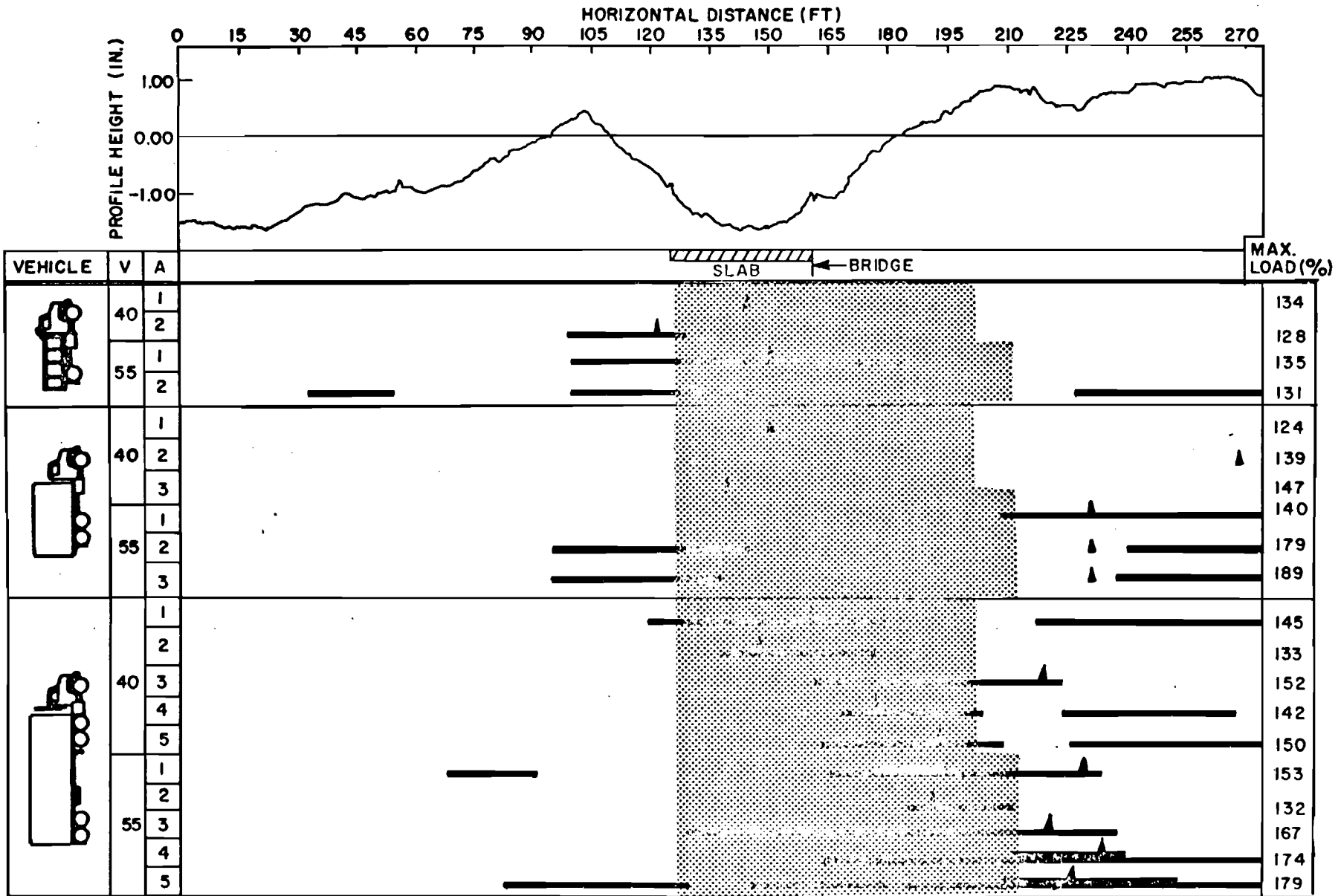


Fig A4.7B. Dynamic wheel load diagram, low frequency oscillation, IH 37 over Durango St., (S.A.), start of bridge.

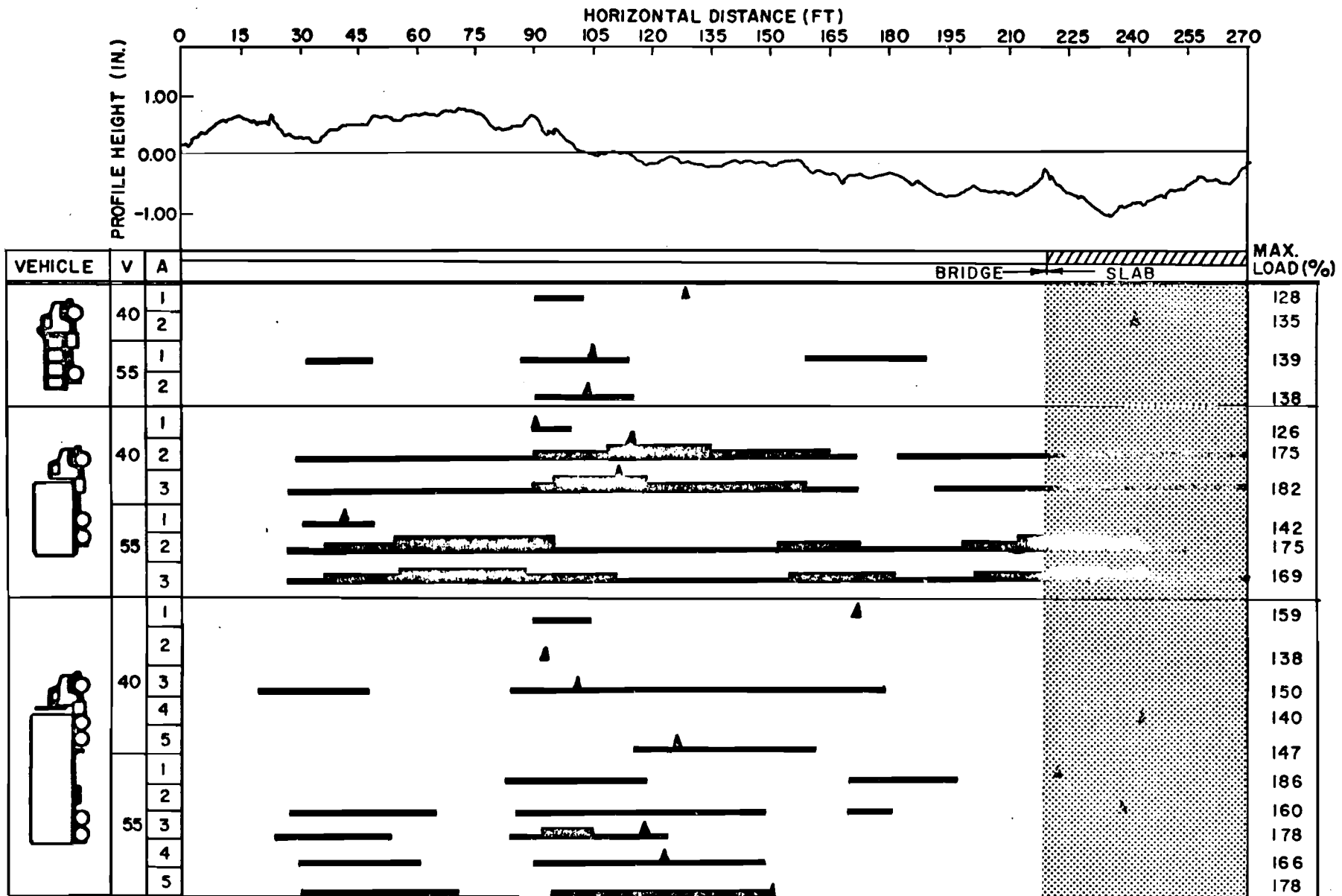


Fig A4.8A. Dynamic wheel load diagram, high frequency oscillation, IH 37 over Durango St., (S.A.), end of bridge.

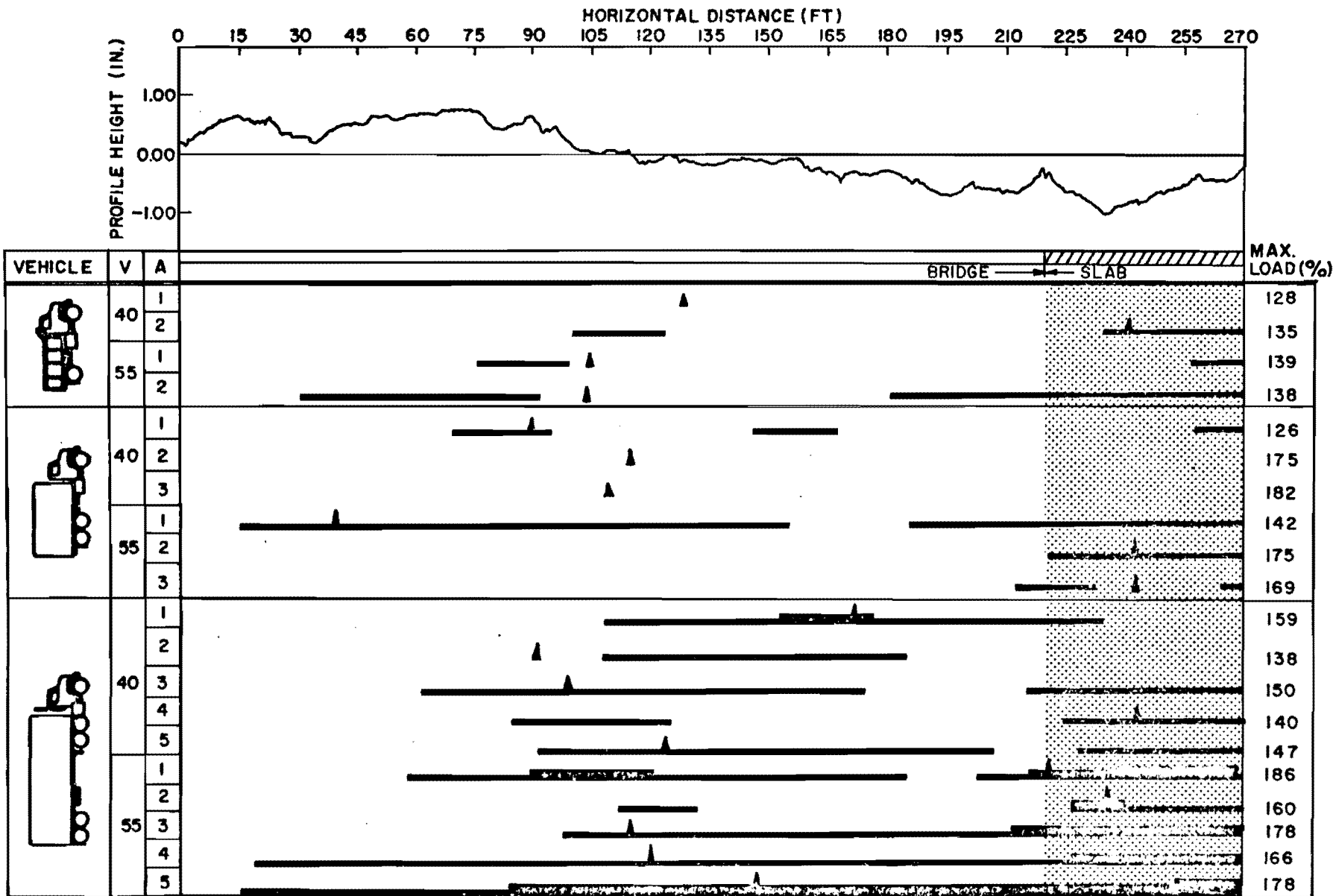


Fig A4.8B. Dynamic wheel load diagram, low frequency oscillation, IH 37 over Durango St., (S.A.), end of bridge.

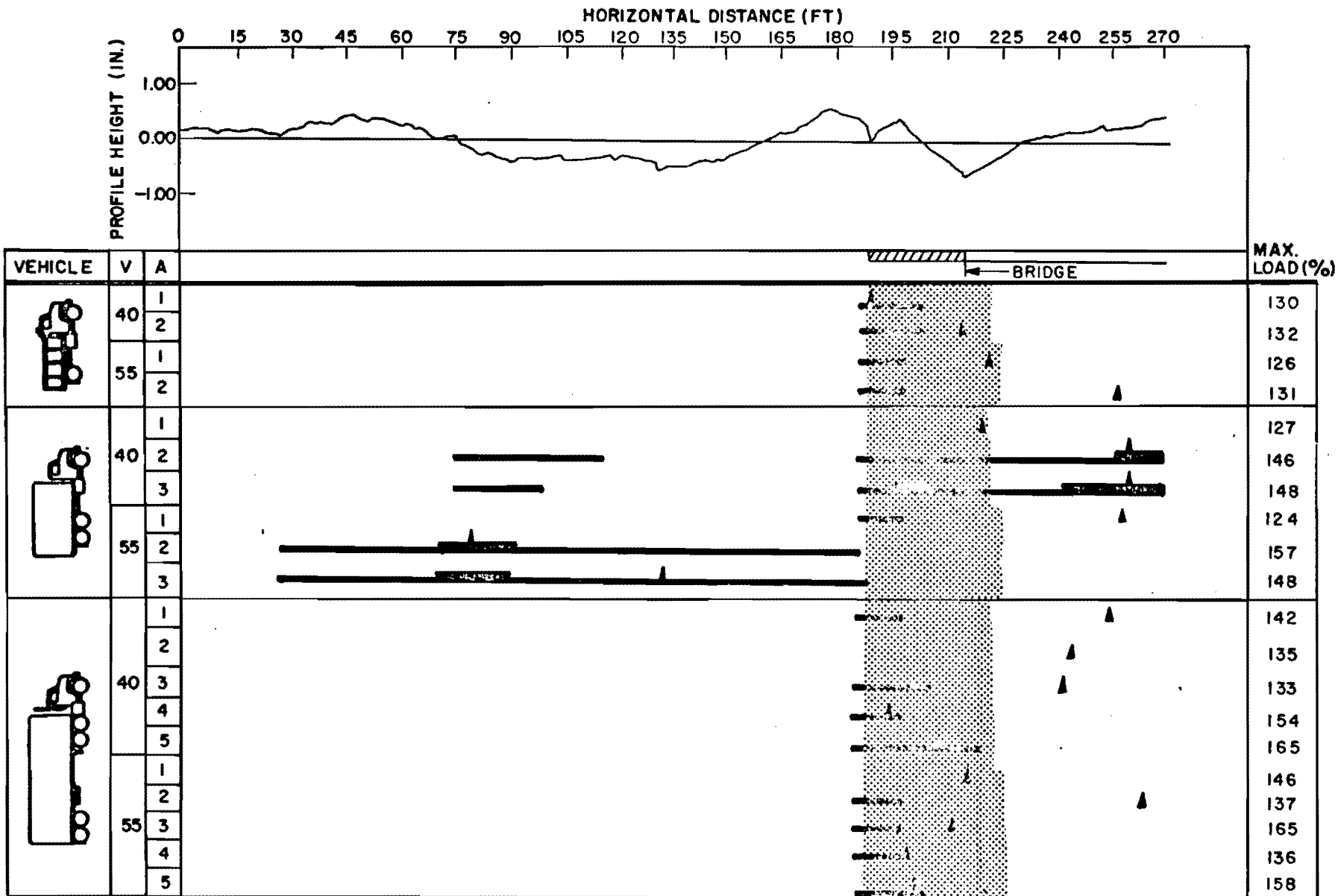
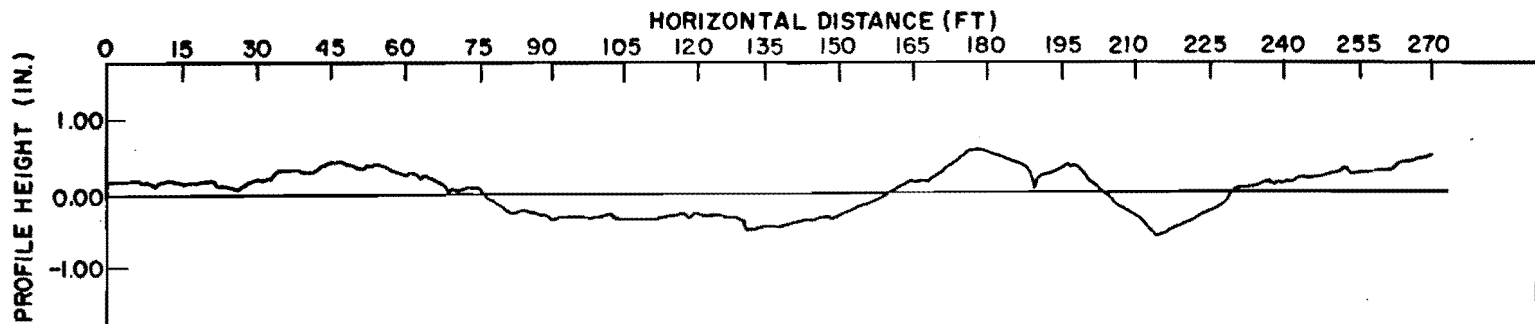


Fig A4.9A. Dynamic wheel load diagram, high frequency oscillation IH 10 over W. W. White Blvd., (S.A.), start of bridge.




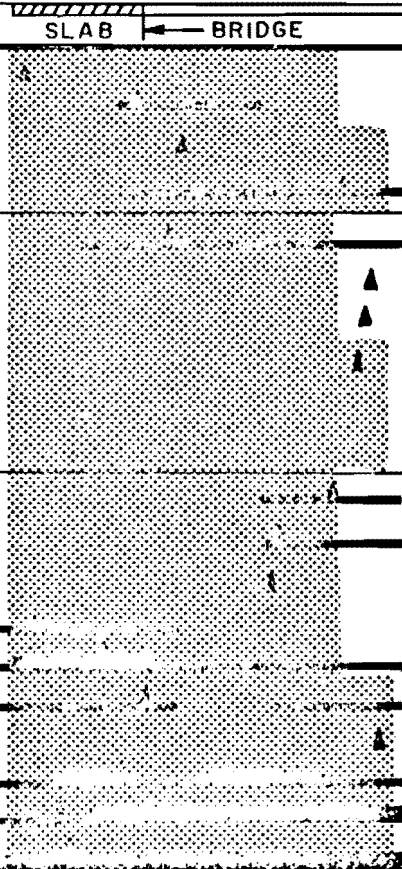



VEHICLE	V	A	SLAB	BRIDGE	MAX. LOAD (%)	
	40	1			130	
		2			132	
	55	1			126	
		2			131	
	40	1				127
		2				146
		3				148
	55	1				124
		2				157
		3				148
	40	1				142
		2				135
		3		133		
		4		154		
		5		165		
	55	1		146		
		2		137		
		3		165		
		4		136		
		5		158		

Fig A4.9B. Dynamic wheel load diagram, low frequency oscillation, IH 10 over W. W. White Blvd., (S.A.), start of bridge.

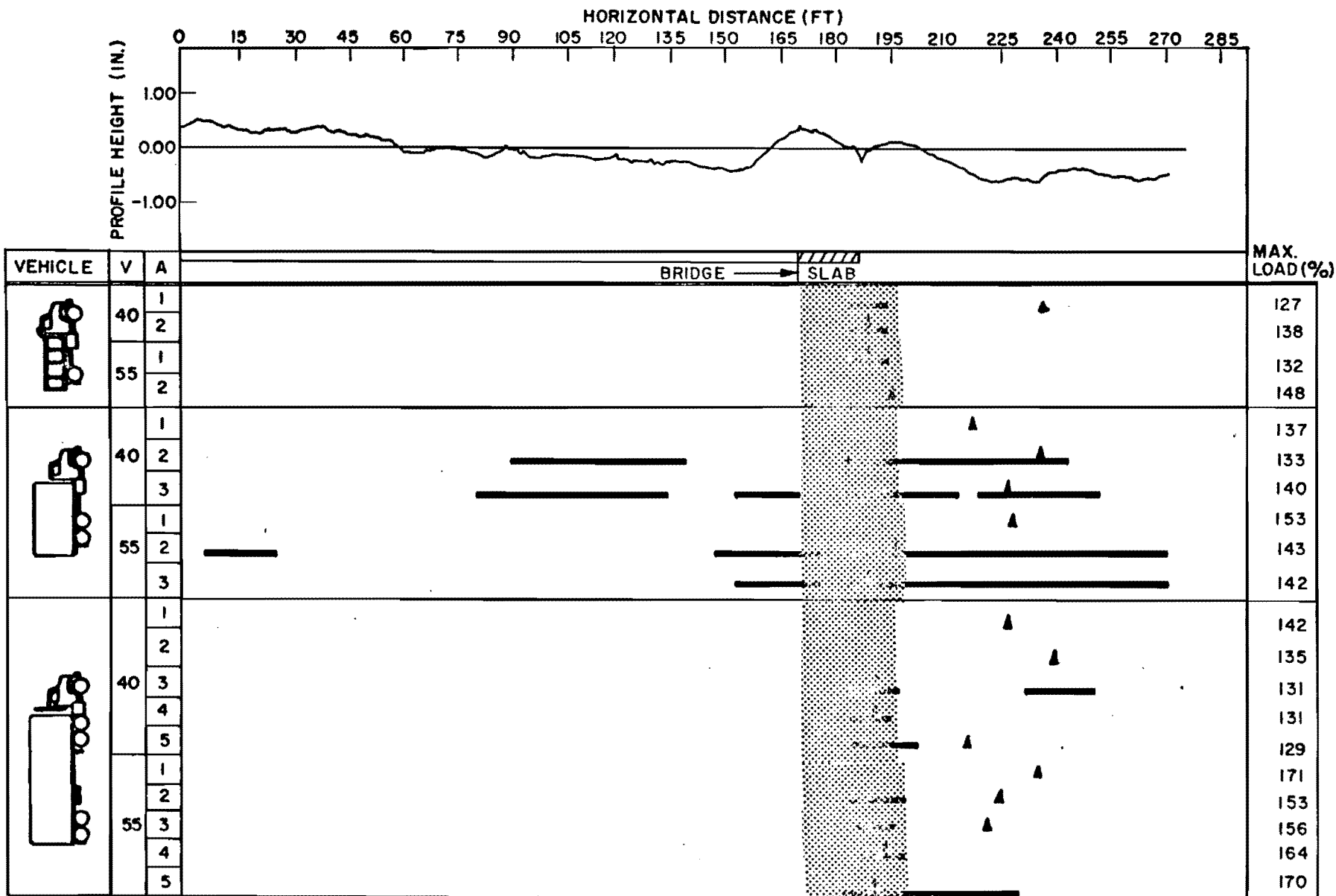


Fig A4.10A. Dynamic wheel load diagram, high frequency oscillation, IH 10 over W. W. White Blvd., (S.A.), end of bridge.

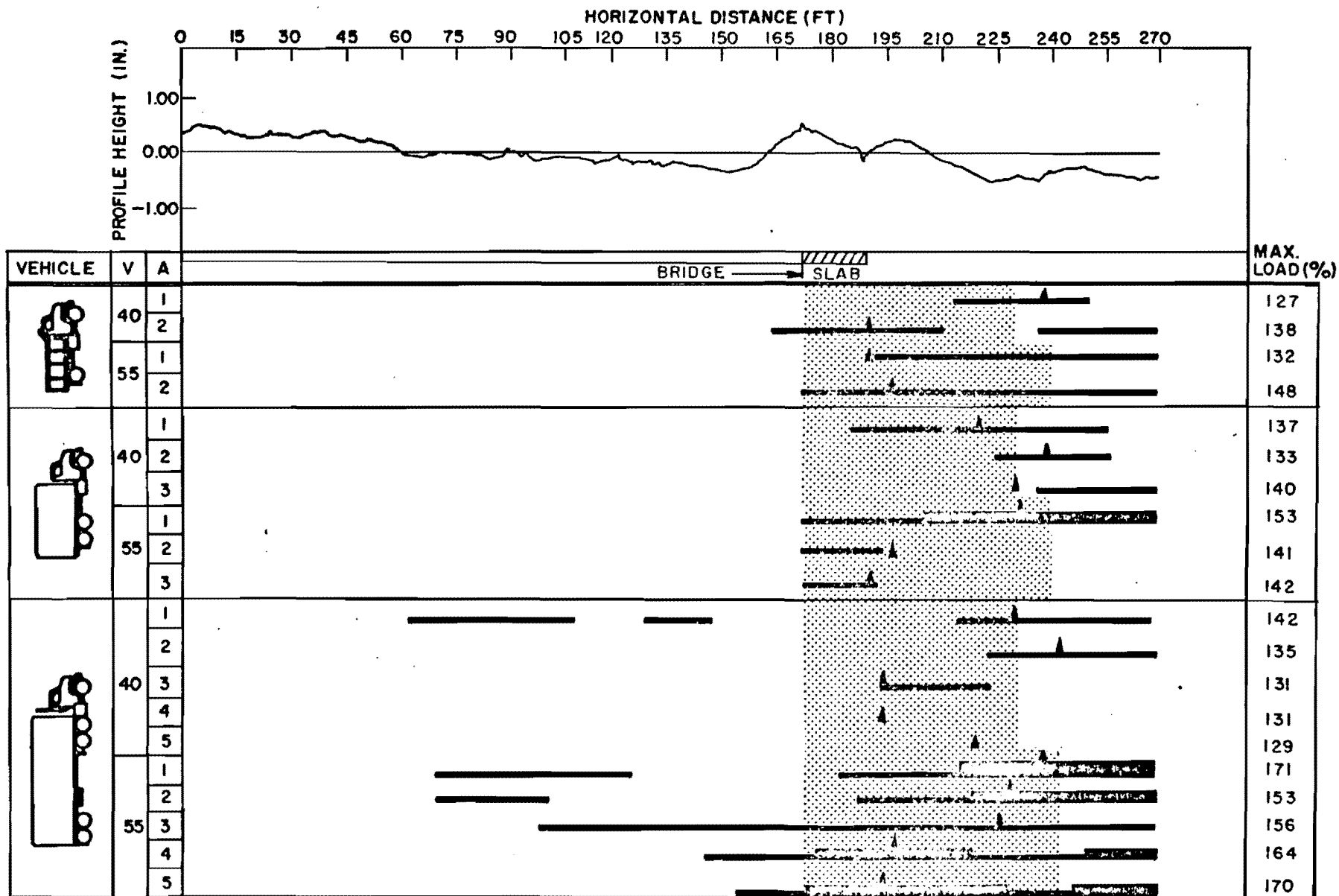


Fig A4.10B. Dynamic wheel load diagram, low frequency oscillation, IH 10 over W. W. White Blvd., (S.A.), end of bridge.

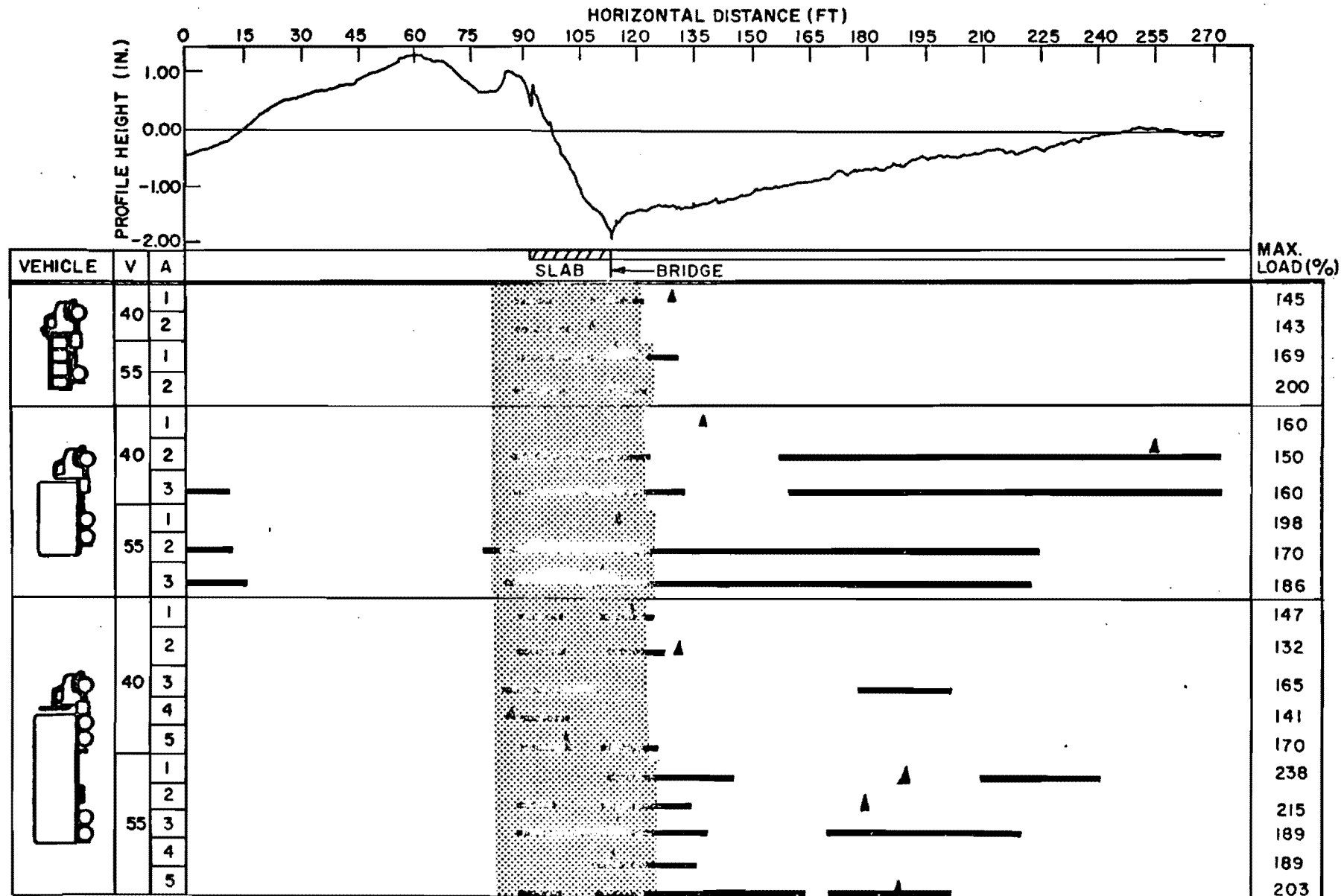
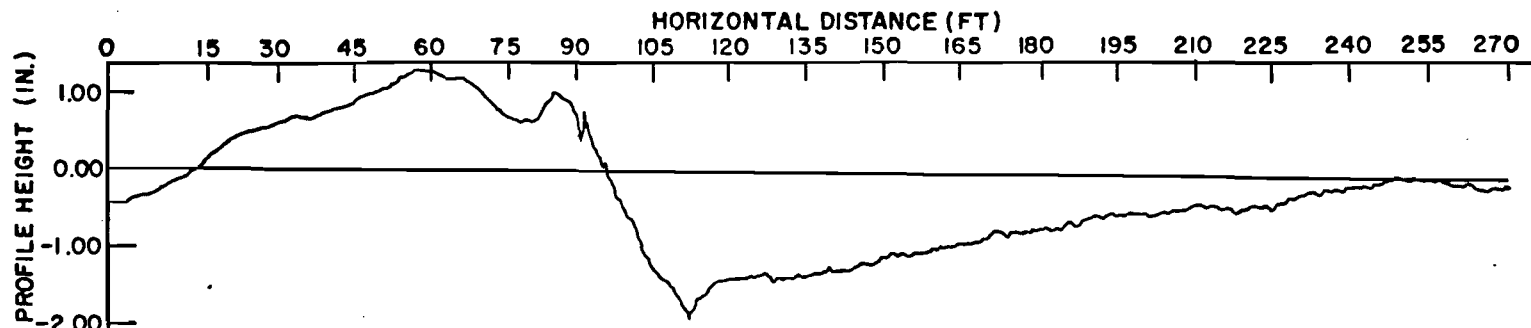
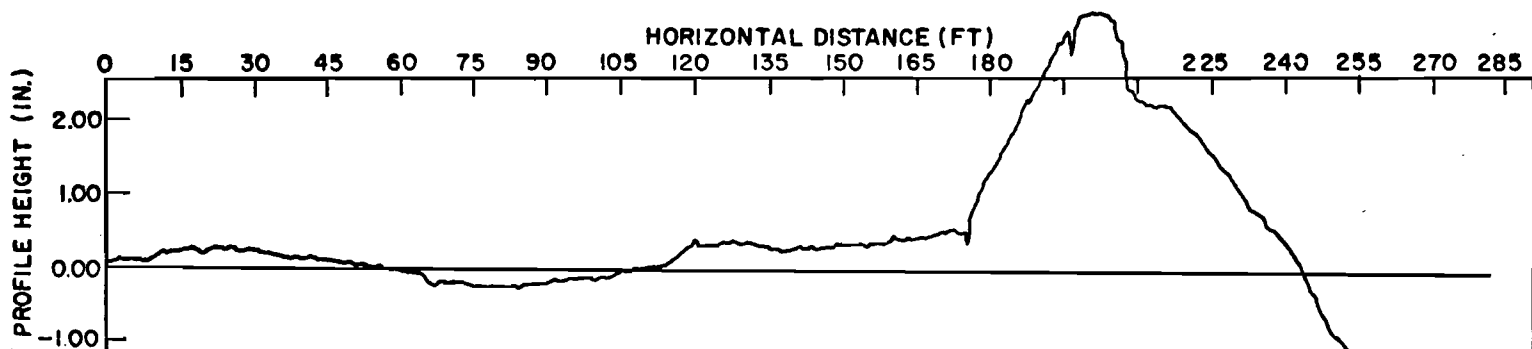


Fig A4.IIA. Dynamic wheel load diagram, high frequency oscillation, IH 10 over Flum Creek, (S.A.), start of bridge.



VEHICLE	V	A	SLAB	BRIDGE	MAX. LOAD (%)
	40	1			145
		2			143
	55	1			169
		2			200
	40	1			160
		2			150
		3			159
	55	1			198
		2			170
		3			186
	40	1			147
		2			132
		3			165
		4			141
		5			170
	55	1			238
		2			215
		3			189
		4			189
		5			203

Fig A4.11B. Dynamic wheel load diagram, low frequency oscillation, IH 10 over Plum Creek, (S.A.), start of bridge.






VEHICLE	V	A	BRIDGE	SLAB	MAX. LOAD (%)
	40	1			140
		2			147
	55	1			160
		2			166
	40	1			138
		2			165
		3			198
	55	1			186
		2			228
		3			227
	40	1			151
		2			133
		3			157
		4			170
		5			173
	55	1			183
		2			137
		3			224
		4			175
		5			211

Fig A4.12A. Dynamic wheel load diagram, high frequency oscillation, IH 10 over Plum Creek, (S.A.), end of bridge.

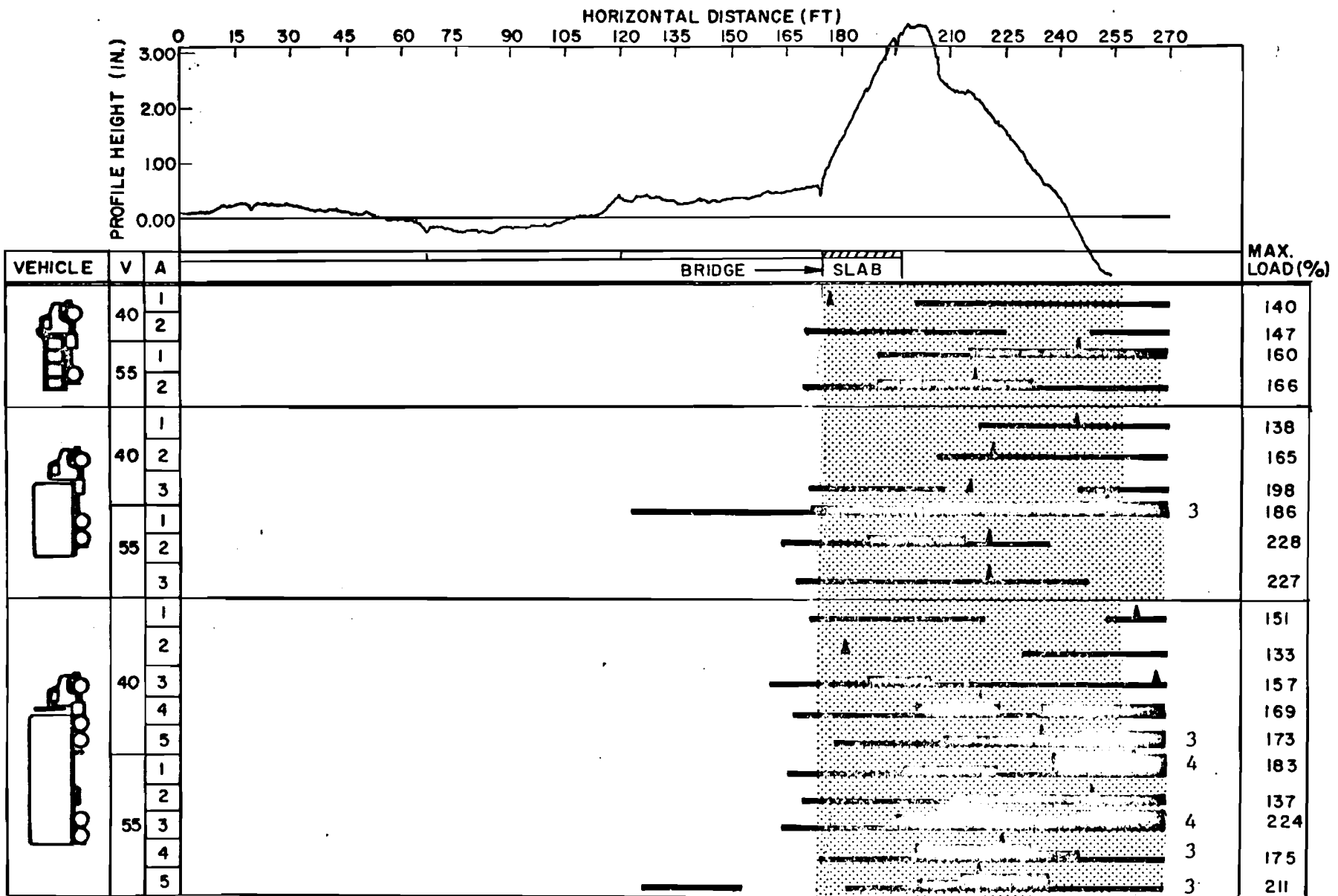


Fig A4.12B. Dynamic wheel load diagram, low frequency oscillation, IH 10 over Plum Creek, (S.A.), end of bridge.

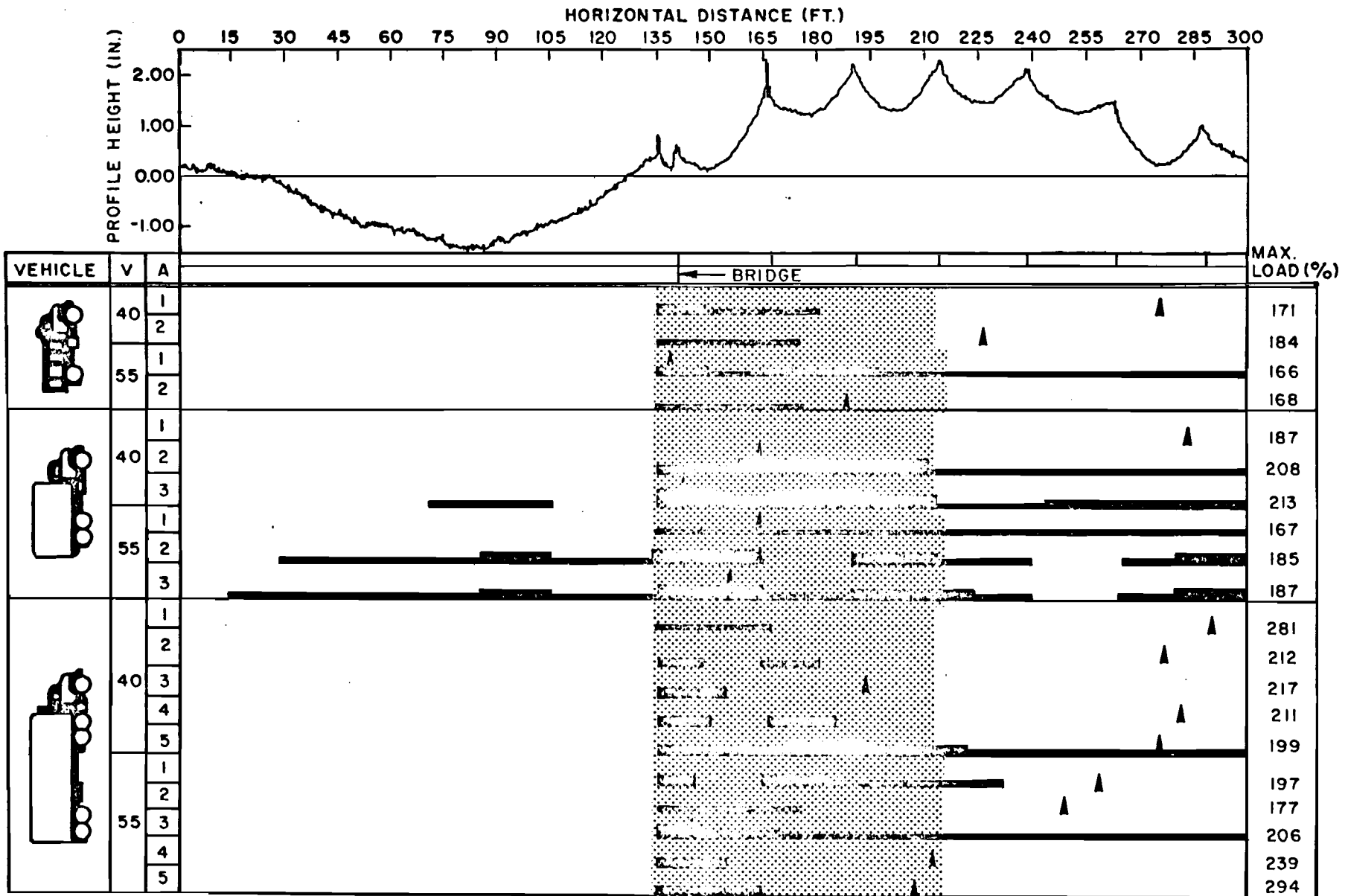


Fig A4.13A. Dynamic wheel load diagram, high frequency oscillation, FM 1065 over Los Linquish Creek (Lubbock), start of bridge.

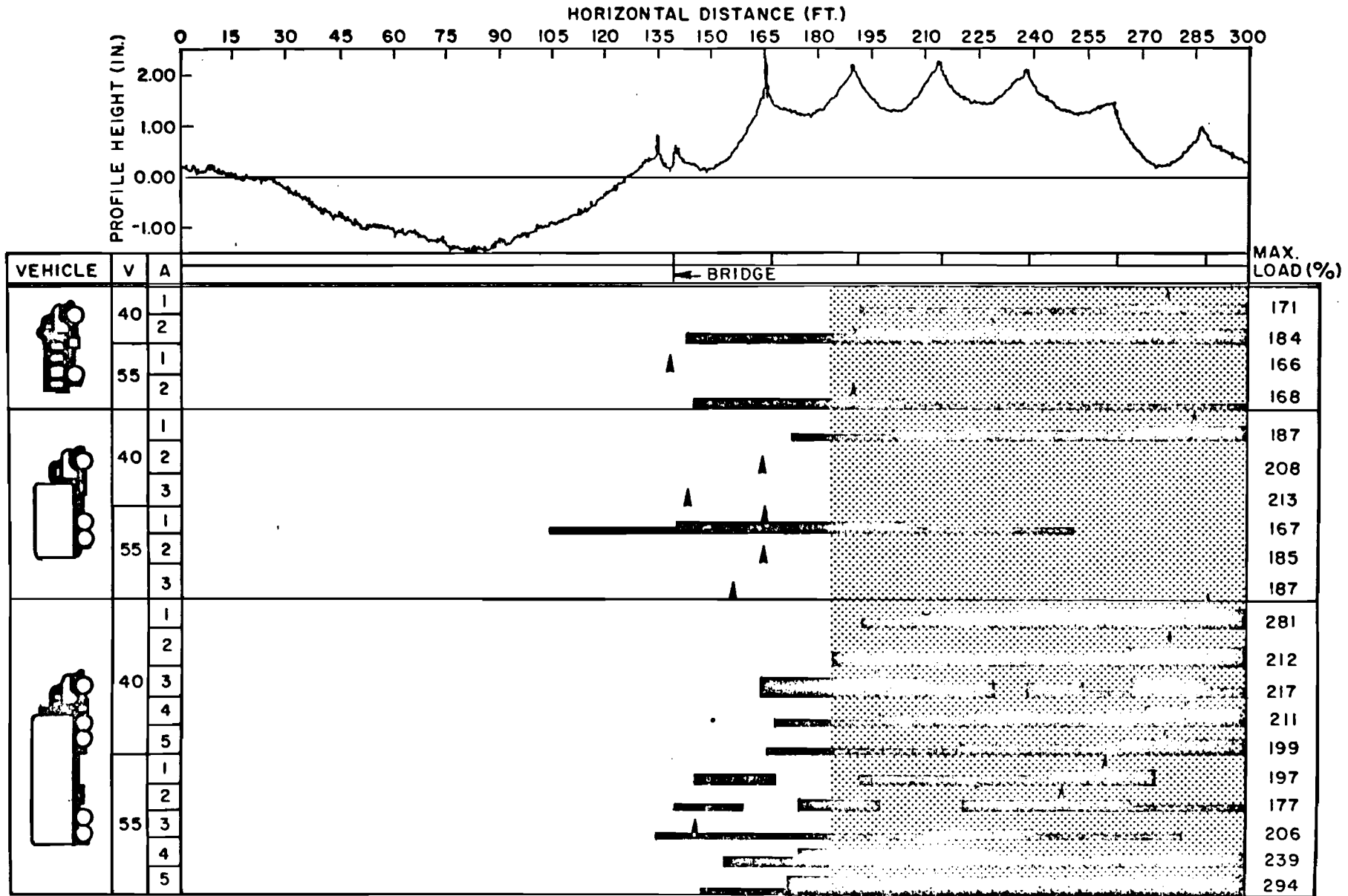


Fig A4.13B. Dynamic wheel load diagram, low frequency oscillation, FM 1065 over Los Linguish Creek (Lubbock), start of bridge.

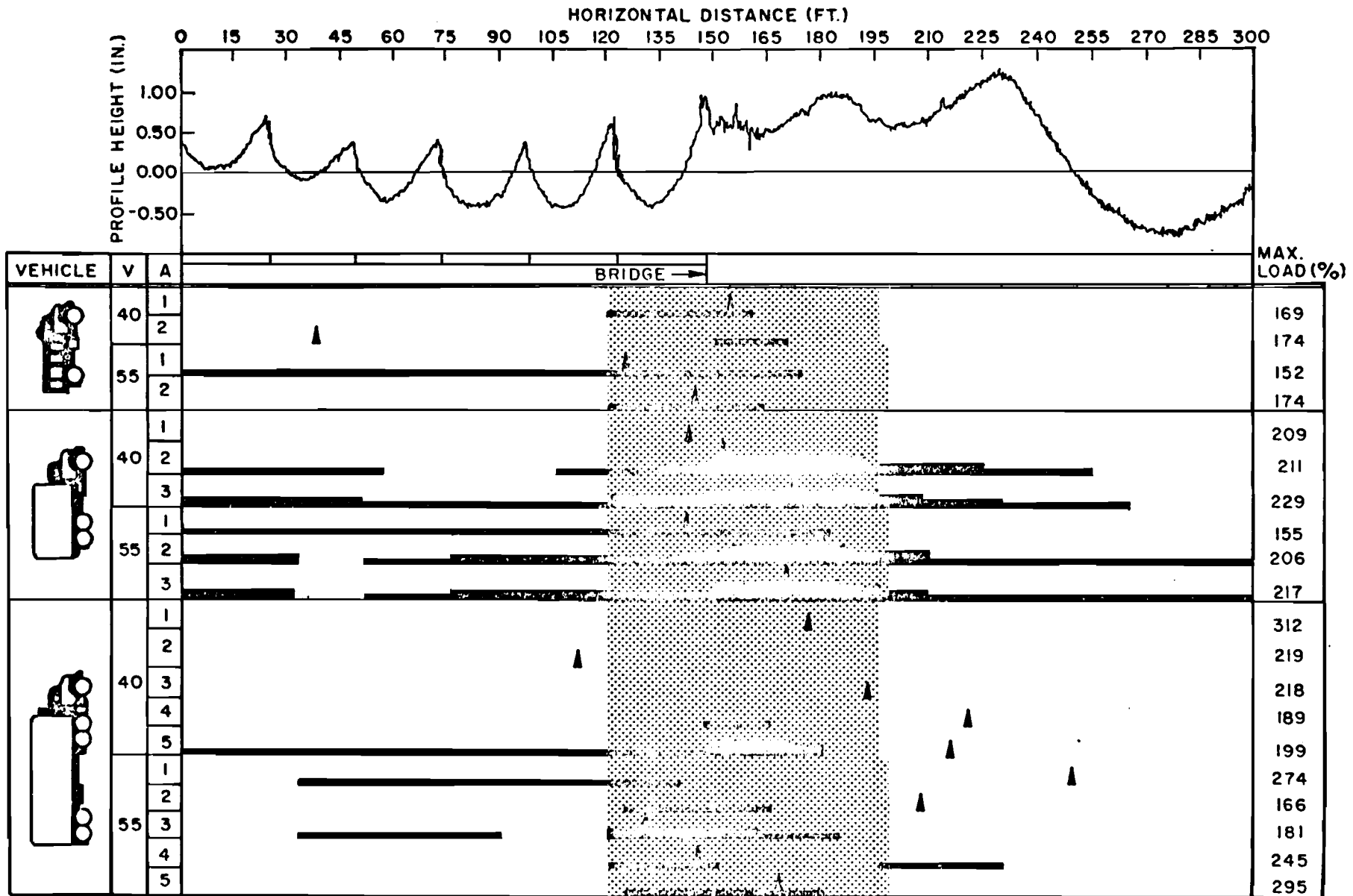
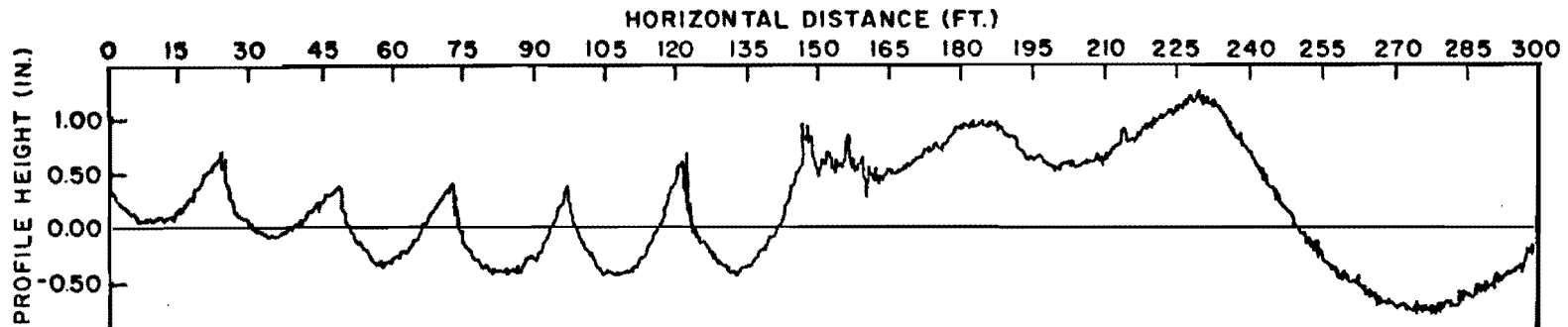


Fig A4.14A.. Dynamic wheel load diagram, high frequency oscillation, FM 1065 over Los Linguish Creek (Lubbock), end of bridge.






VEHICLE	V	A	BRIDGE →	MAX. LOAD (%)
	40	1		169
		2		174
	55	1		152
		2		174
	40	1		209
		2		211
		3		229
	55	1		155
		2		206
		3		217
	40	1		312
		2		219
		3		218
		4		189
		5		199
	55	1		274
		2		166
		3		181
		4		245
		5		295

Fig A4.14B.. Dynamic wheel load diagram, low frequency oscillation, FM 1065 over Los Linguish Creek (Lubbock), end of bridge.

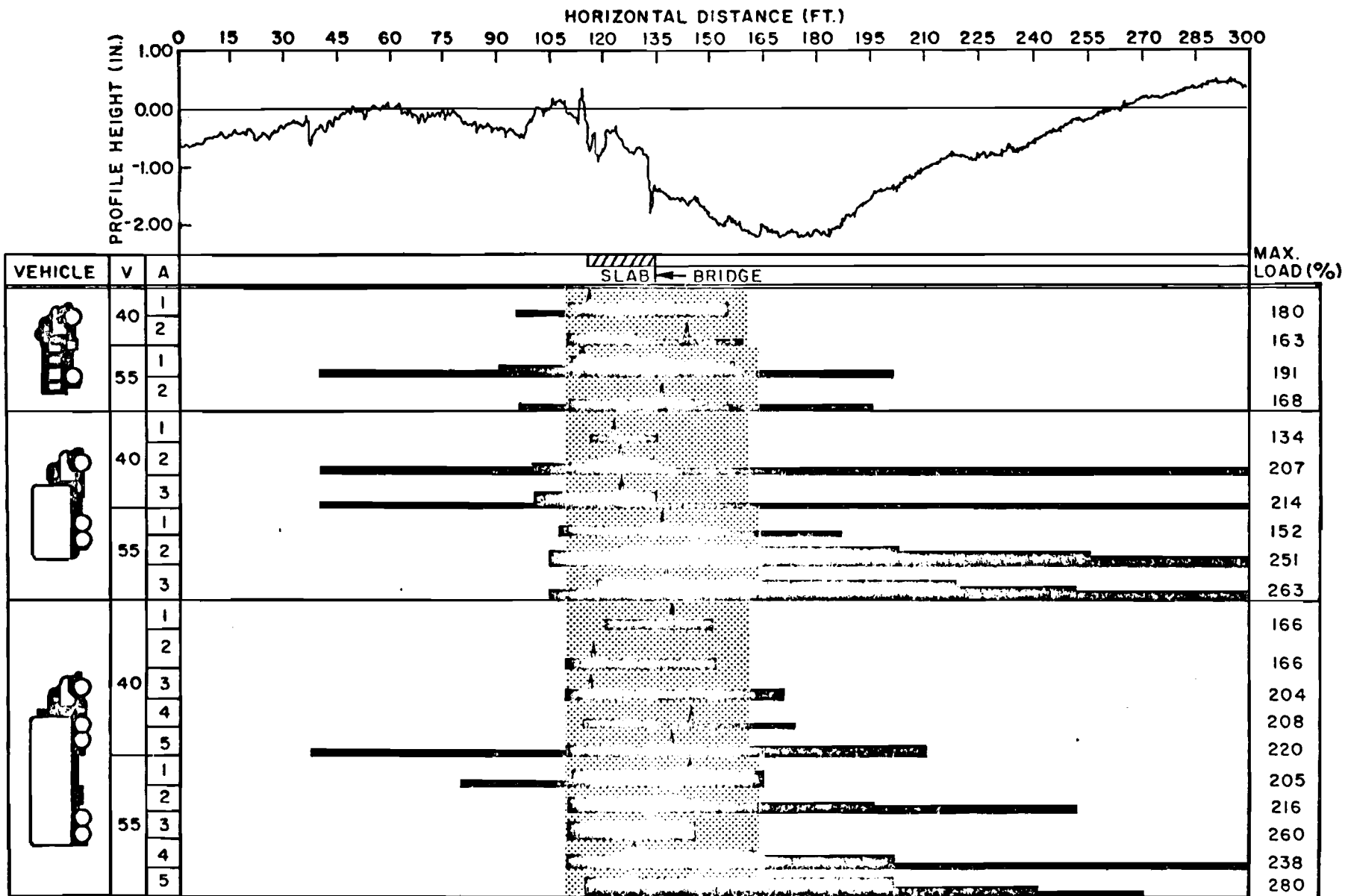


Fig A4.15A. Dynamic wheel load diagram, high frequency oscillation, Spur 326 over AT & SF Railroad (Lubbock), start of bridge.

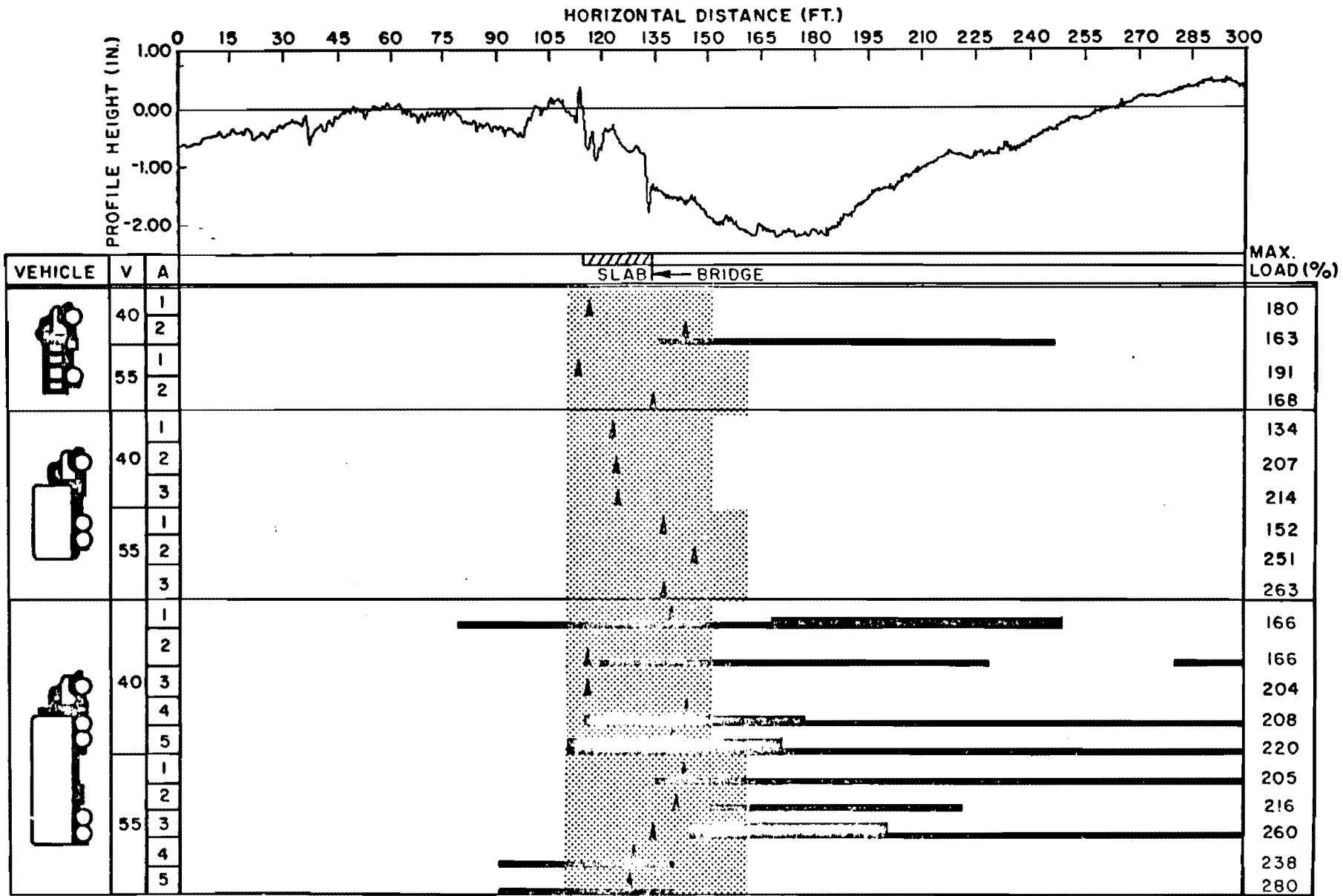


Fig A4.15B. Dynamic wheel load diagram, low frequency oscillation, Spur 326 over AT & SF Railroad (Lubbock), start of bridge.

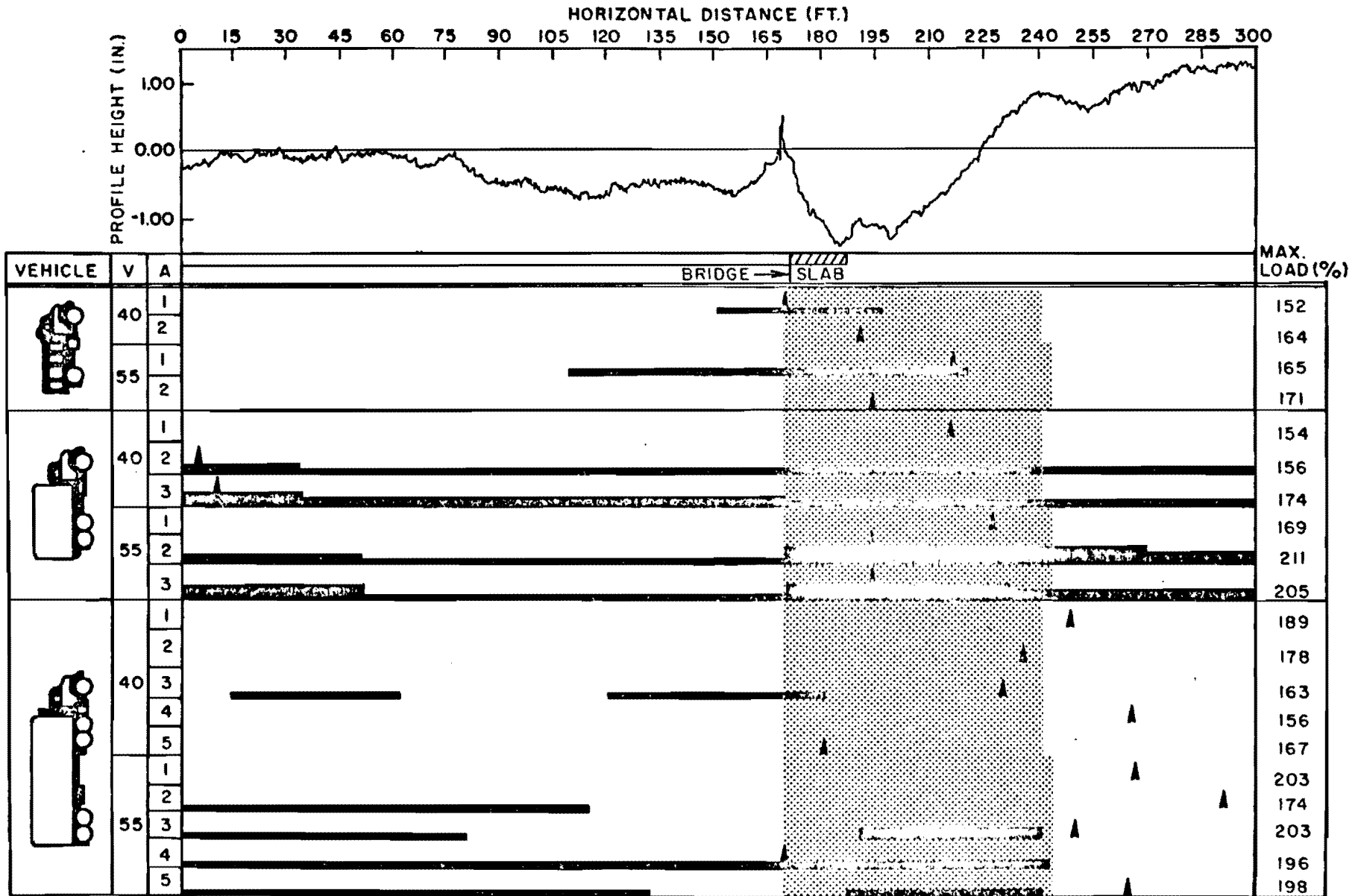


Fig A4.16A. Dynamic wheel load diagram, high frequency oscillation, Spur 326 over AT & SF Railroad (Lubbock), end of bridge.

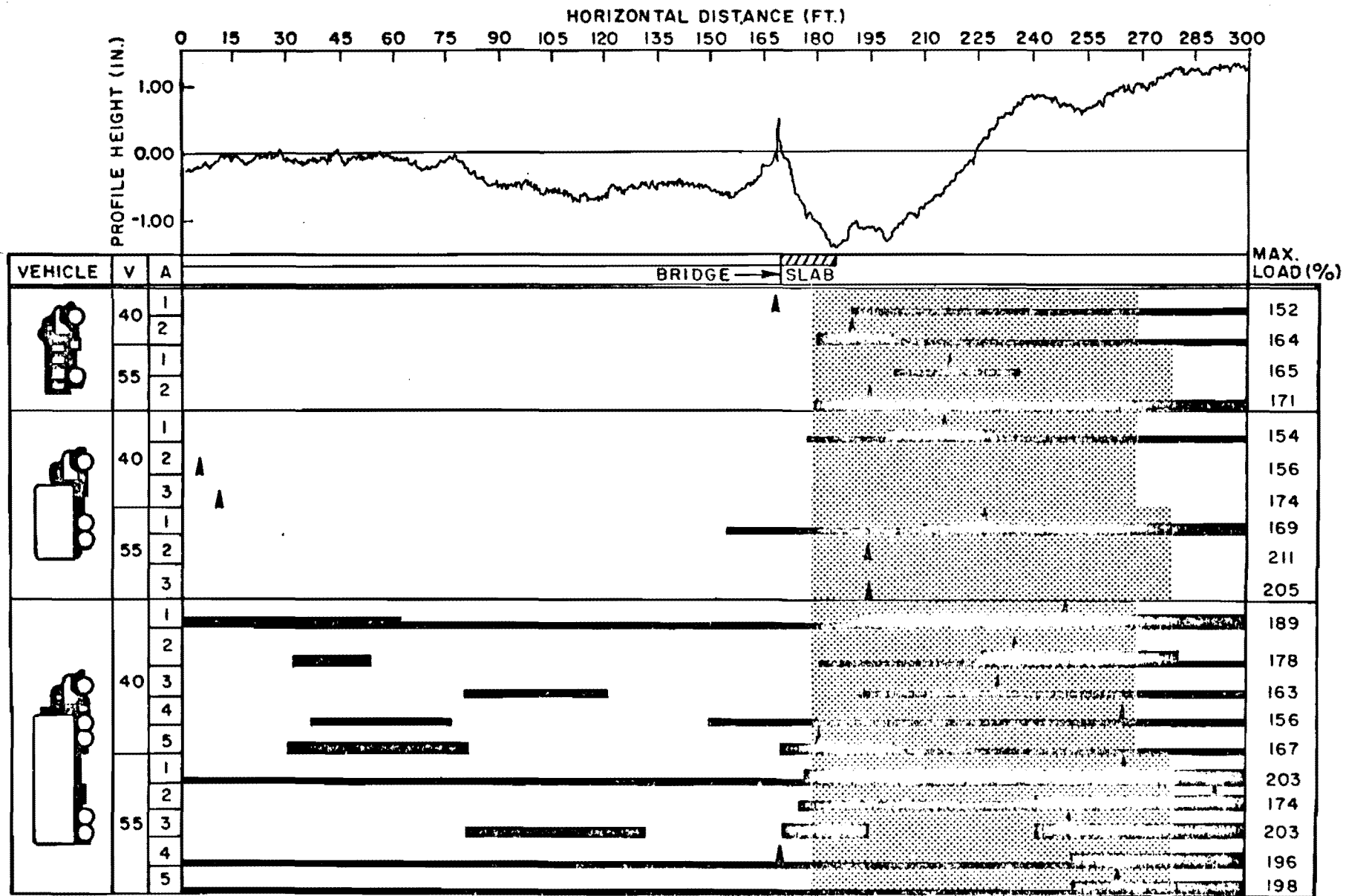


Fig A4.16B. Dynamic wheel load diagram, low frequency oscillation, Spur 326 over At & SF Railroad (Lubbock), end of bridge.

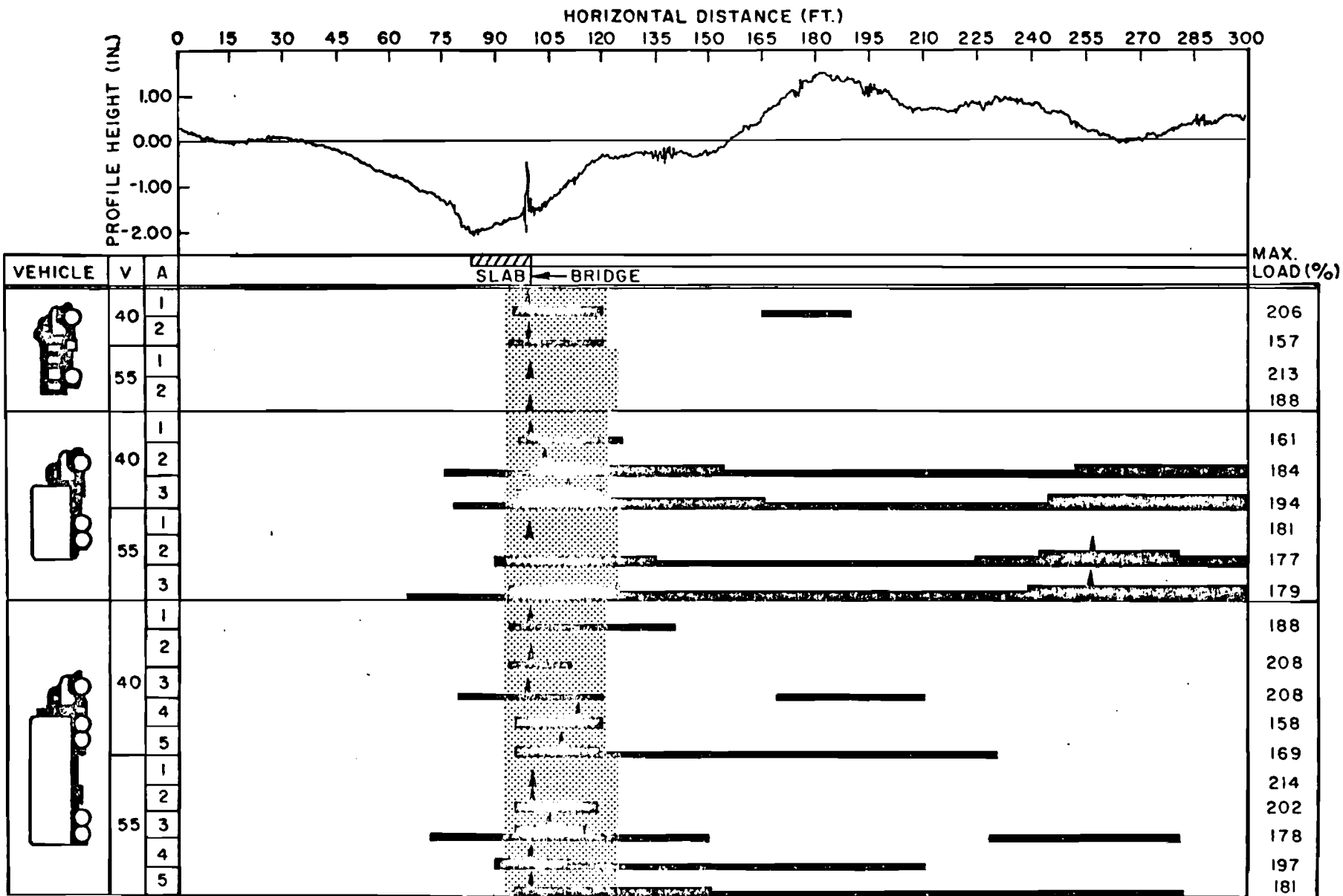


Fig A4.17A. Dynamic wheel load diagram, high frequency oscillation, Loop 289 over US 87 South (Lubbock), start of bridge.

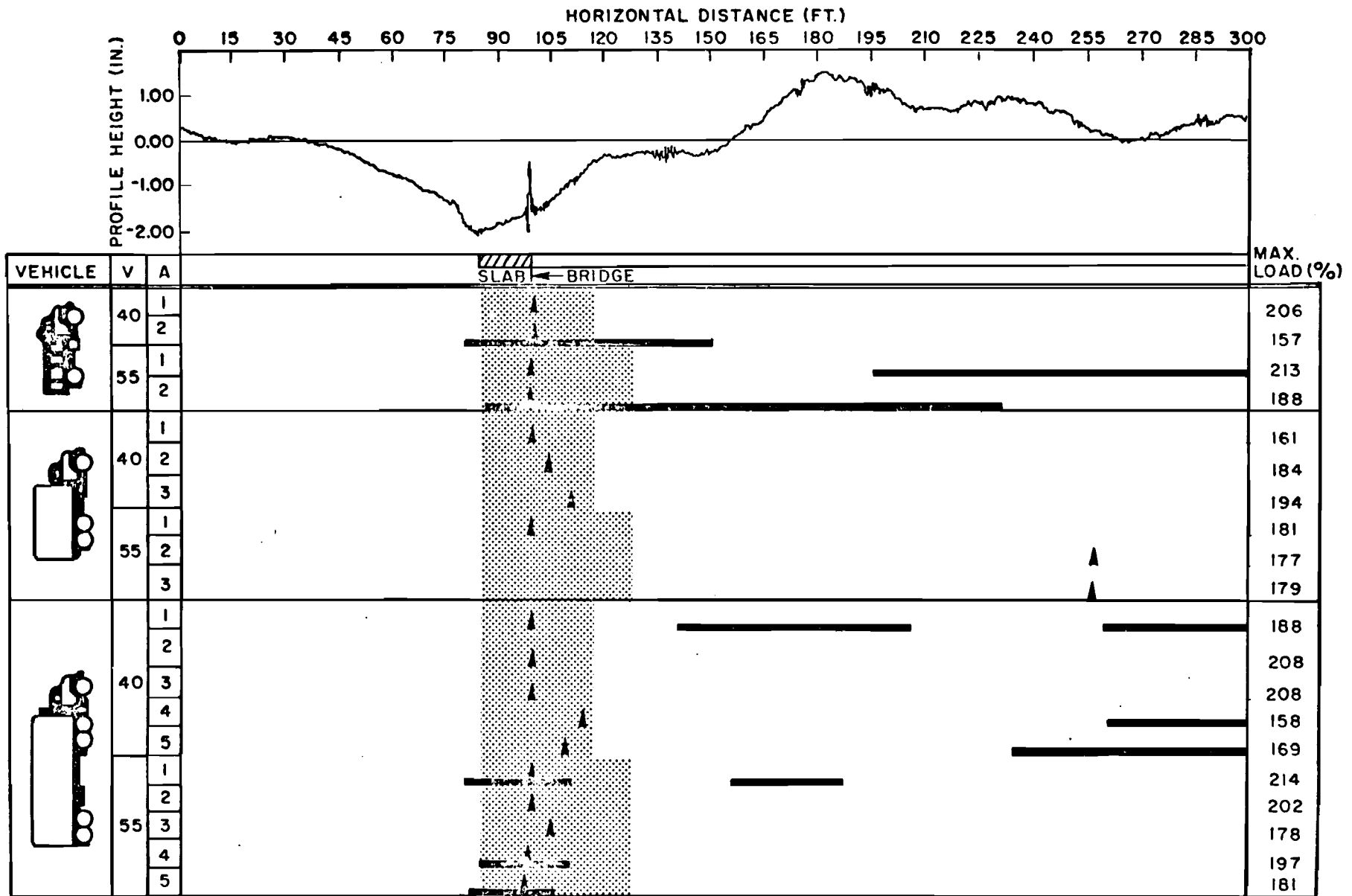
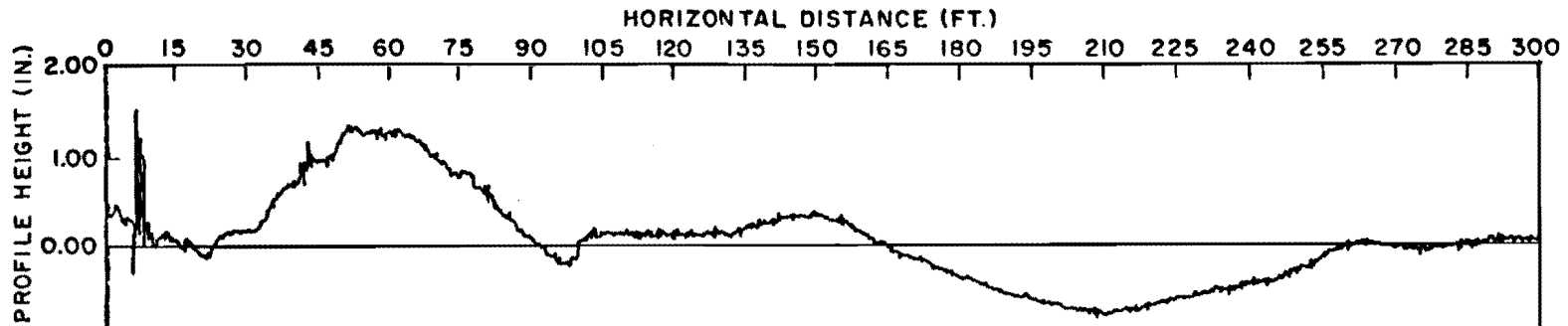


Fig A4.17B. Dynamic wheel load diagram, low frequency oscillation, Loop 289 over US 87 South (Lubbock), start of bridge.






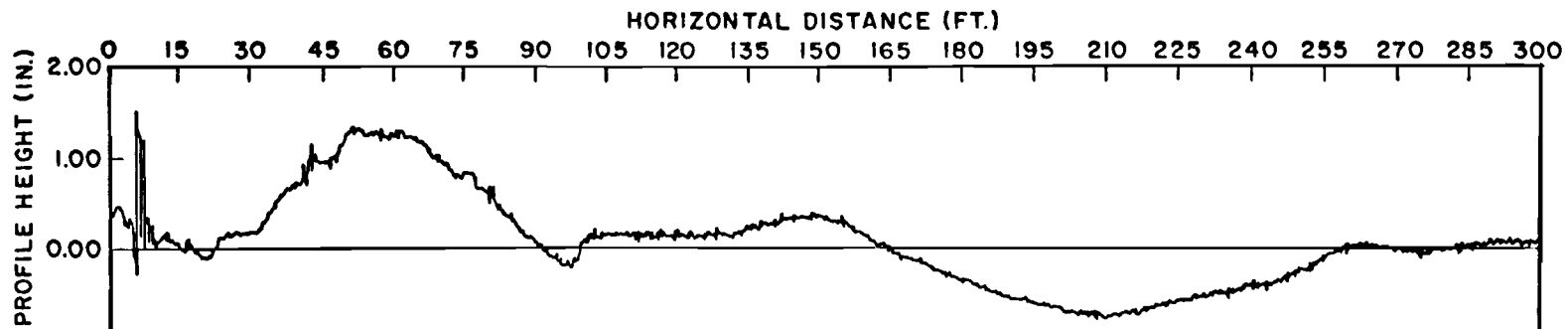
VEHICLE	V	A	BRIDGE → SLAB	MAX. LOAD (%)
	40	1	[Hatched area]	213
		2	[Hatched area]	159
	55	1	[Hatched area]	200
		2	[Hatched area]	169
	40	1	[Hatched area]	178
		2	[Hatched area]	266
		3	[Hatched area]	277
	55	1	[Hatched area]	173
		2	[Hatched area]	195
		3	[Hatched area]	203
	40	1	[Hatched area]	193
		2	[Hatched area]	228
		3	[Hatched area]	229
		4	[Hatched area]	191
		5	[Hatched area]	259
	55	1	[Hatched area]	215
		2	[Hatched area]	224
		3	[Hatched area]	223
		4	[Hatched area]	244
		5	[Hatched area]	259

Fig A4.18A. Dynamic wheel load diagram, high frequency oscillation, Loop 289 over US 87 South (Lubbock), end of bridge.



VEHICLE	V	A	BRIDGE → SLAB	MAX. LOAD (%)
	40	1		213
		2		159
	55	1		200
		2		169
	40	1		178
		2		266
		3		277
	55	1		173
		2		195
		3		203
	40	1		193
		2		228
		3		229
		4		191
		5		259
	55	1		215
		2		224
		3		223
		4		244
		5		259

Fig A4.18B. Dynamic wheel load diagram, low frequency oscillation, Loop 289 over US 87 South (Lubbock), end of bridge.

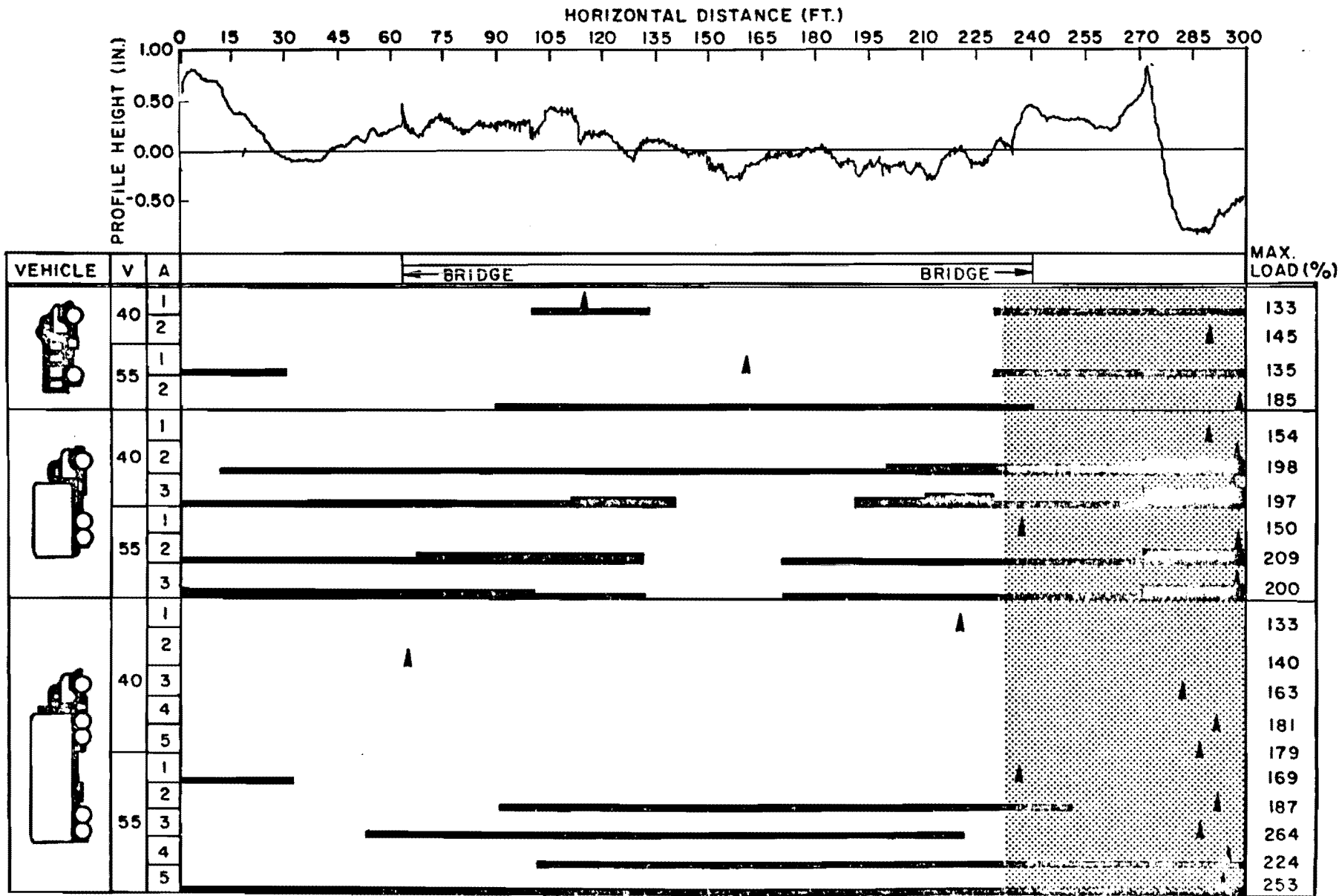


Fig A4.19A. Dynamic wheel load diagram, high frequency oscillation, US 87 South over 98th street (Lubbock).

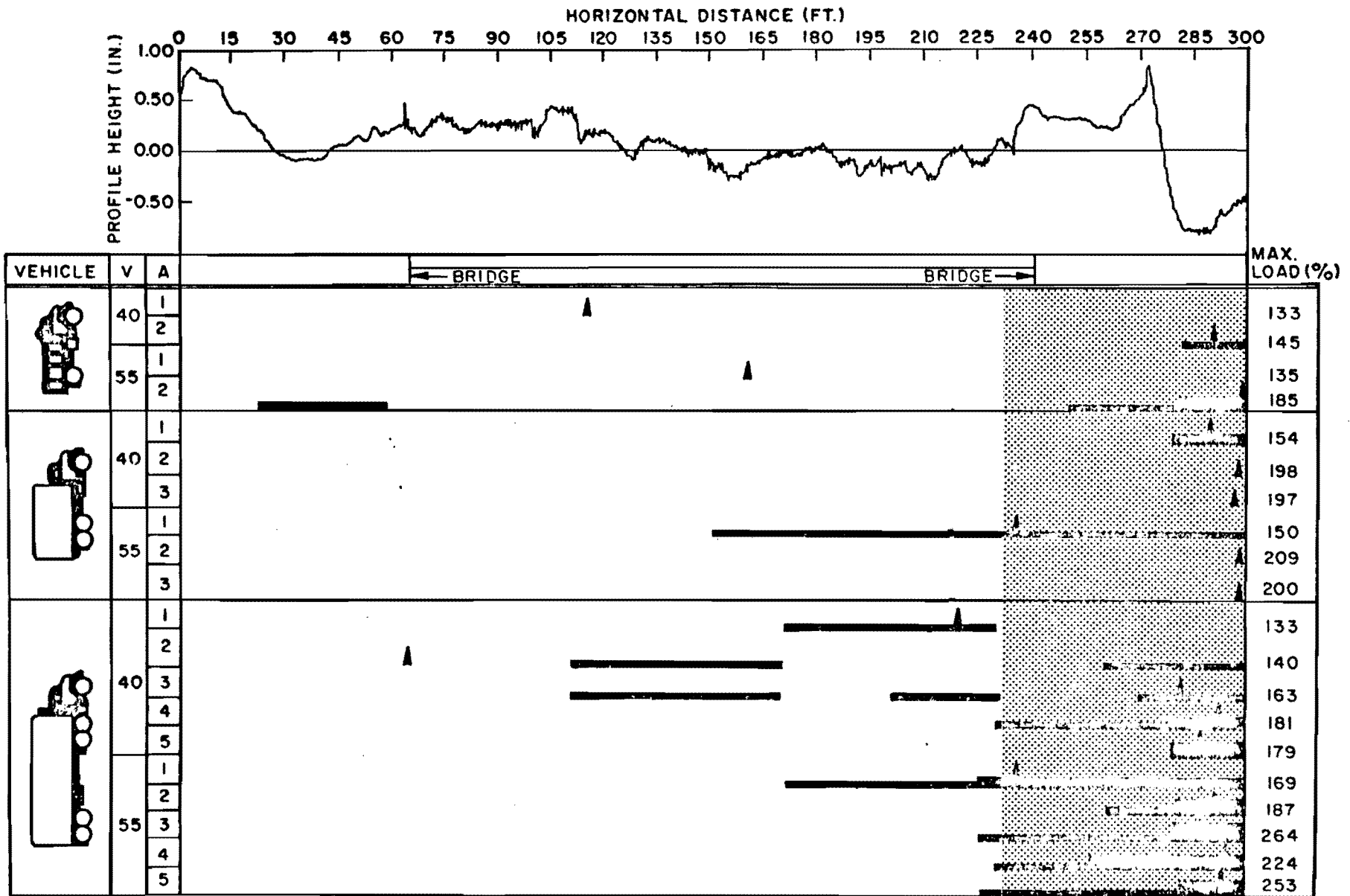


Fig A4.19B. Dynamic wheel load diagram, low frequency oscillation, US 87 South over 98th Street (Lubbock).

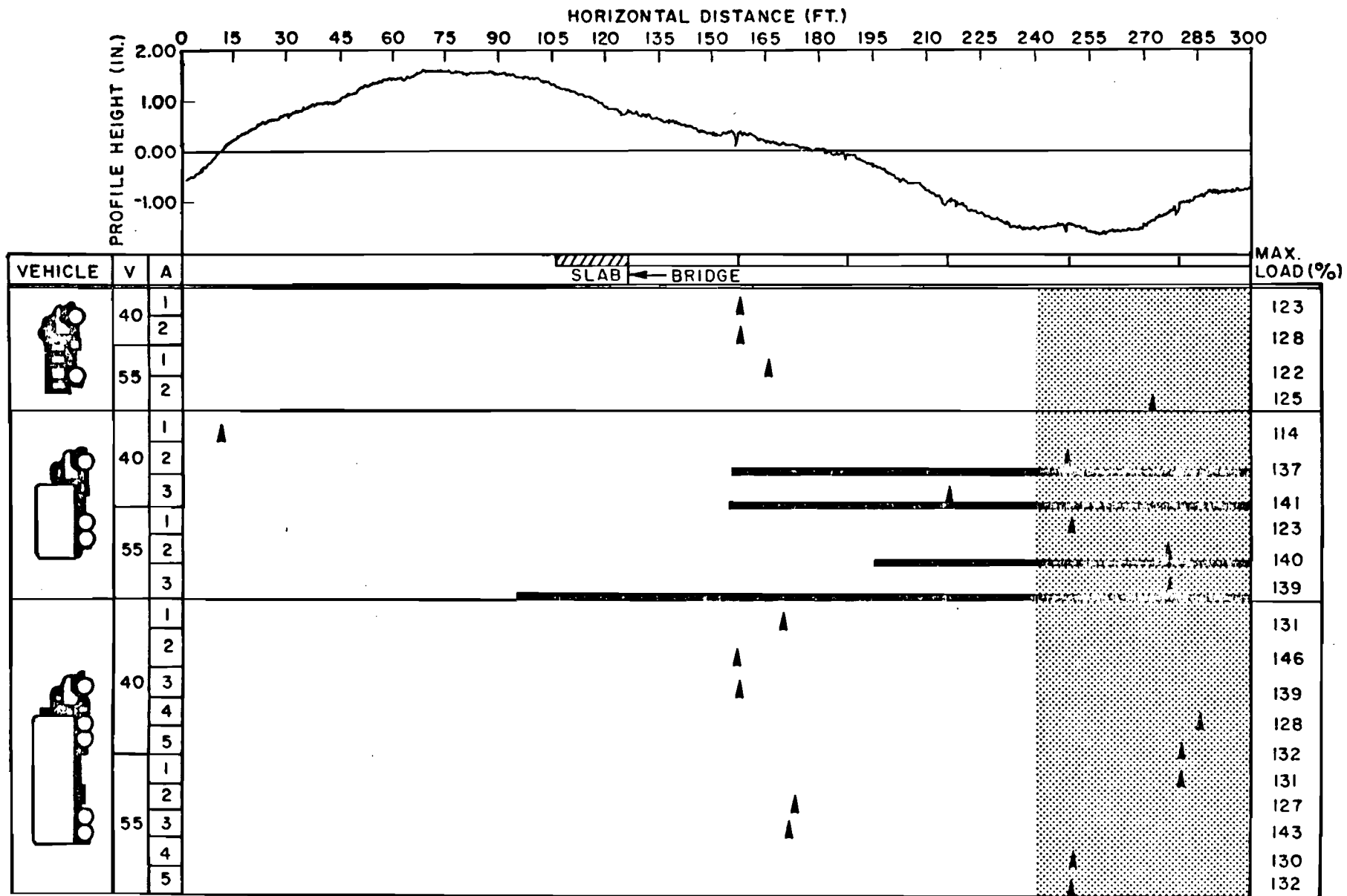


Fig A4.20A. Dynamic wheel load diagram, high frequency oscillation, US 84 over Brazos River (Lubbock), old structure, start of bridge.

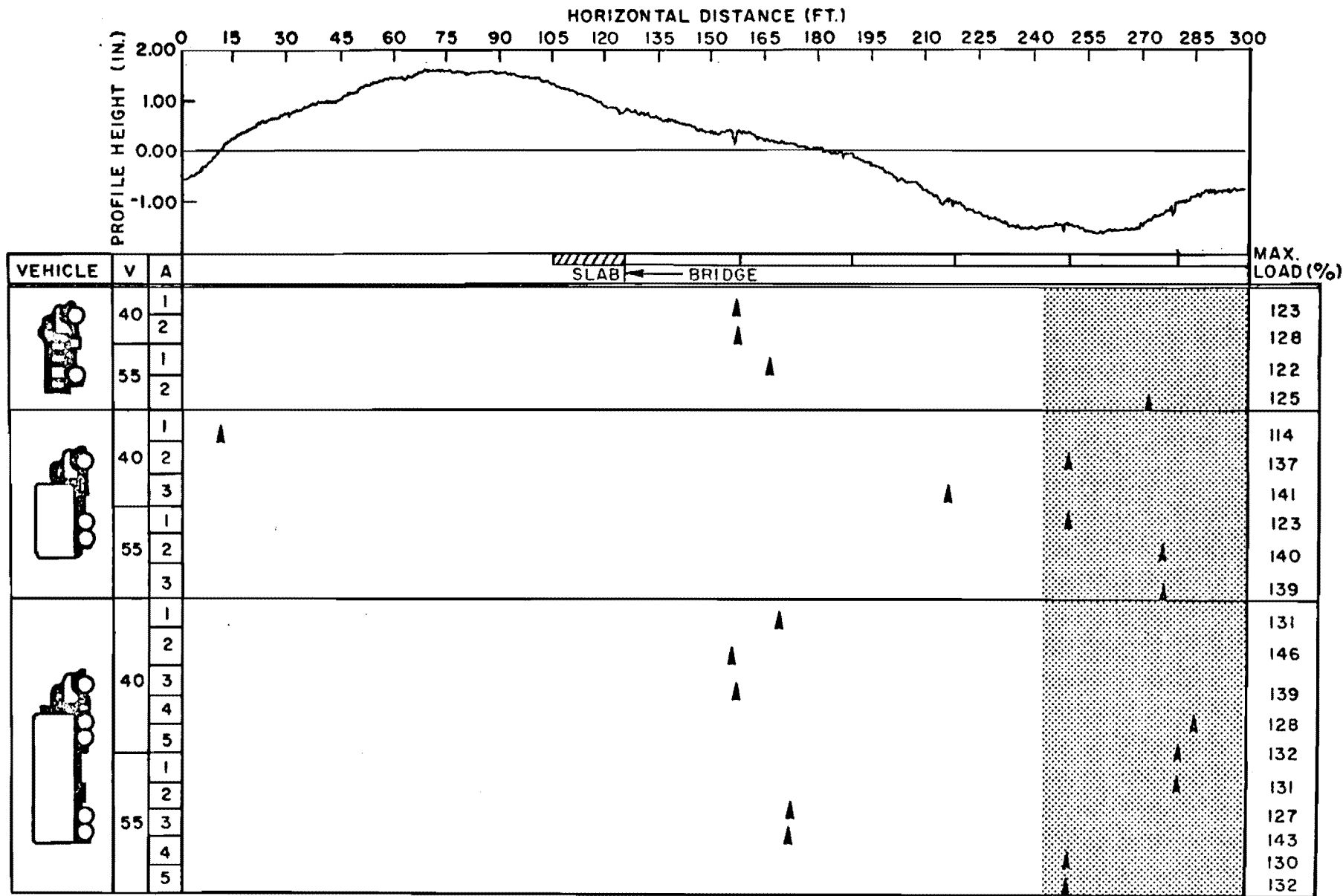


Fig A4.20B. Dynamic wheel load diagram, low frequency oscillation, US 84 over Brazos River (Lubbock), old structure, start of bridge.

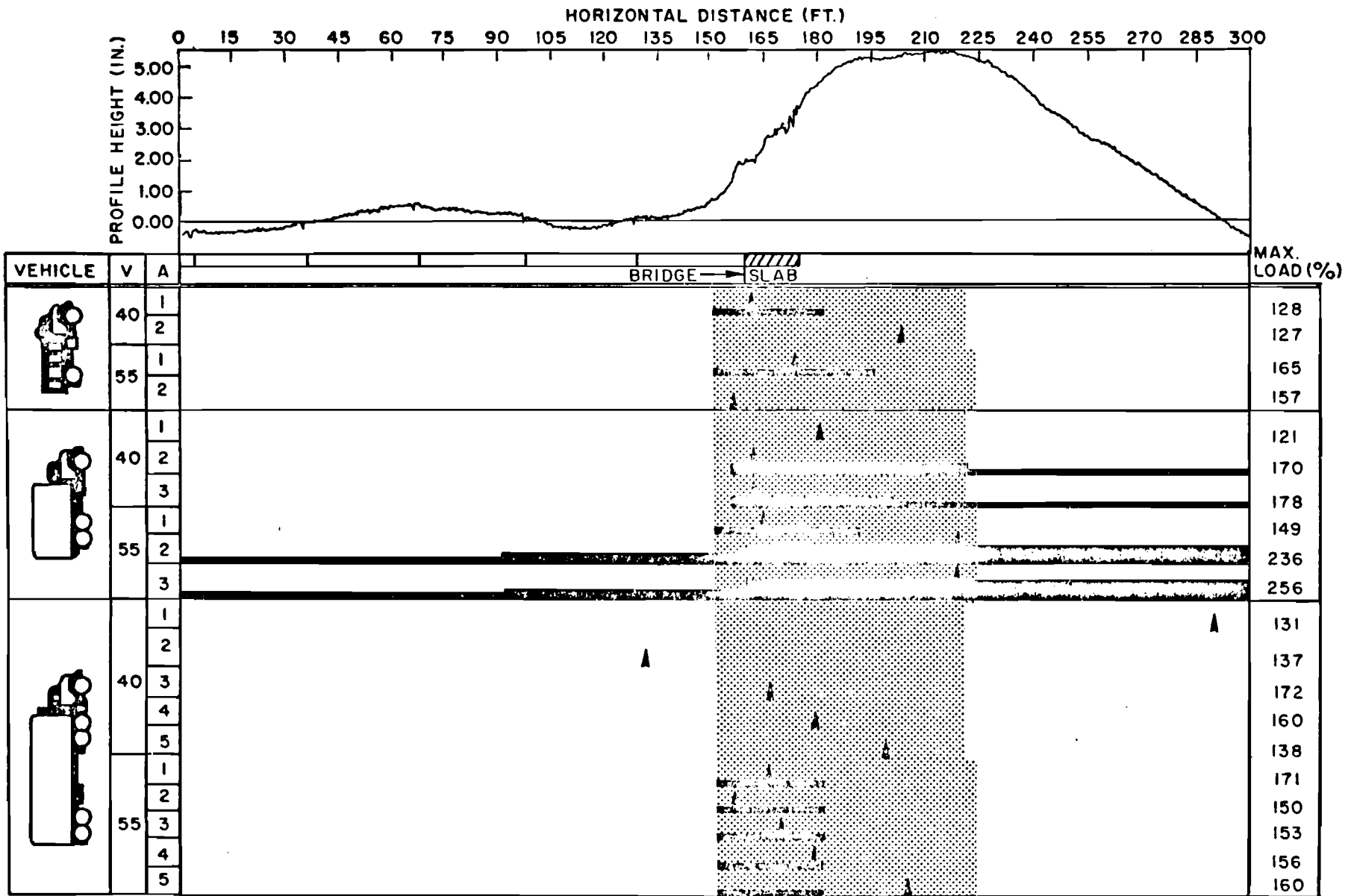


Fig A4.21A. Dynamic wheel load diagram, high frequency oscillation, US 84 over Brazos River (Lubbock), old structure, end of bridge.

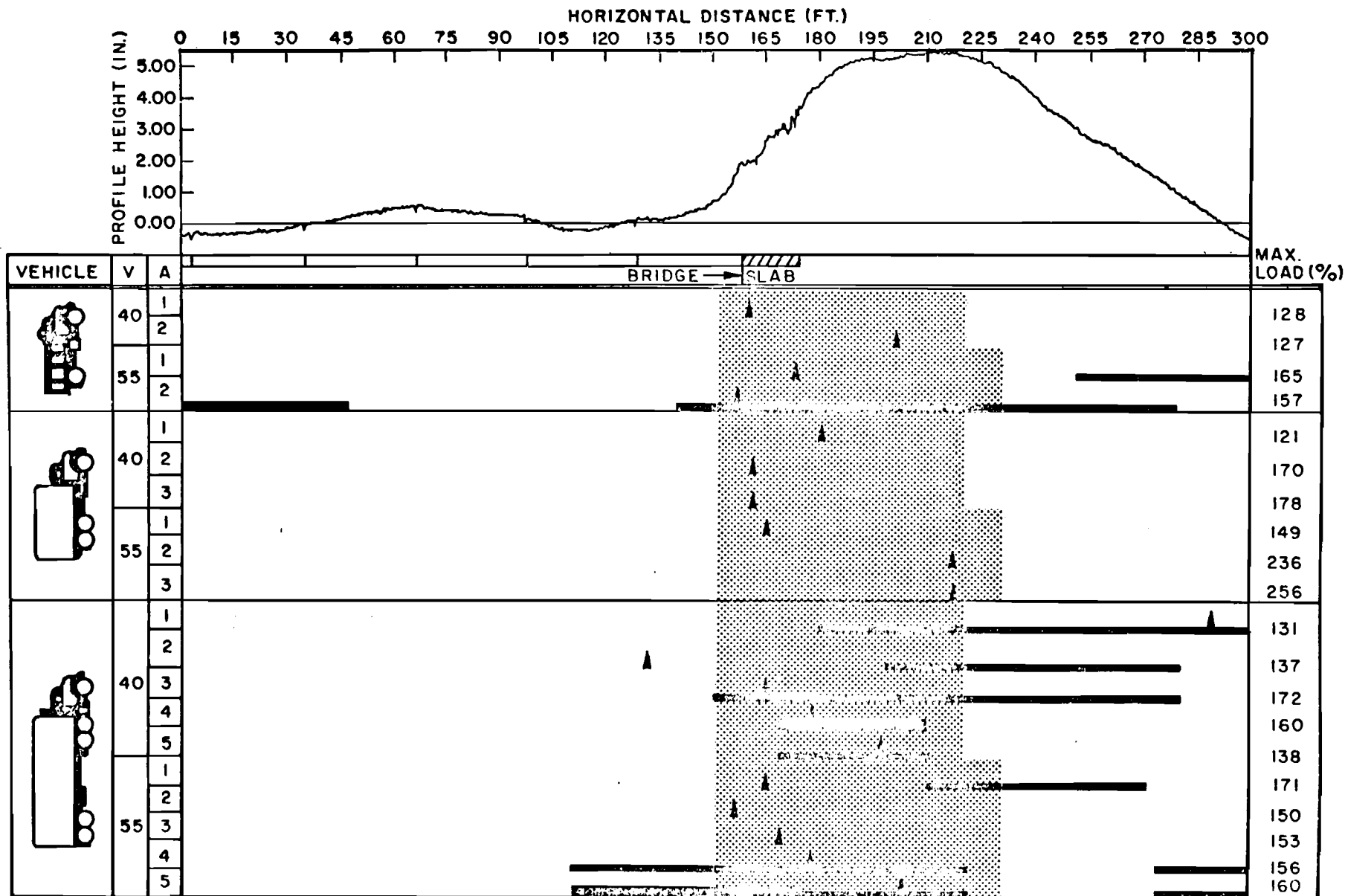


Fig A4.21B. Dynamic wheel load diagram, low frequency oscillation, US 84 over Brazos River (Lubbock), old structure, end of bridge.

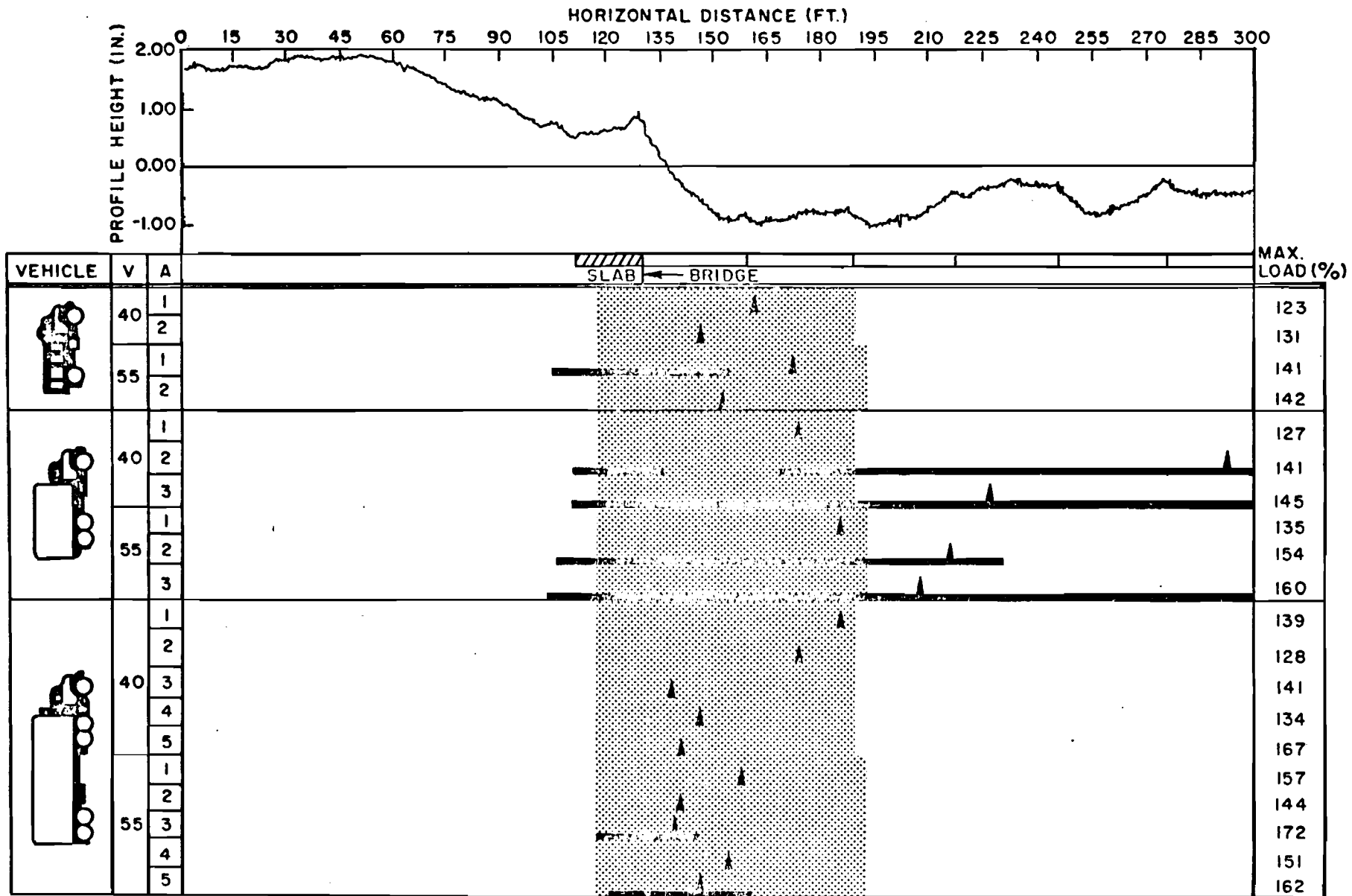


Fig A4.22A. Dynamic wheel load diagram. high frequency oscillation, US 84 over Brazos River (Lubbock), new structure, start of bridge.

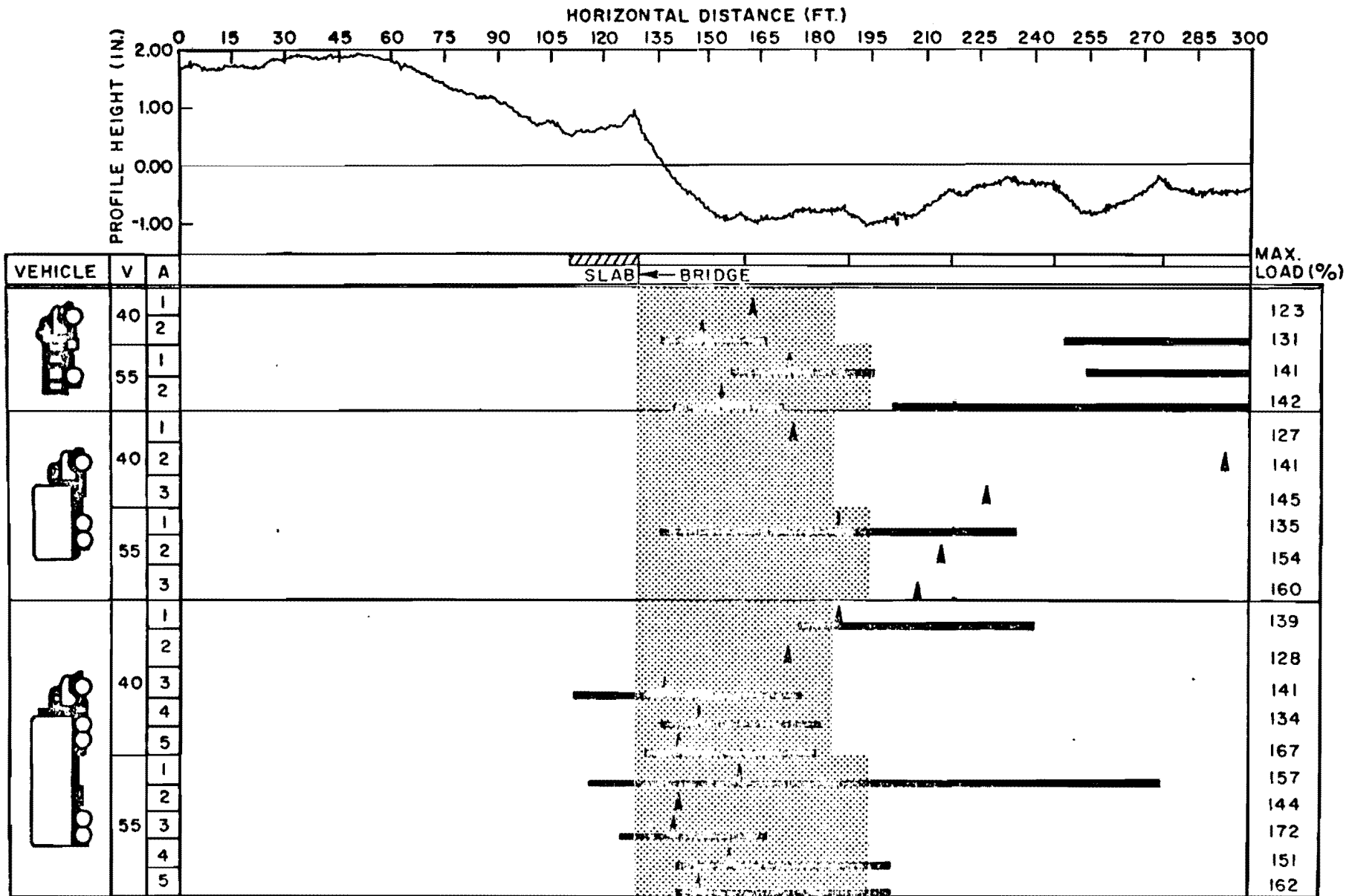


Fig A4.22B. Dynamic wheel load diagram, low frequency oscillation, US 84 over Brazos River (Lubbock), new structure, start of bridge.

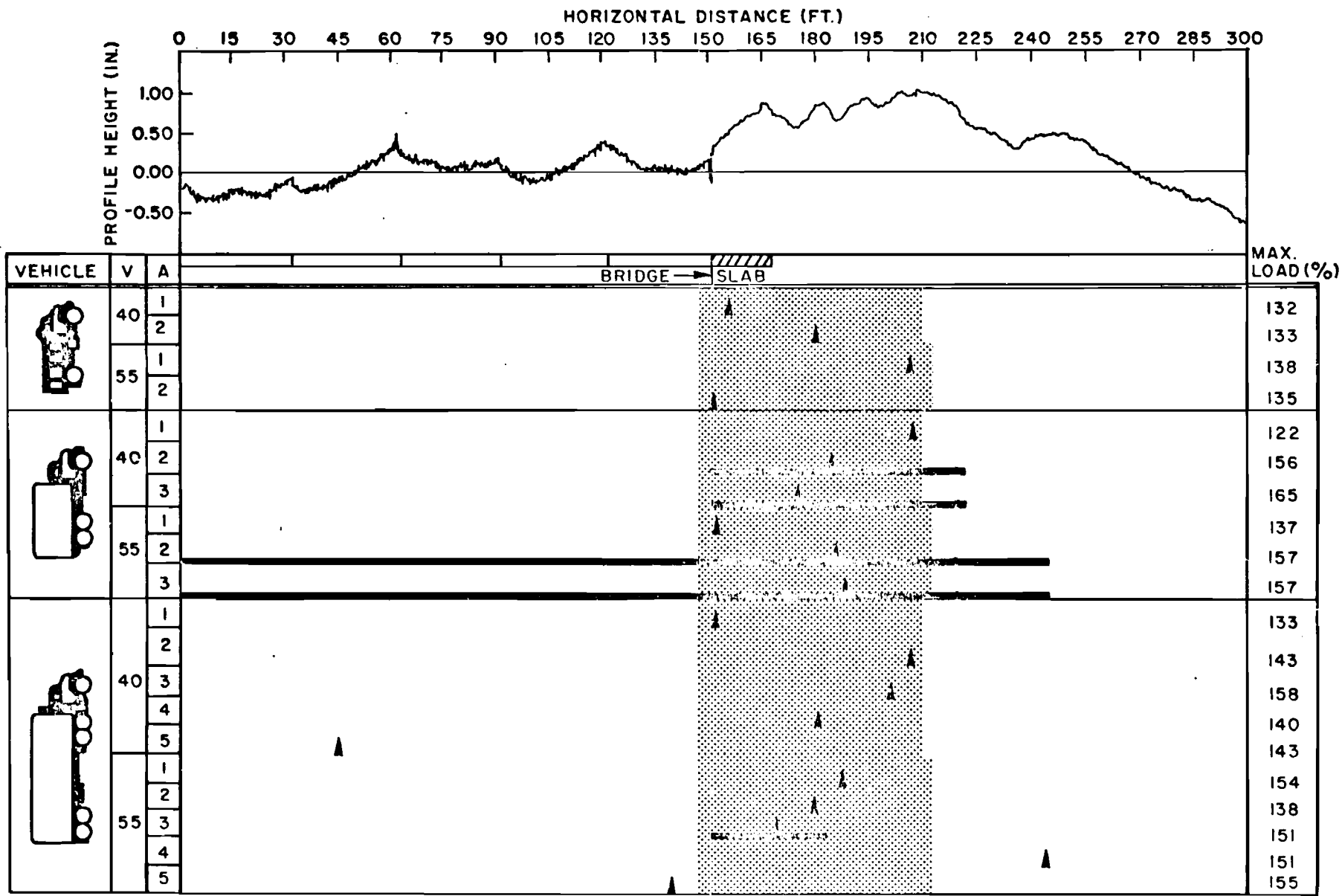


Fig. A4.23A. Dynamic wheel load diagram, high frequency oscillation, US 84 over Brazos River (Lubbock), new structure, end of bridge.

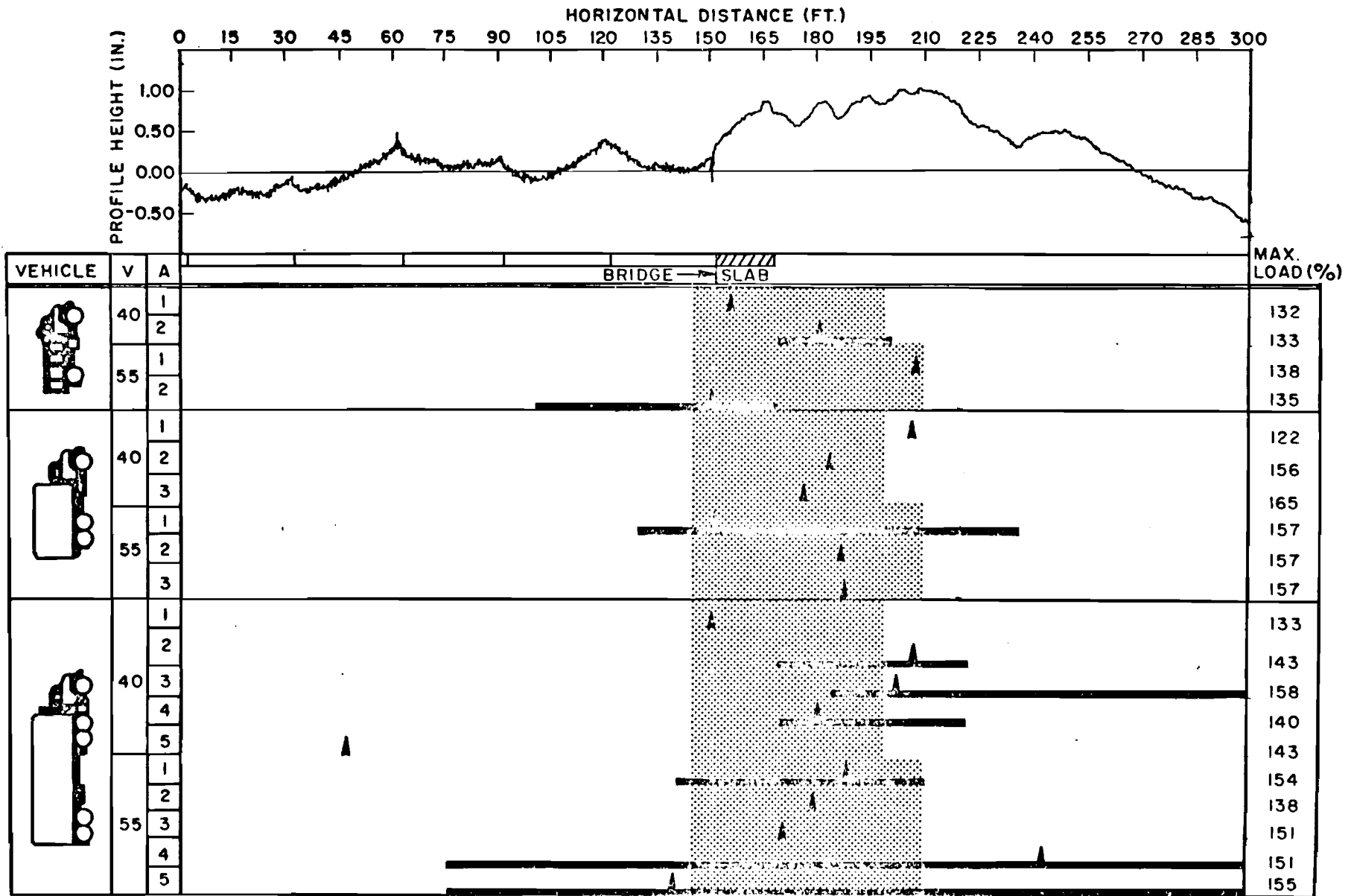


Fig A4.23B. Dynamic wheel load diagram, low frequency oscillation, US 84 over Brazos River (Lubbock), new structure, end of bridge.

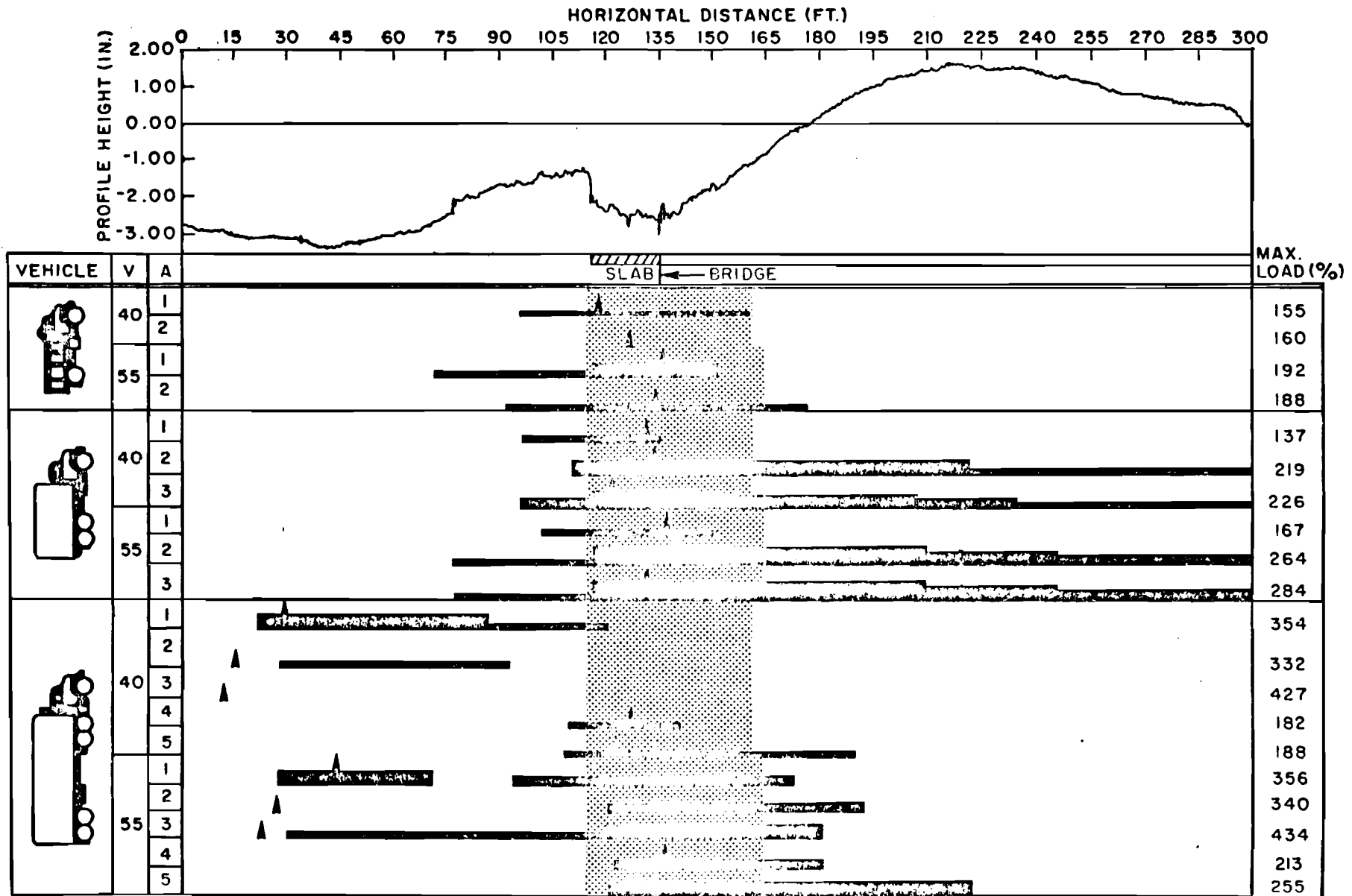


Fig A4. 24A. Dynamic wheel load diagram, high frequency oscillation, IH 45 over South Belt (Houston), start of bridge.

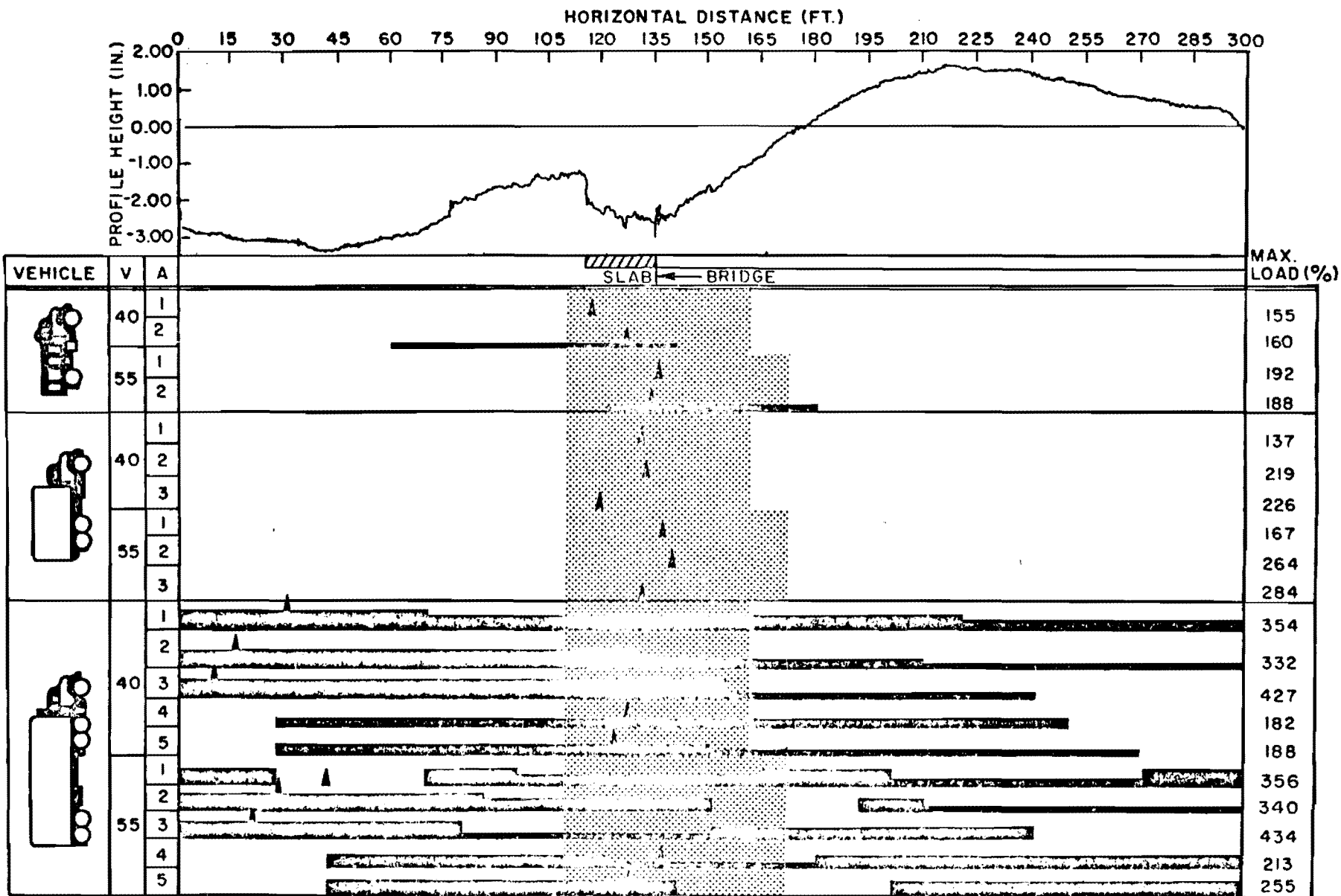


Fig A4. 24B. Dynamic wheel load diagram, low frequency oscillation, IH 45 over South Belt (Houston), start of bridge.

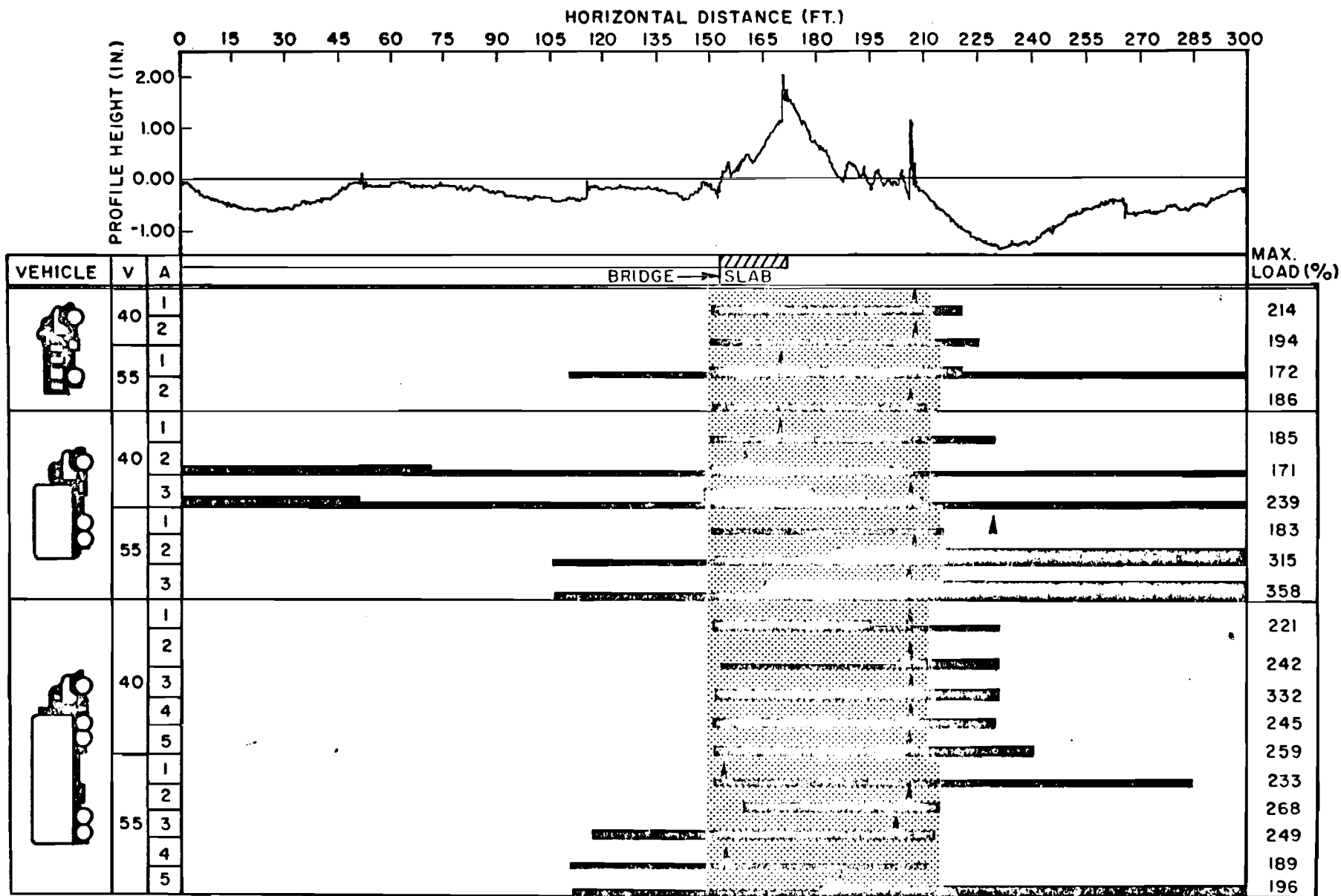


Fig A4.25A. Dynamic wheel load diagram, high frequency oscillation, IH 45 over South Belt (Houston), end of bridge.

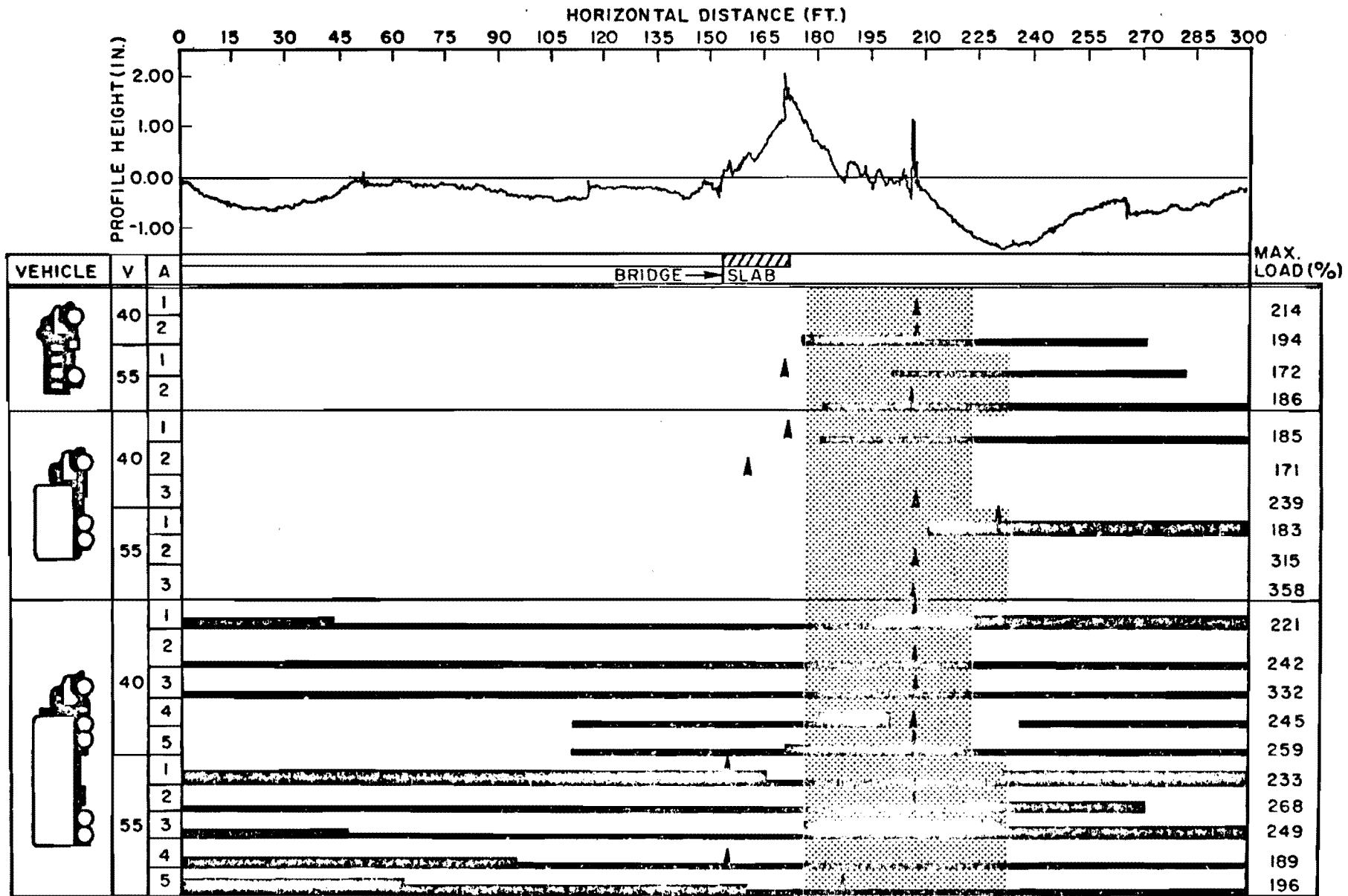
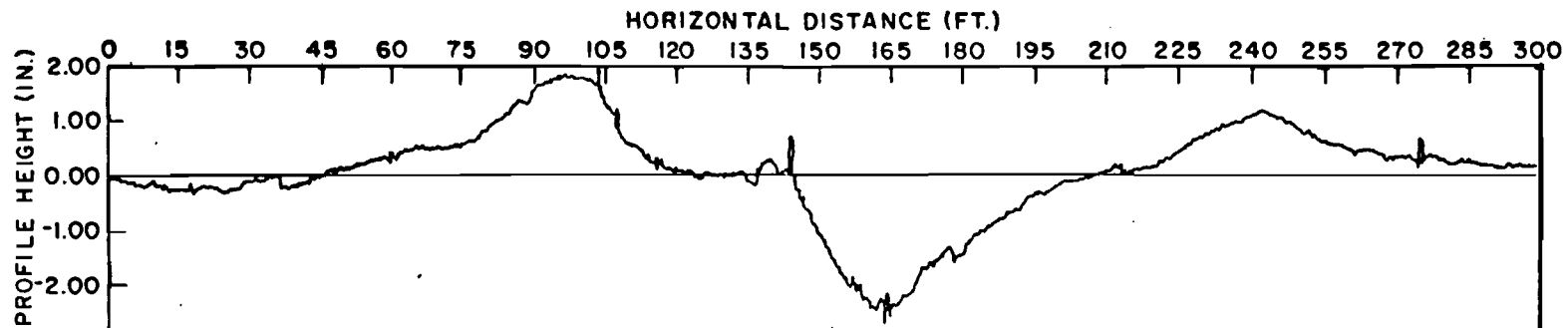


Fig A4.25B. Dynamic wheel load diagram, low frequency oscillation, IH 45 over South Belt (Houston), end of bridge.



VEHICLE	V	A	SLAB ← BRIDGE	MAX. LOAD (%)
	40	1		174
		2		197
	55	1		194
		2		190
	40	1		163
		2		219
		3		314
	55	1		189
		2		194
		3		192
	40	1		190
		2		177
		3		189
		4		169
		5		228
	55	1		203
		2		194
		3		228
		4		198
		5		214

Fig A4.26A. Dynamic wheel load diagram, high frequency oscillation, SH 225 Shell Overpass (Houston), start of bridge.

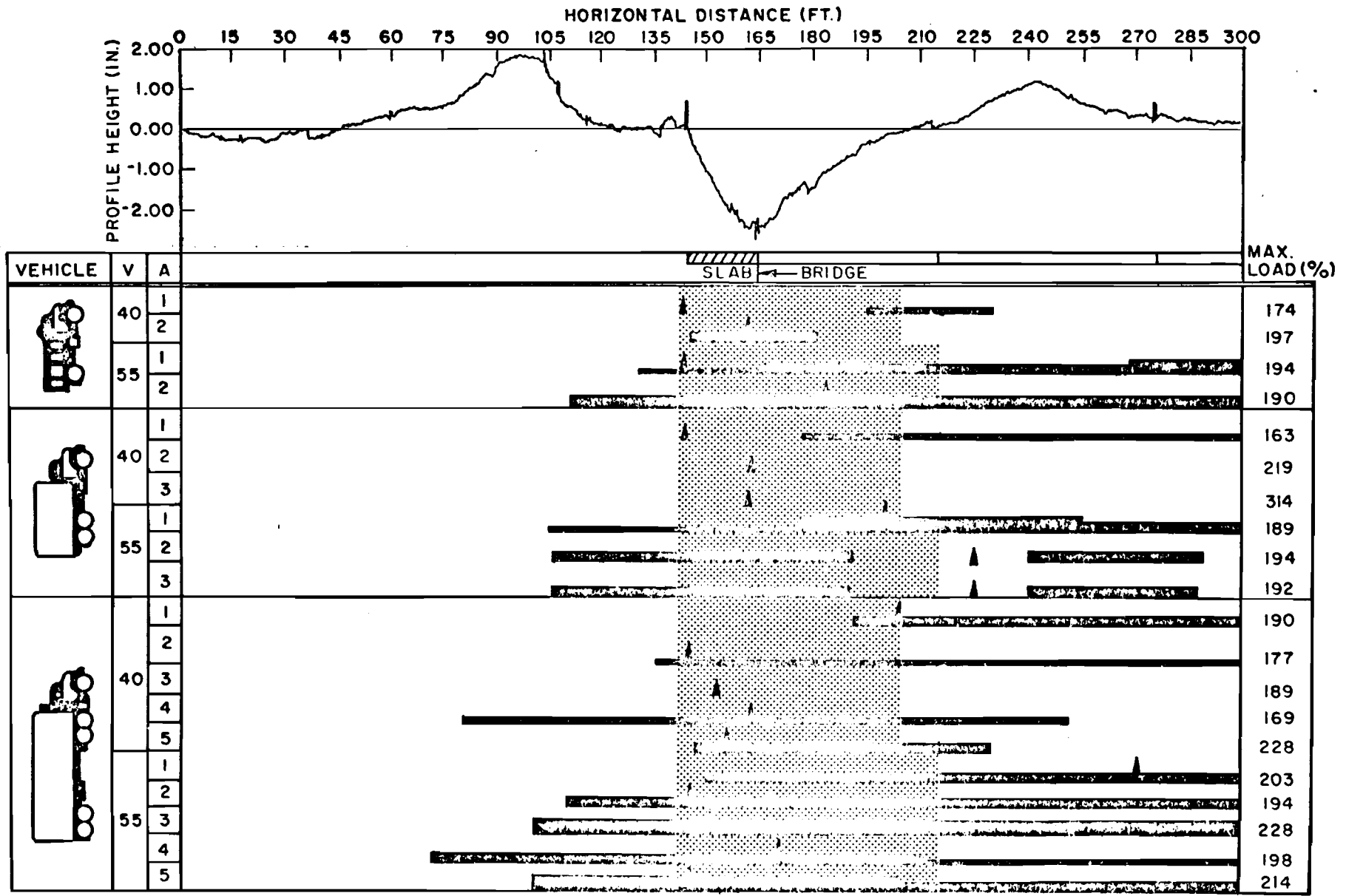


Fig A4.26B. Dynamic wheel load diagram, low frequency oscillation. SH 225 Shell Overpass (Houston), start of bridge.

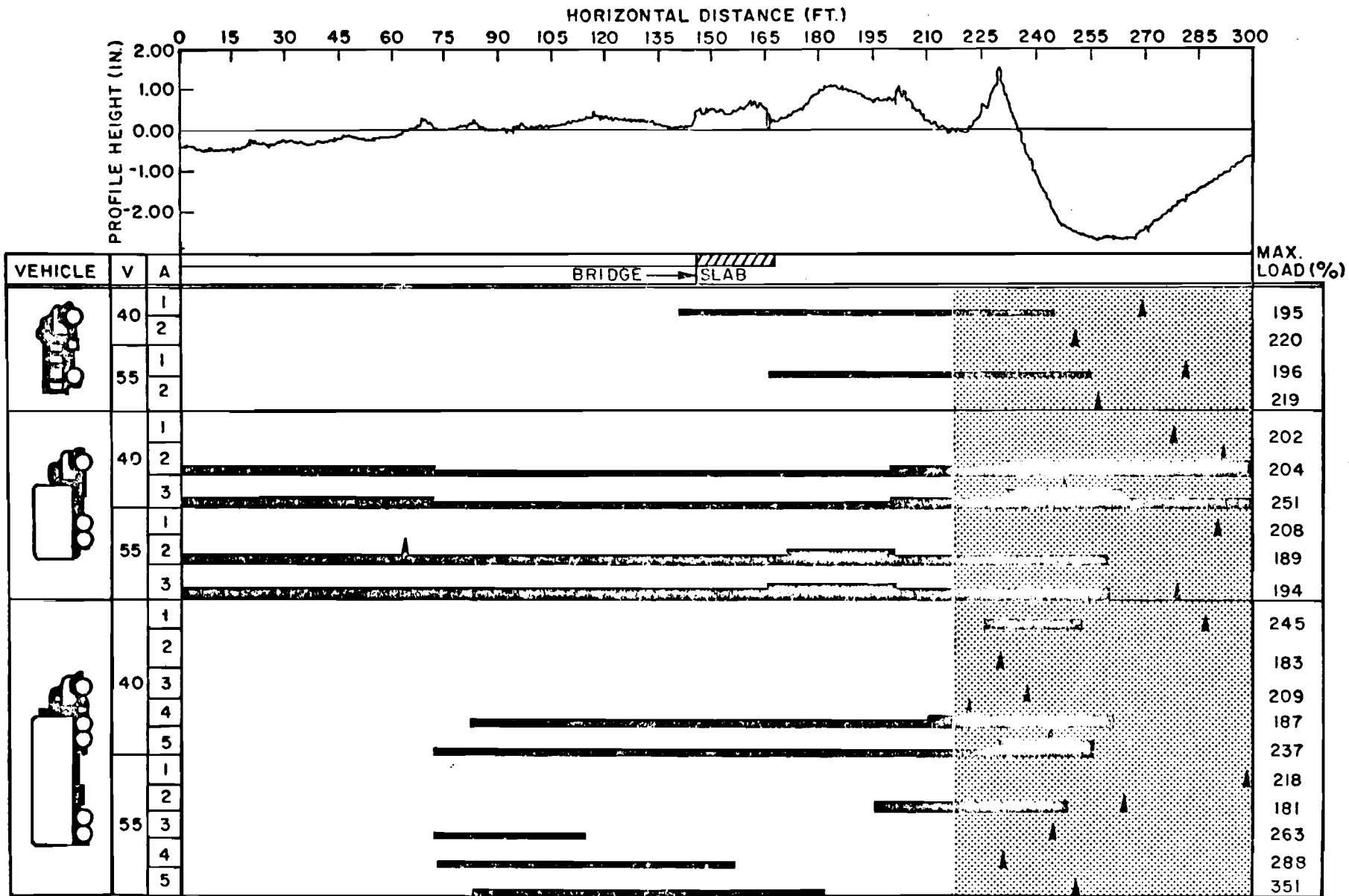


Fig A4.27A. Dynamic wheel load diagram, high frequency oscillation, SH 225 Shell Overpass (Houston), end of bridge.

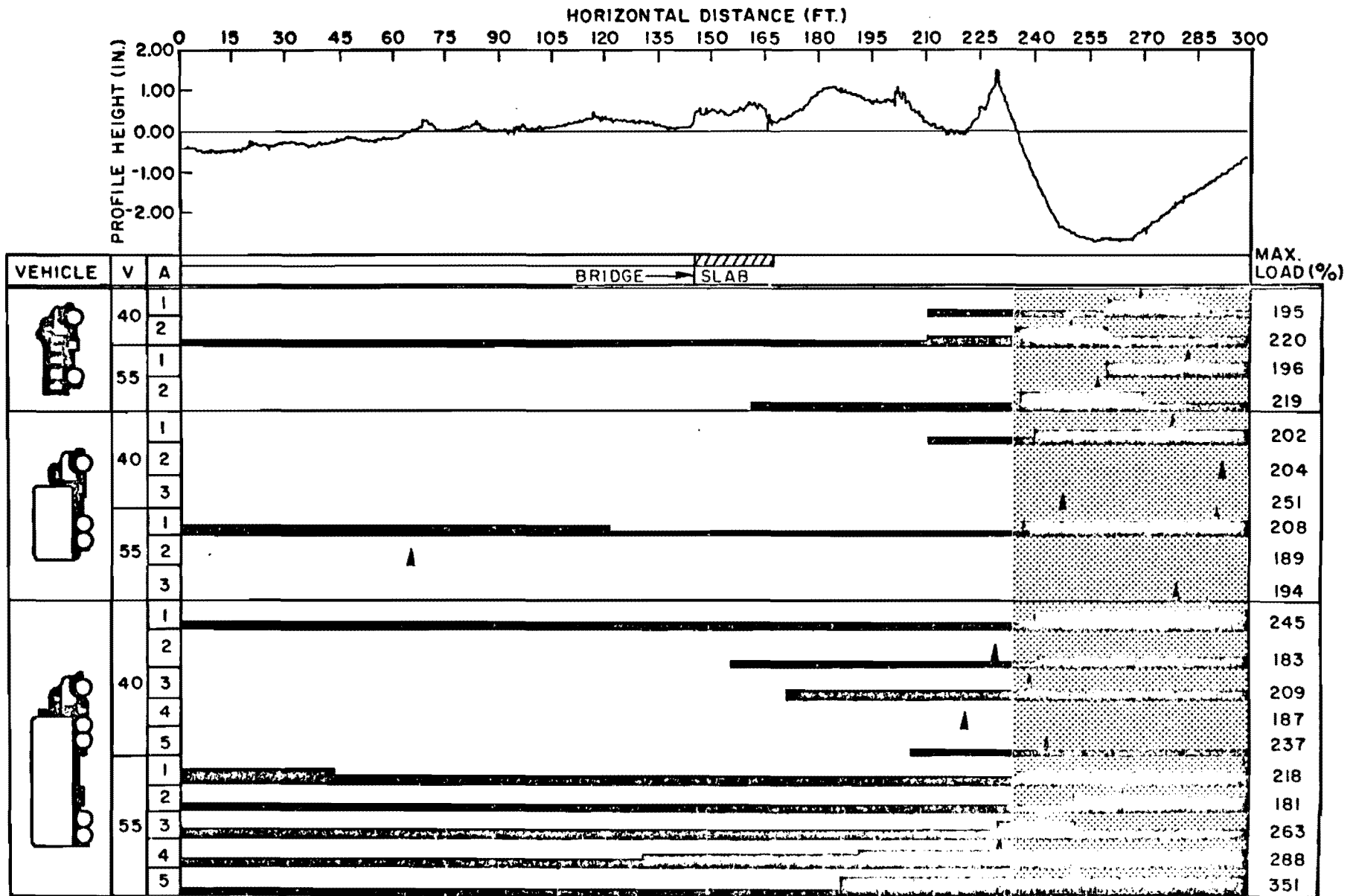


Fig A4.27B. Dynamic wheel load diagram, low frequency oscillation, SH 225 Shell Overpass (Houston), end of bridge.

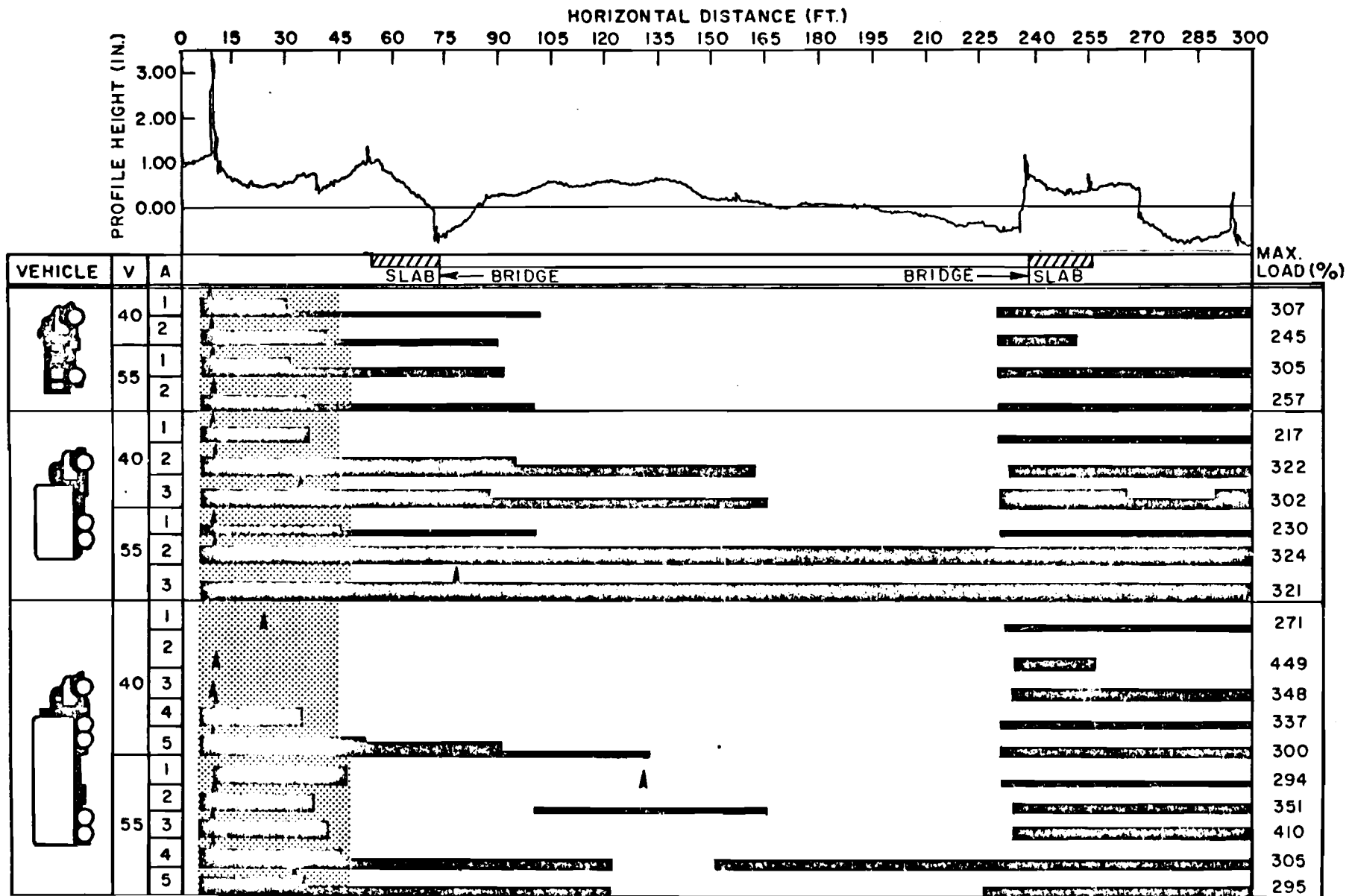


Fig A4.28A. Dynamic wheel load diagram, high frequency oscillation, SH 225 over Scarborough Lane (Houston).

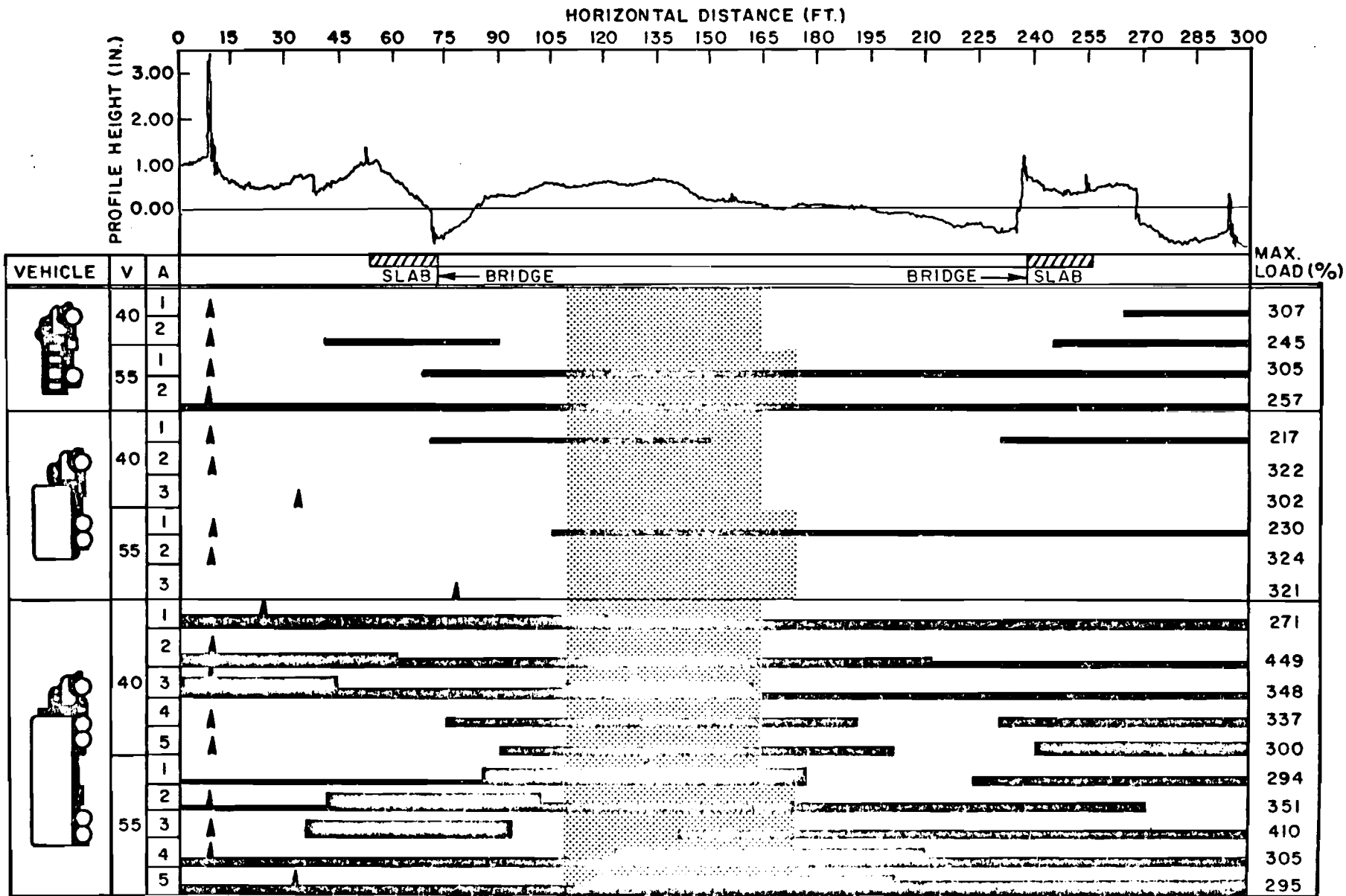
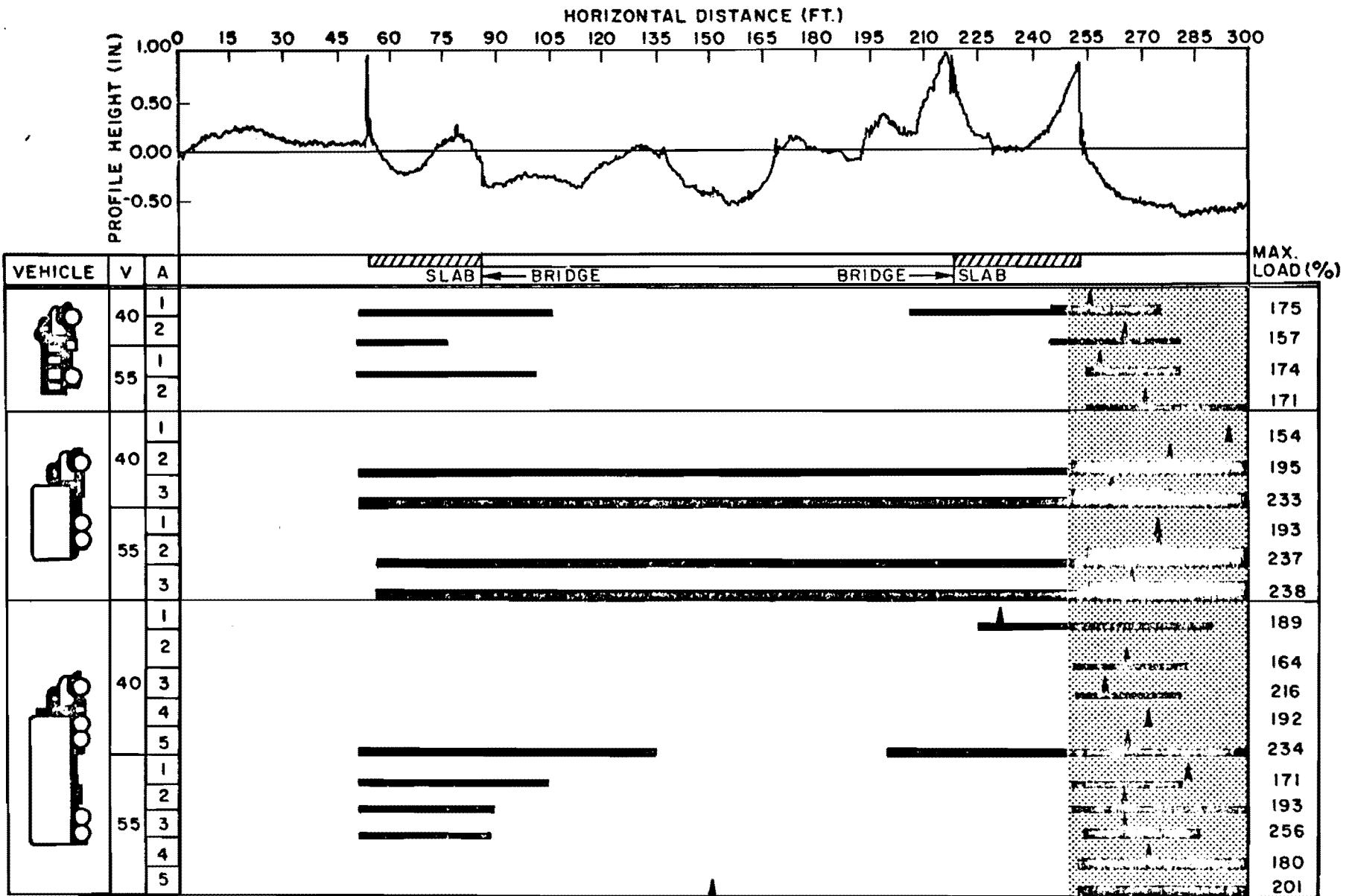


Fig A4. 28B. Dynamic wheel load diagram, low frequency oscillation, SH 225 over Scarborough Lane (Houston).



FigA4. 29A. Dynamic wheel load diagram, high frequency oscillation, South Loop over Calais Street (Houston).

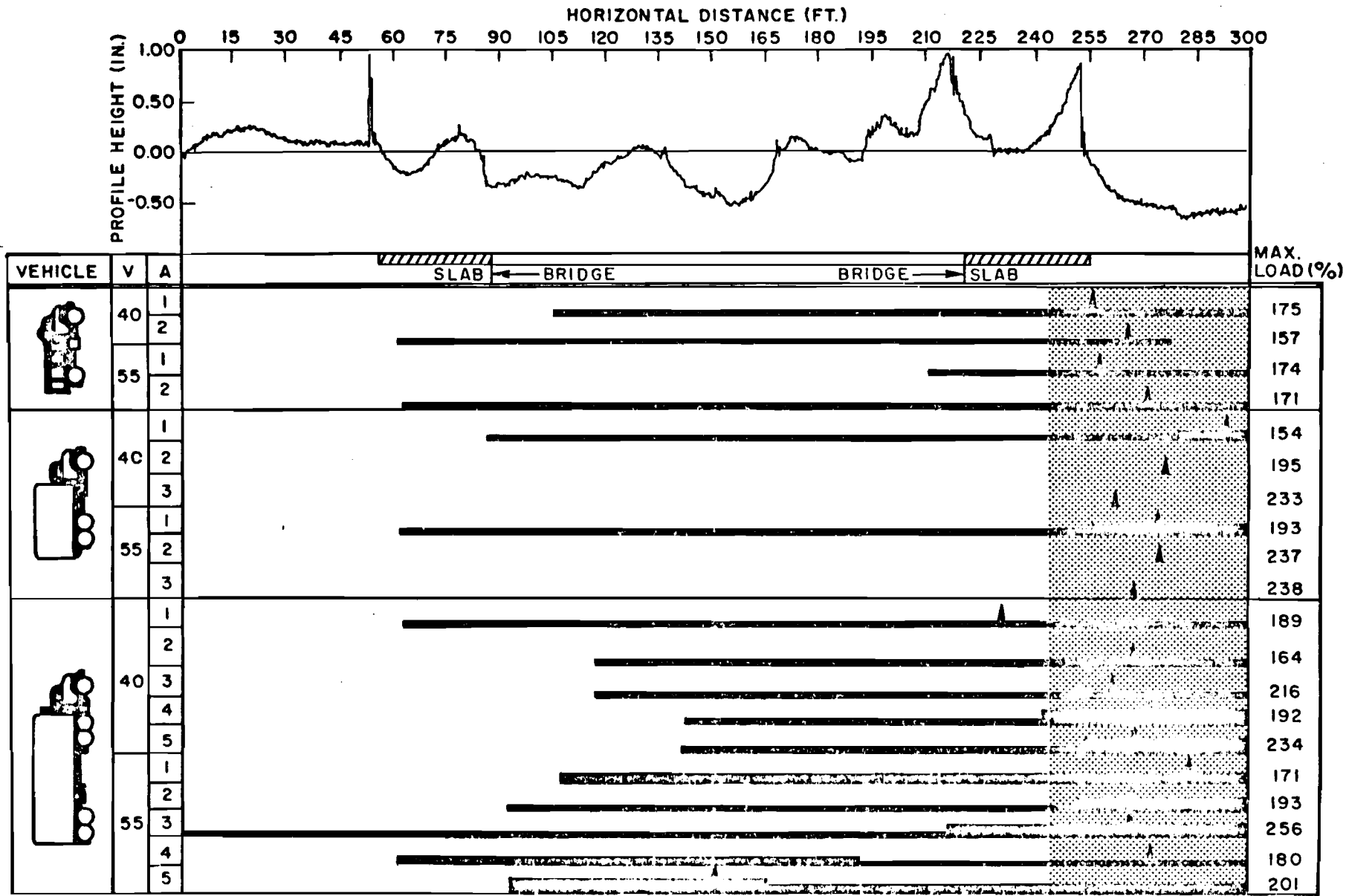


Fig A4. 29B. Dynamic wheel load diagram, low frequency oscillation, South Loop over Calais Street (Houston).

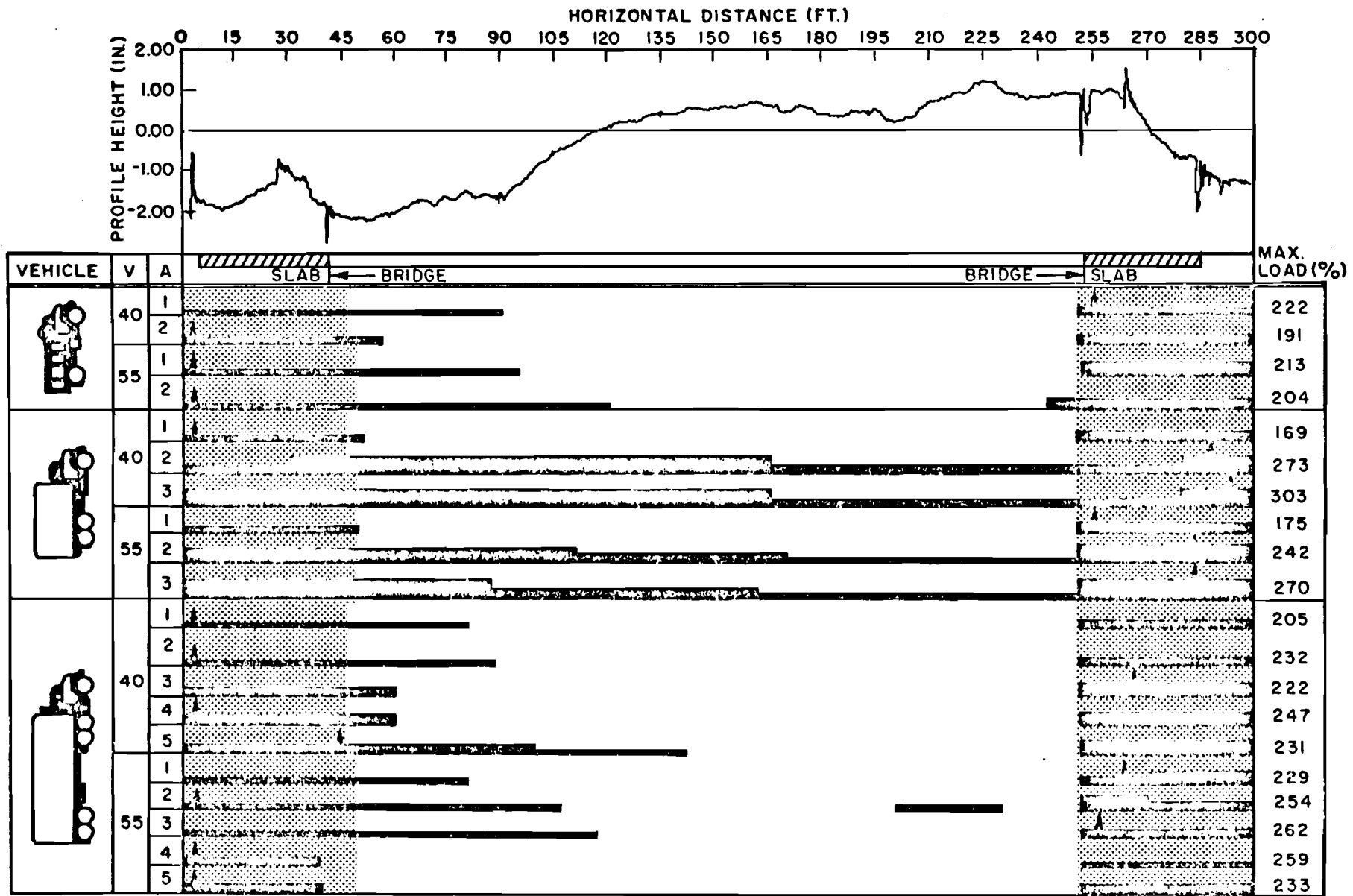


Fig A4. 30A. Dynamic wheel load diagram, high frequency oscillation, South Loop over SH 288 (Houston).

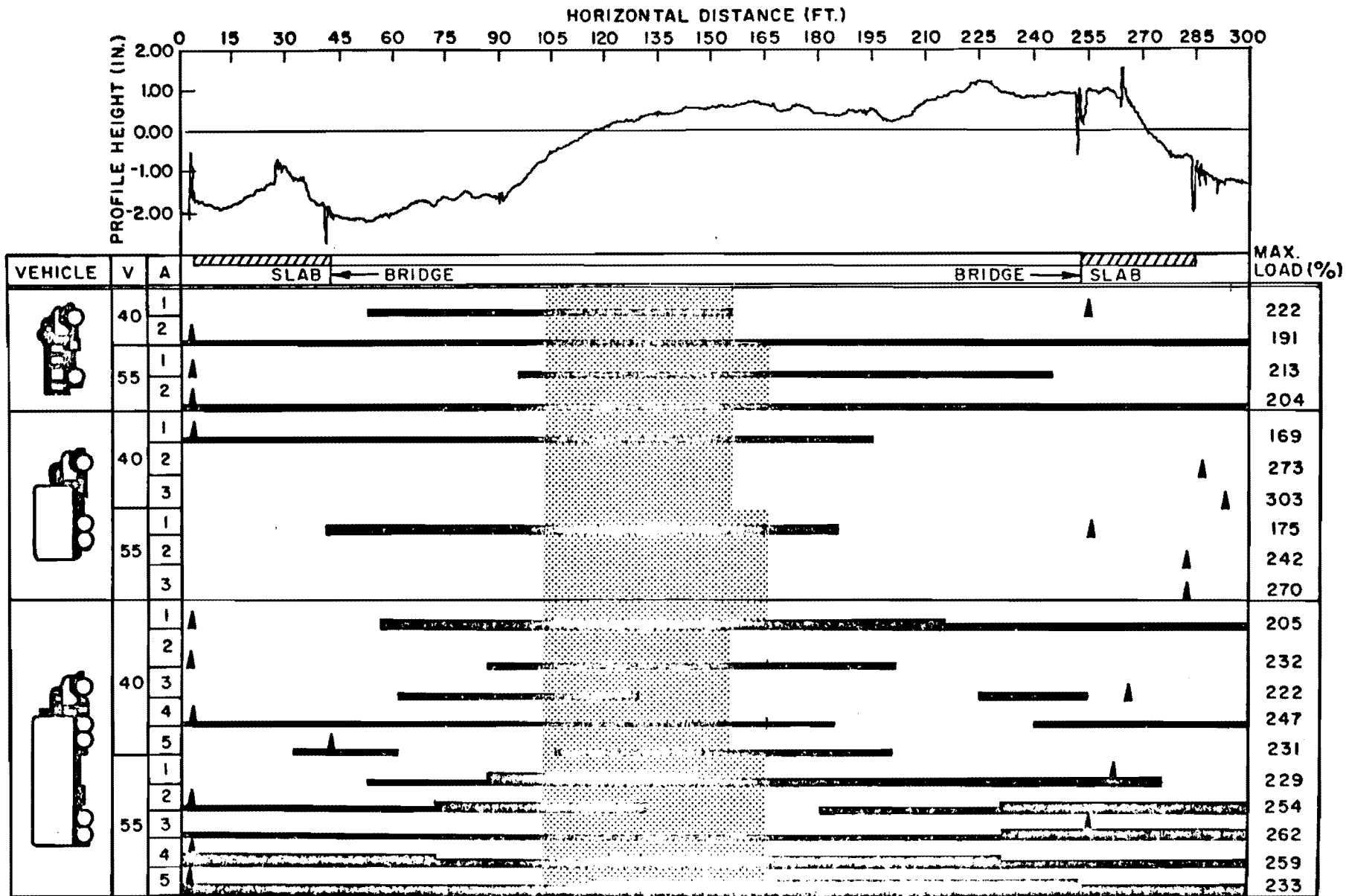


Fig A4.30B. Dynamic wheel load diagram, low frequency oscillation, South Loop over SH 288 (Houston).

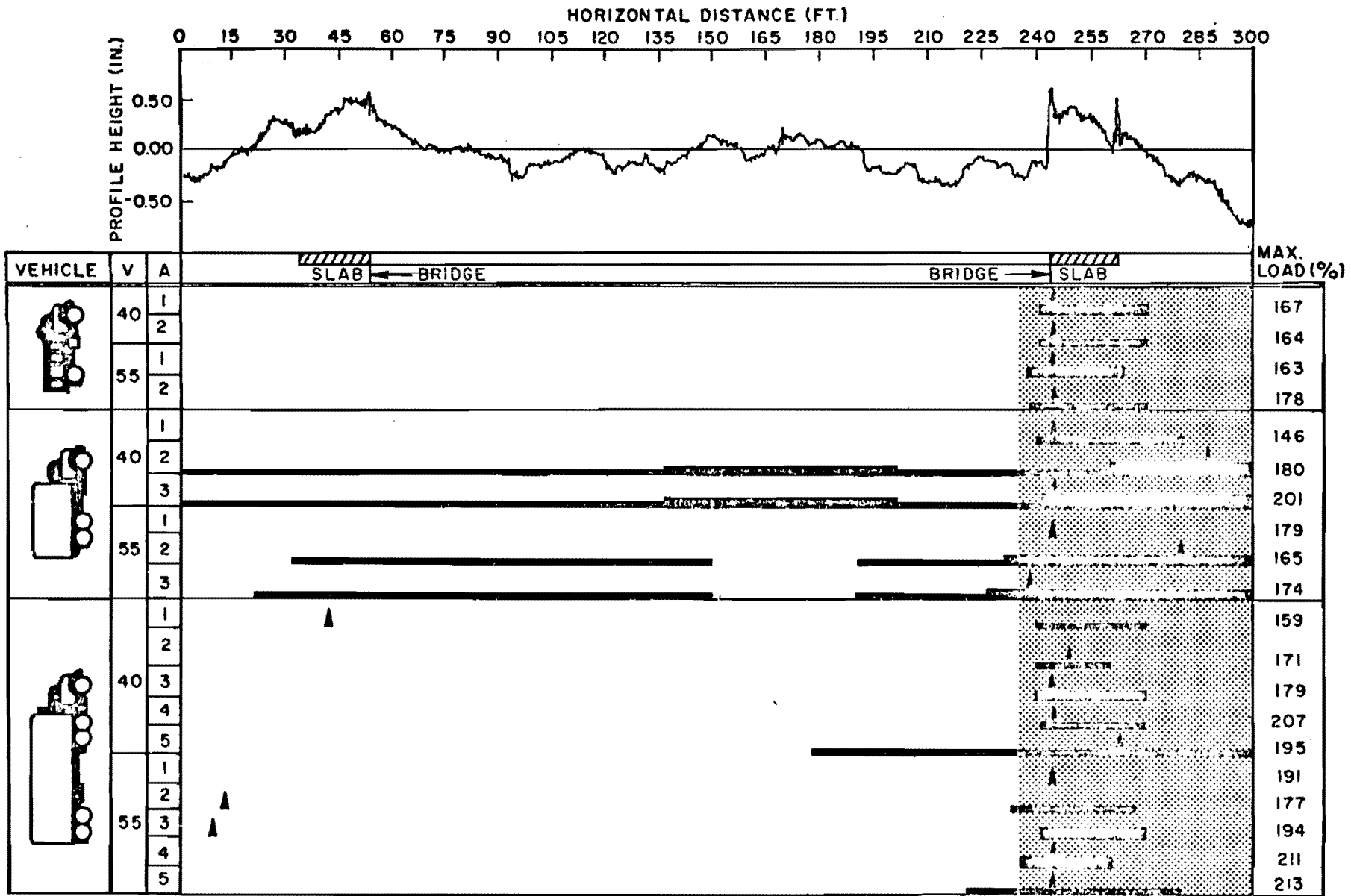


Fig A4. 31A. Dynamic wheel load diagram, high frequency oscillation, North Loop over McCarty Road (Houston).

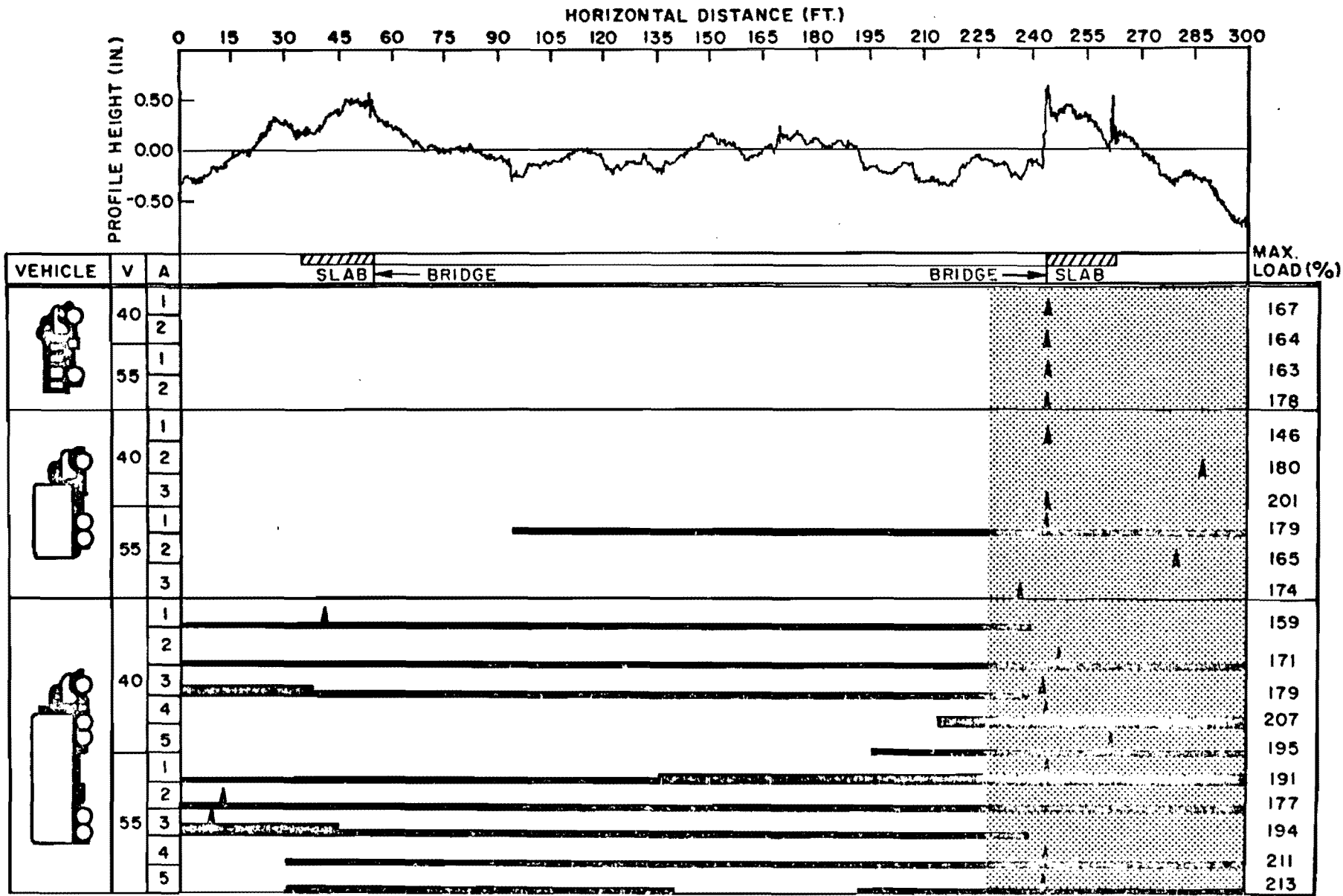


Fig A4. 31B. Dynamic wheel load diagram, low frequency oscillation, North Loop over McCarty Road (Houston).

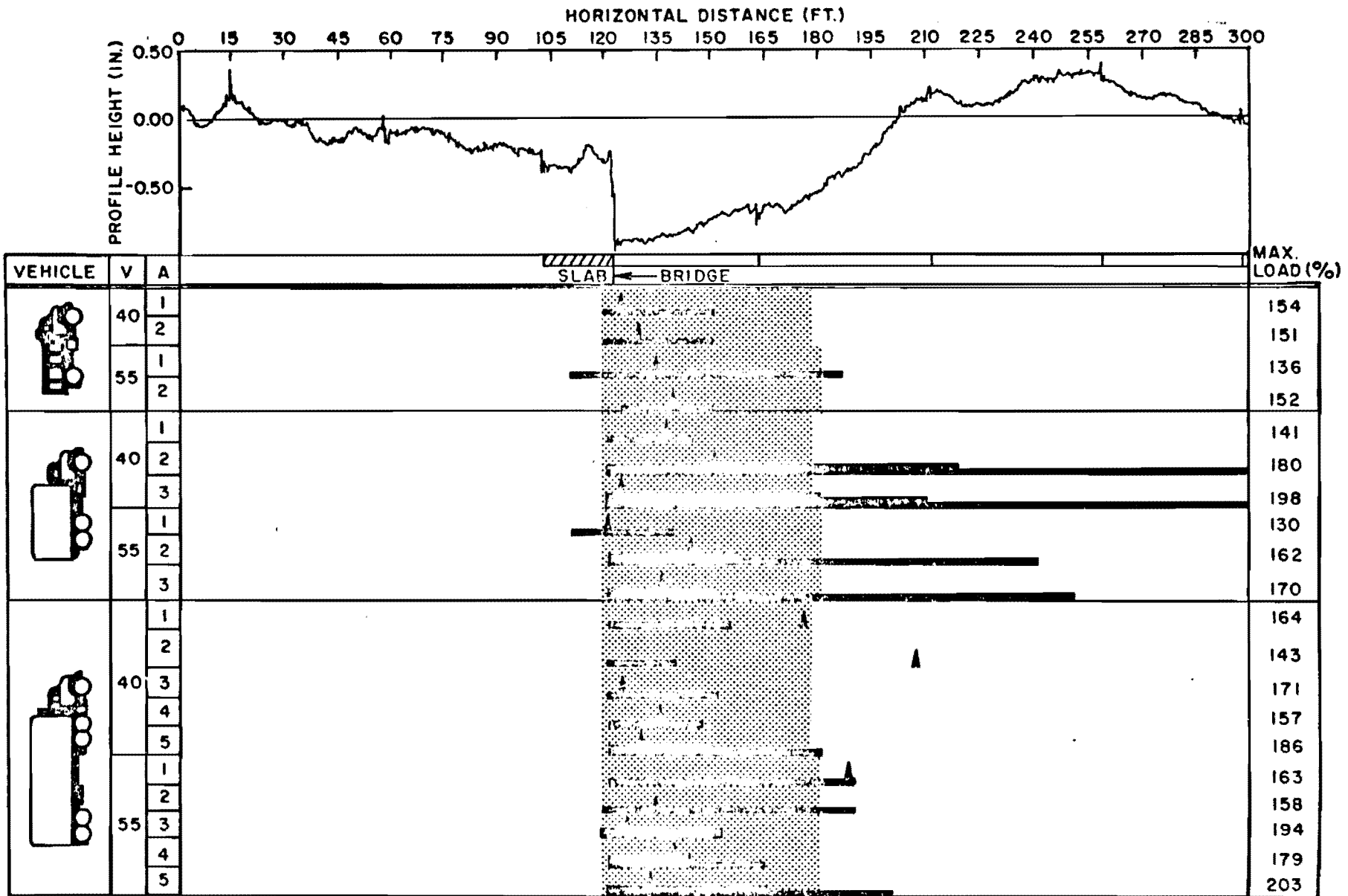


Fig A4.32A. Dynamic wheel load diagram, high frequency oscillation, IH 10 over West Belt (Houston), start of bridge.

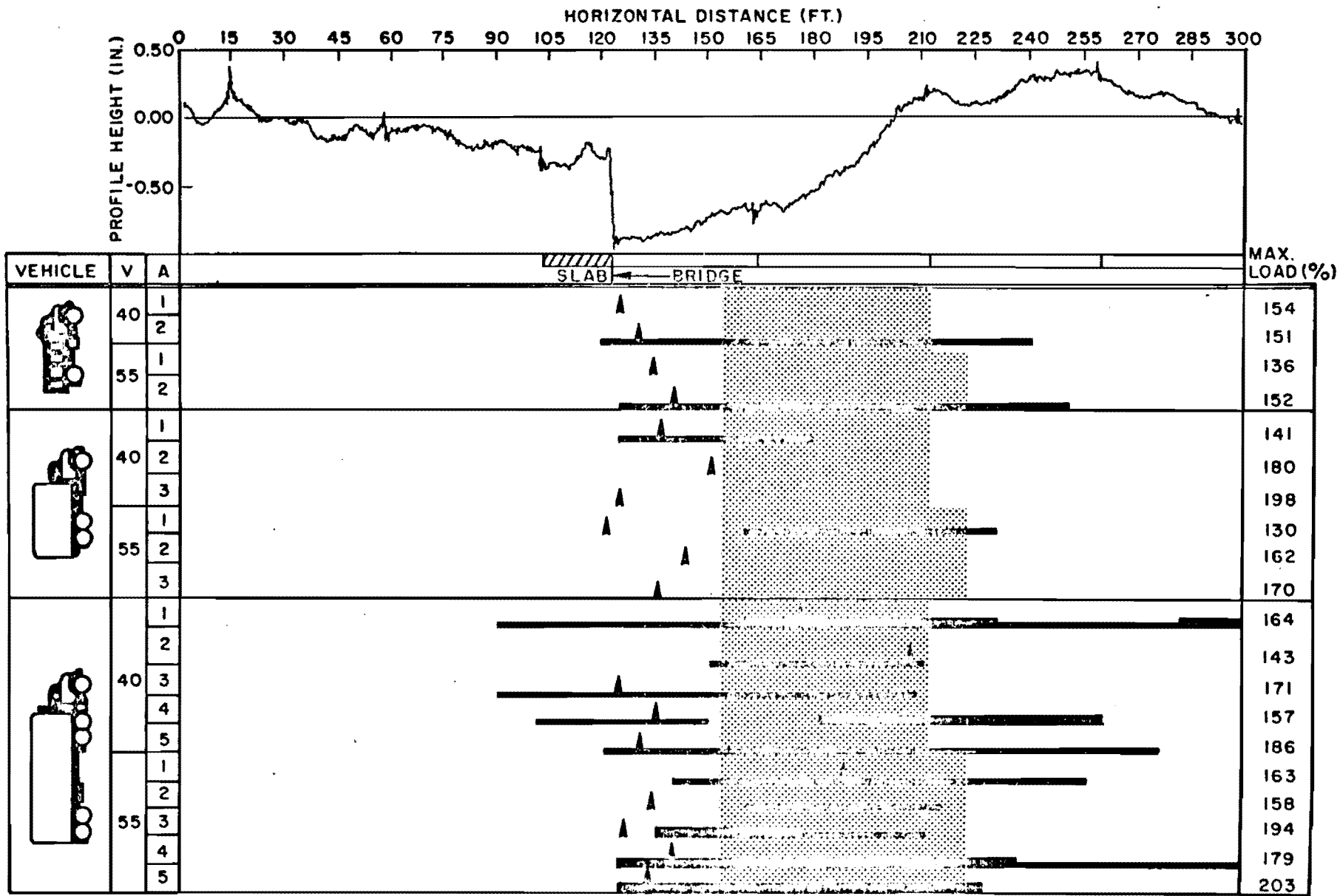
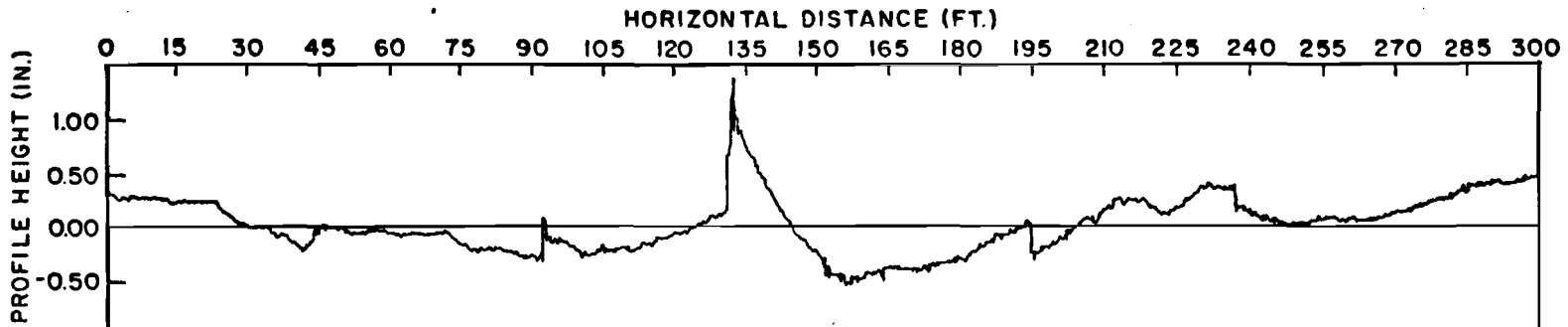


Fig A4.32B. Dynamic wheel load diagram, low frequency oscillation, III 10 over West Belt (Houston), start of bridge.



VEHICLE	V	A	BRIDGE	SLAB	MAX. LOAD (%)
	40	1			186
		2			152
	55	1			191
		2			164
	40	1			155
		2			194
		3			228
	55	1			158
		2			206
		3			221
	40	1			192
		2			179
		3			187
		4			184
		5			181
	55	1			187
		2			214
		3			228
		4			203
		5			239

Fig A4.32A. Dynamic Wheel load diagram, high frequency oscillation, IH 10 over West Belt (Houston), end of bridge.

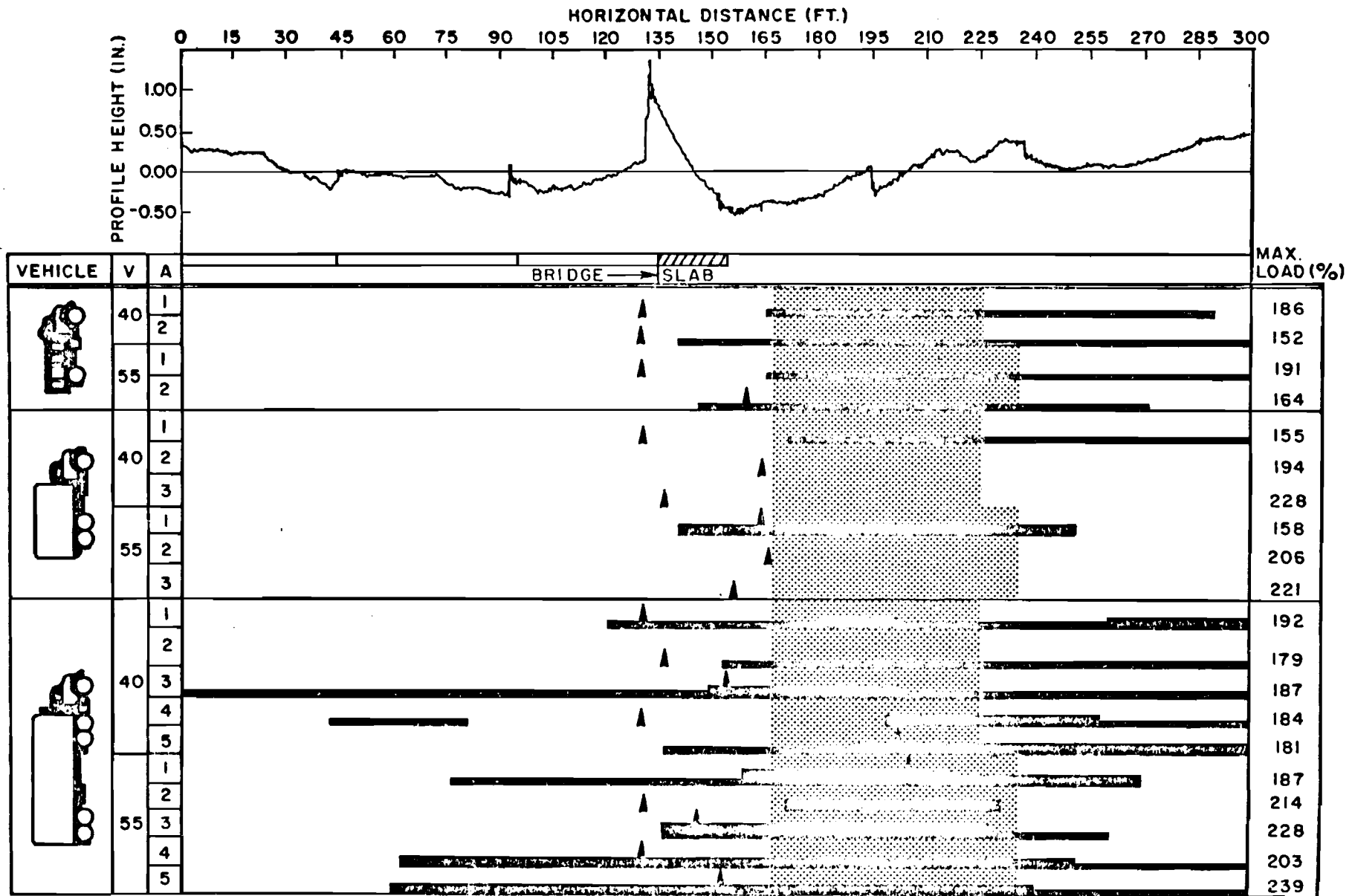


Fig A4. 33B. Dynamic wheel load diagram, low frequency oscillation, IH 10 over West Belt (Houston), end of bridge.

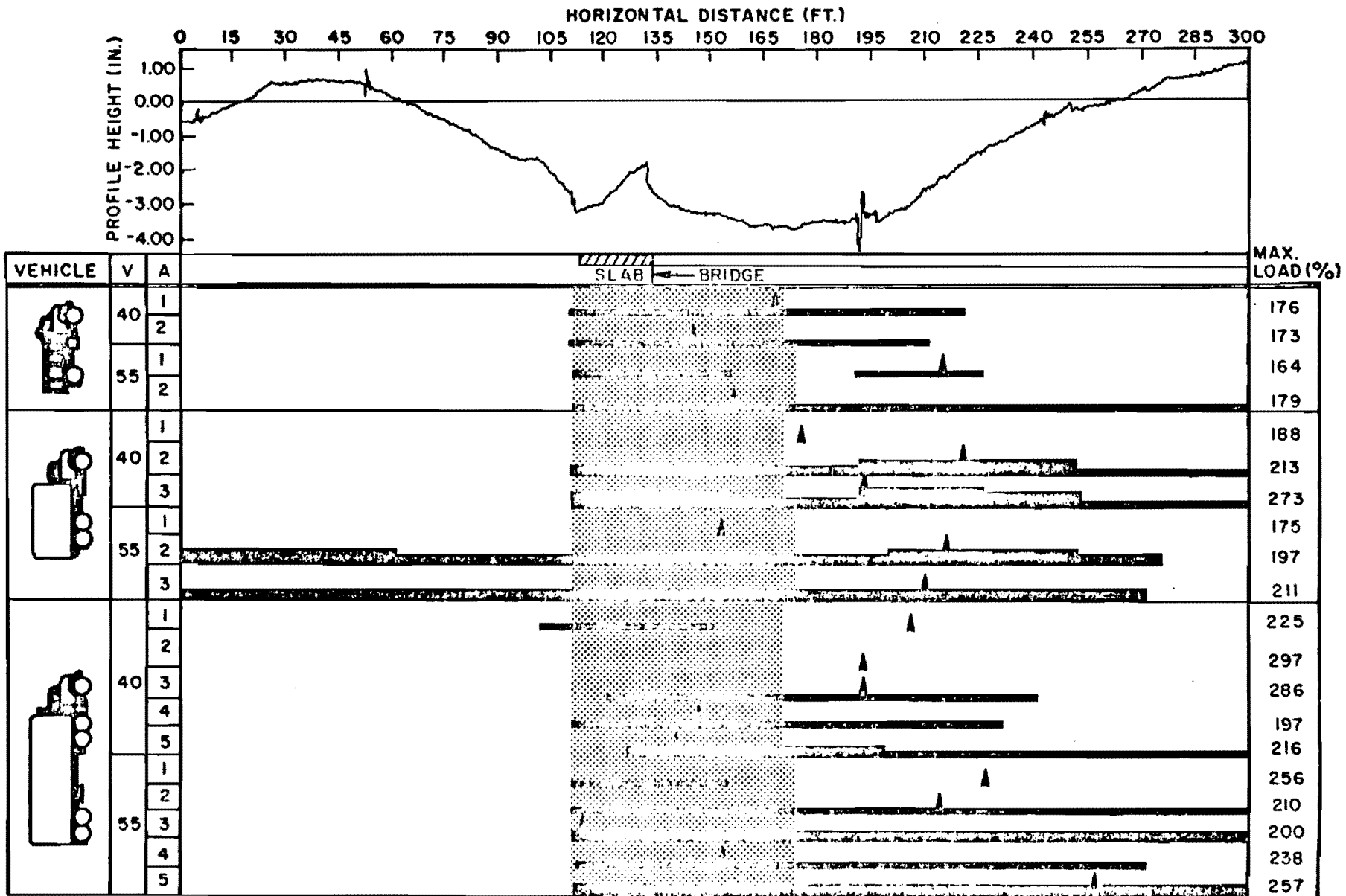


Fig A4. 34A. Dynamic wheel load diagram, high frequency oscillation, North Loop over Railroad (Houston), start of bridge.

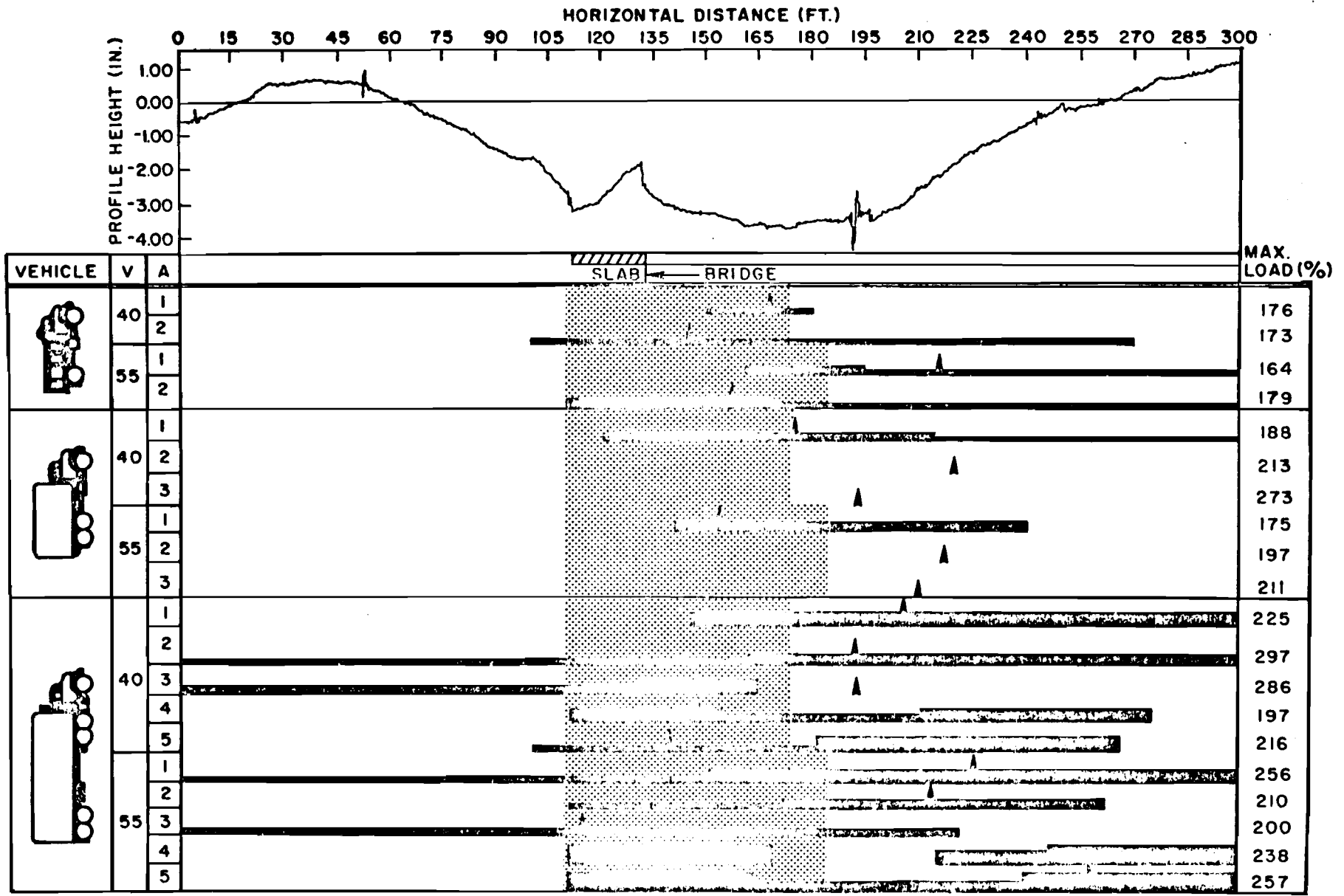


Fig A4. 34B. Dynamic wheel load diagram, low frequency oscillation, North Loop over Railroad (Houston), start of bridge.

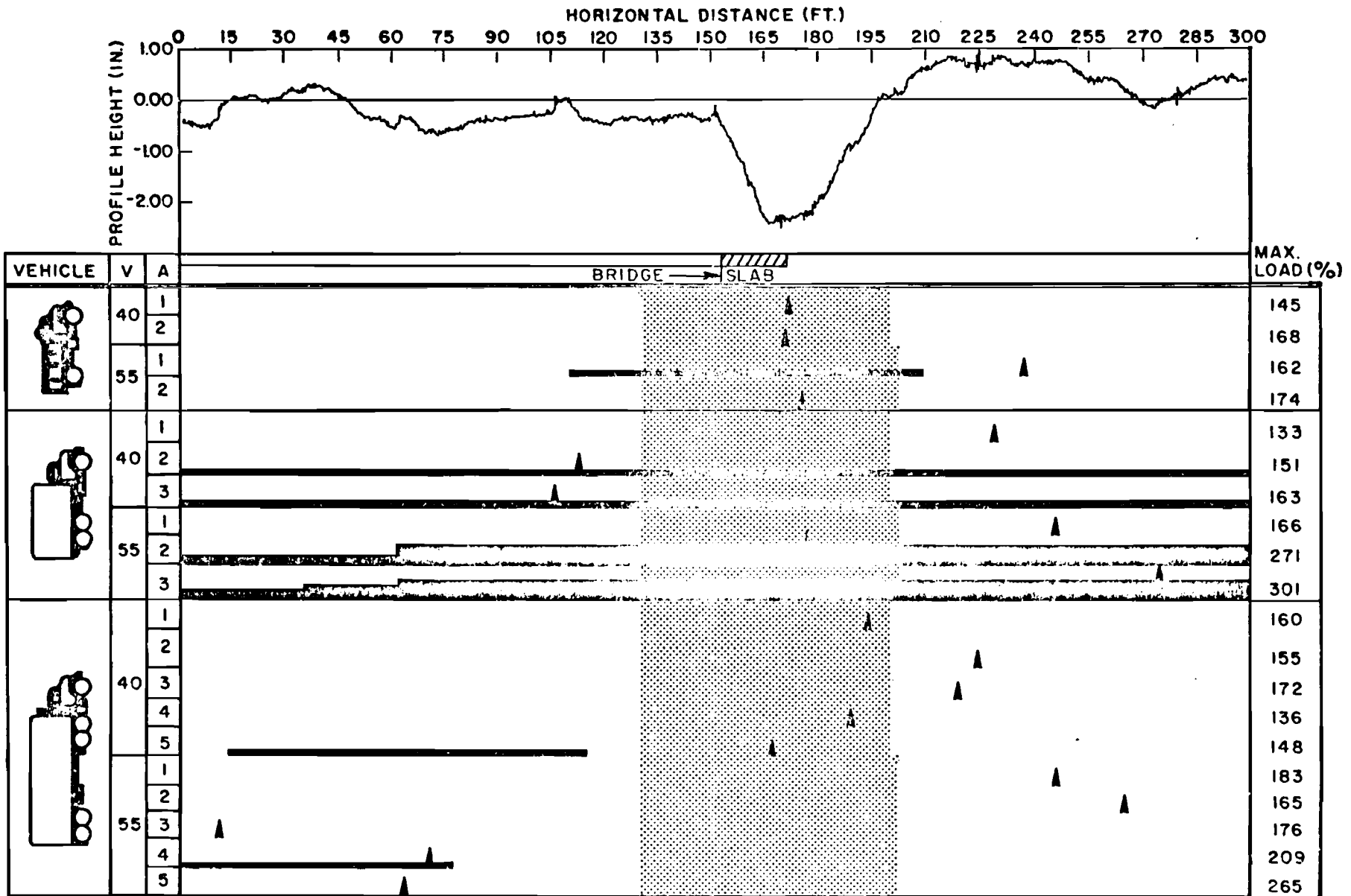


Fig A4. 35A. Dynamic wheel load diagram, high frequency oscillation, North Loop over Railroad (Houston), end of bridge.

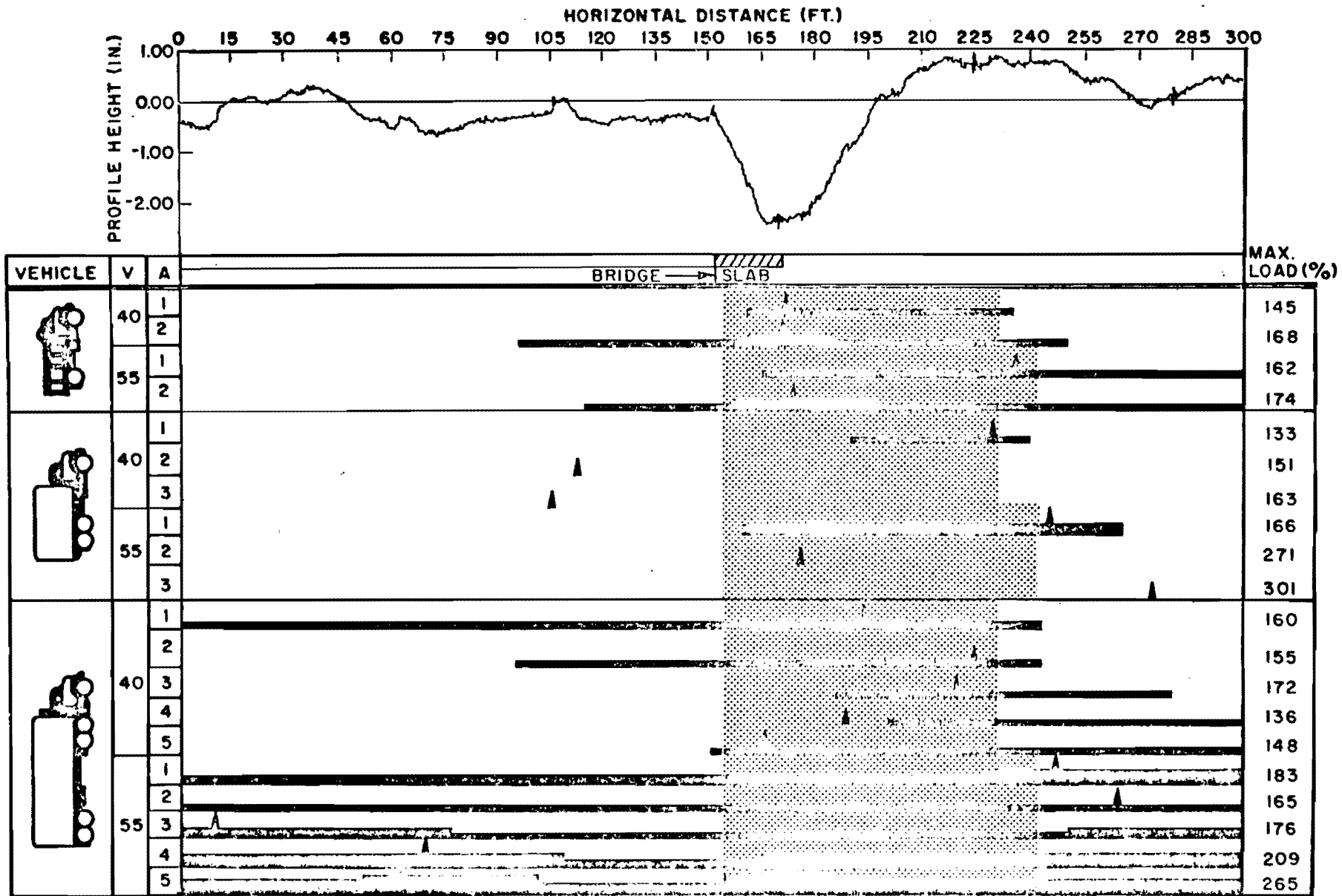


Fig A4.35B. Dynamic wheel load diagram, low frequency oscillation, North loop over Railroad (Houston), end of bridge.

REFERENCES

1. "Pavement Rehabilitation-Materials and Techniques," National Cooperative Highway Research Program Synthesis of Highway Practice (NCHRP SYN) No. 9, Highway Research Board, 1972.
2. "Bridge Approach Design and Construction Practices," NCHRP SYN No. 2, Highway Research Board, 1969.
3. "AASHTO Interim Guide for Design of Pavement Structures - 1972," American Association of State Highway and Transportation Officials, Washington, DC, 1972.
4. "Dynamic Studies of Bridges on the AASHTO Road Test," Special Report 71, Highway Research Board, 1962.
5. General Motors Corporation, "Dynamic Pavement Loads of Heavy Highway Vehicles," NCHRP Report 105, Highway Research Board, 1970.
6. Kaplar, C. W., "Phenomenon and Mechanism of Frost Heaving," Highway Research Record No. 304, Highway Research Board, 1970, pp. 1-13.
7. Jessberger, H. L., and D. L. Carbee, "Influence of Frost Action on the Bearing Capacity of Soils," Highway Research Record No. 304, Highway Research Board, 1970, pp. 14-26.
8. McCullough, B. F., and T. F. Sewell, "An Evaluation of Terminal Anchorage Installation on Rigid Pavements," Departmental Research Report No. 39-4F, Texas Highway Department, 1966.
9. Yoder, E. J., and M. W. Witczak, "Principles of Pavement Design," Second Edition, John Wiley & Sons, 1975.
10. Hopkins, T. C., and R. C. Deen, "The Bump at the End of the Bridge," Highway Research Record No. 302, Highway Research Board, 1970, pp. 72-75.
11. Moore, L. H., "Summary of Treatments for Highway Embankments on Soft Foundations," Highway Research Record No. 133, Highway Research Board, 1966, pp. 45-59.
12. "Treatment of Soft Foundations for Highway Embankments," NCHRP SYN No. 29, Transportation Research Board, 1975.

13. Johnson, S. J., "Precompression for Improving Foundation Soils," Journal of the Soil Mechanics and Foundations Division, Proceedings of the American Society of Civil Engineers, Vol. 96, No. SM1, January 1970, pp. 111-144.
14. Johnson, S. J., "Foundation Precompression with Vertical Sand Drains," Journal of the Soil Mechanics and Foundations Divisions, ASCE, Vol. 96, No. SM1, January 1970, pp. 145-175.
15. Landau, R.E., "Method of Installation as a Factor in Sand Drain Stabilization Design," Highway Research Record No. 133, Highway Research Board, 1966, pp. 75-97.
16. Hopkins, T.C., and G.D. Scott, "Estimated and Observed Settlements of Bridge Approaches," Highway Research Record No. 302, Highway Research Board, 1970, pp. 76-86.
17. "Construction of Embankments," NCHRP SYN No. 8, Highway Research Board, 1971.
18. Nelson, D. S., and W. L. Allen Jr., "Sawdust as Lightweight Fill Material," Public Roads 39-2, Federal Highway Administration, September 1975, pp. 63-67.
19. Lea, N.D., "Highway Design and Construction over Peat Deposits in Lower British Columbia," Highway Research Record No. 7, Highway Research Board, 1963, pp. 1-31.
20. Gray, D.H., "Properties of Compacted Sewage Ash," Journal of the Soil Mechanics and Foundations Division, ASCE, Vol. 96, No. SM2, March 1970, pp. 439-451.
21. Margason, G., and J. E. Cross, "Settlement Behind Bridge Abutments, The use of pulverised fuel ash in constructing the approach embankments to bridges on the Staines By-pass," RRL Report No. 48, Road Research Laboratory, England, 1966.
22. McLaren, D., "Settlement Behind Bridge Abutments, The performance of a medium-clay fill used to form the approach embankment to a bridge on the M.1 Motorway," RRL Report LR 76, Road Research Laboratory, England, 1967.
23. McLaren, D., "Settlement Behind Bridge Abutments, The performance of a silty clay fill in an approach embankment on the M4 Motorway," RRL Report LR309, Road Research Laboratory, England, 1970.
24. Cross, J.E., "Settlement Behind Bridge Abutments, The performance of a uniformly-graded sand fill in an approach embankment on the M4 Motorway," RRL Report LR310, Road Research Laboratory, England, 1970.

25. Margason, G., "Settlement Behind Bridge Abutments, The performance of a stony-clay fill in an approach embankment to an overbridge on the M4 Motorway," RRL Report LR311, Road Research Laboratory, England, 1970.
26. Wise, J.R., and W. R., Hudson, "An Examination of Expansive Clay Problems in Texas," Research Report 118-5, Center for Highway Research, The University of Texas at Austin, 1971.
27. Grover, R., "Bridge and Approach Settlements Cured by Major Design Revisions," Rural and Urban Roads, July 1978, pp. 63-65.
28. Harris, F.A., "Asphalt Membranes in Expressway Construction," Highway Research Record No. 7, Highway Research Board, 1963, pp. 34-46.
29. Hu, Y. C., "A Study of Roughness at the Pavement-Bridge Interface," M.S.E. Thesis, The University of Texas at Austin, 1977.
30. Spangler, E.B., and W. J. Kelley, "GMR Profilometer - A Method for Measuring Road Profile," Highway Research Record No. 121, Highway Research Board, 1966, pp. 27-54.
31. Hudson, W.R., "High-Speed Road Profile Equipment Evaluation," Research Report 73-1, Center for Highway Research, The University of Texas at Austin, 1966.
32. Walker, R.S., F.L. Roberts, and W.R. Hudson, "A Profile Measuring, Recording, and Processing System," Research Report 73-2, Center for Highway Research, The University of Texas at Austin, 1970.
33. Al-Rashid, N.I., C.E. Lee, and W.P. Dawkins, "A Theoretical and Experimental Study of Dynamic Highway Loading," Research Report 108-1F, Center for Highway Research, The University of Texas at Austin, 1972.
34. Wu, Tsu-Long, "Roughness at the Bridge-Pavement Interface," M.S. Thesis, The University of Texas at Austin, 1979.